MAKERERE UNIVERSITY

COLLEGE OF NATURAL SCIENCES
SCHOOL OF PHYSICAL SCIENCES

DEPARTMENT OF GEOLOGYAND PETROLEUM STUDIES

A SEMILIKI BASIN FIELD STUDY REPORT

SUBMITTED TO THE DEPARTMENT OF GEOLOGY AND PETROLEUM STUDIES, MAKERERE UNIVERSITY IN PARTIAL FULFILMENT OF THE AWARD OF BACHELOR OF SCIENCE DEGREE IN PETROLEUM GEOSCIENCE AND PRODUCTION.

BY:

ETENGU EMMANUEL

REGISTRATION NUMBER: 21/U/18892

STUDENT NUMBER:2100718892

DATE OF SUBMISSION: 2ND JUNE, 2025

DECLARATION

I, **ETENGU EMMANUEL** hereby declare that the content of this report, submitted to the Department of Geology and Petroleum studies at Makerere University for the award of a Bachelor of Science degree in Petroleum Geoscience and Production, is based on my own work and field observations carried out during the Isingiro field trip under the supervision of various lecturers, and has never been presented before to this institution or any other institution.

I strongly assert the statements made and conclusions drawn are purely the outcome of my research work. I further certify that; I have followed to the dot the guidelines provided by the department in writing the report.

..... 02/06/2025.

Signature Date

APPROVAL

Project Coordinator

..... 2nd/June/2025

Signature Date

Dr. Betty Nagudi.

DEDICATION

I dedicate this report first and foremost to **Almighty God**, whose guidance and blessings have been my strength throughout my academic journey and life.

I also extend my deepest gratitude to my **exceptional lecturers**, whose wisdom, expertise, and unwavering support have shaped my understanding and growth.

To my **wonderful friends and groupmates**, thank you for your encouragement, teamwork, and camaraderie, this achievement is as much yours as it is mine.

In a very special way, I dedicate this work to my **beloved parents, uncles, and aunts**, whose endless love, sacrifices, and unwavering belief in me have made this milestone possible. Your support has been my greatest motivation.

ACKNOWLEDGEMENT

First and foremost, I give all glory and thanks to **Almighty God** for His grace, love, and protection, as well as the strength and wisdom He bestowed upon me to successfully complete the field exercise and report.

I am deeply grateful to **Makerere University**, particularly the **Department of Geology and Petroleum Studies**, for their unwavering academic support and dedication to our learning.

My heartfelt appreciation goes to my lecturers—**Dr. A. Batte, Dr. Nagudi Betty, Assoc.Prof. Echegu Simon, Dr. John Mary Kiberu and Mr.Mugwano Patrick,** for their expert guidance, intellectual mentorship, encouragement, and supervision during and after the fieldwork. Their invaluable contributions were instrumental in the successful completion of this exercise and report.

I extend my sincere thanks to my fellow students, especially my **Area F groupmates Mr. Meen John Maper, Mrs. Nalumba Deborah, Mrs. Asaba Scovia Makume, and Mrs. Nansereko Diana,** for their unwavering support, cooperation, and teamwork throughout the challenging phases of fieldwork and report writing.

Finally, I greatly appreciate the **support staff, Mr. Tonny, Mr. Enoch, Mr. Enoch and Madam Grace**, for taking excellent care of our welfare and any support needed before, during and after the field camp. Their efforts ensured a smooth and productive fieldwork experience.

ABSTRACT

This report presents findings from fieldwork conducted in Uganda's Semliki Basin (Albertine Graben) from 30/06/2024 to 10/07/2024, analyzing stratigraphic, sedimentologic, and structural data critical for petroleum exploration. The basin, formed by tensional tectonics, contains Middle Miocene-Recent sediments overlying Jurassic/Permo-Triassic to Early Tertiary strata unconformably deposited on Precambrian basement (granite/gneiss/amphibolite).

Lithologies include variably sorted sands (white/yellow), clays, polymictic/monomictic conglomerates, and siltstones showing cyclic fluvial-deltaic (coarsening/fining upward) and lacustrine (blocky) deposition. Paleocurrent analysis (Stereonet rose diagrams) suggests braided/meandering river systems, while gypsum/iron(III) minerals indicate semi-arid conditions. Stratigraphy comprises (ascending): Kisegi, Kasande, Kakara, Oluka, Nyaburogo, Nyakabingo, and Nyabusosi Formations.

Structural analysis reveals NE-SW trending basement faults/joints (minor SE-NW trend) influencing sedimentary structures (cross-bedding, unconformities, mud cracks). Sempaya Hot Springs evidence active crustal thinning, providing sufficient thermal maturity (TTI) for hydrocarbon generation in Kasande Formation source rocks, with Kisegi Formation as reservoirs. Reservoir compartmentalization by thin clays/gypsum poses production challenges, while joints facilitate migration and normal faults create traps. The basin also shows significant geothermal potential.

TABLE OF CONTENTS

LIST OF FIGURES

LIST OF APPENDICES

LIST OF TABLES

CHAPTER 0NE: INTRODUCTION

1.0 Project Background

This field study aims to develop essential fieldwork competencies for third-year Petroleum Geoscience and Production students from Makerere University's Department of Geology and Petroleum Studies (College of Natural Sciences). The program focuses on the Kichwamba and Semliki basins within Uganda's Albertine Graben region, located south and east of Lake Albert.

As a mandatory component of the degree requirements, the study provides hands-on training in geological field techniques. This report documents the field observations and findings, serving as partial fulfillment for the Bachelor's degree program in Petroleum Geoscience and Production at Makerere University.

1.1 Location of the Study area.

The Kichwamba and Semliki Basins, the focus of this study, are situated in Uganda's Karugutu-Ntoroko district within the Albertine Graben. This region forms the northernmost section of the western branch of the East African Rift System (EARS), located south and east of Lake Albert.

The Semliki Basin covers approximately 1200 km², with 740 km² in Uganda's Albertine Graben and the remainder in the Democratic Republic of Congo. Our research specifically targeted Block 3 of the Albertine Graben (Fig. 1.1), encompassing the Semliki flats and Toro Plain southwest of Lake Albert. The area is bounded by a dramatic 1000-meter fault escarpment connecting to the Rwenzori Mountains' northern foothills.

Notably, the basin's elevation averages just 650 meters above sea level, contrasting sharply with neighboring rift shoulders that rise 1100-1800 meters in Uganda and DRC. Current estimates suggest 700m of exposed Neogene sediments in Semliki River tributaries, though previous studies by Wayland, Pickford (≈600m) and Bishop (≥1300m) show significant variation in these depth assessments.

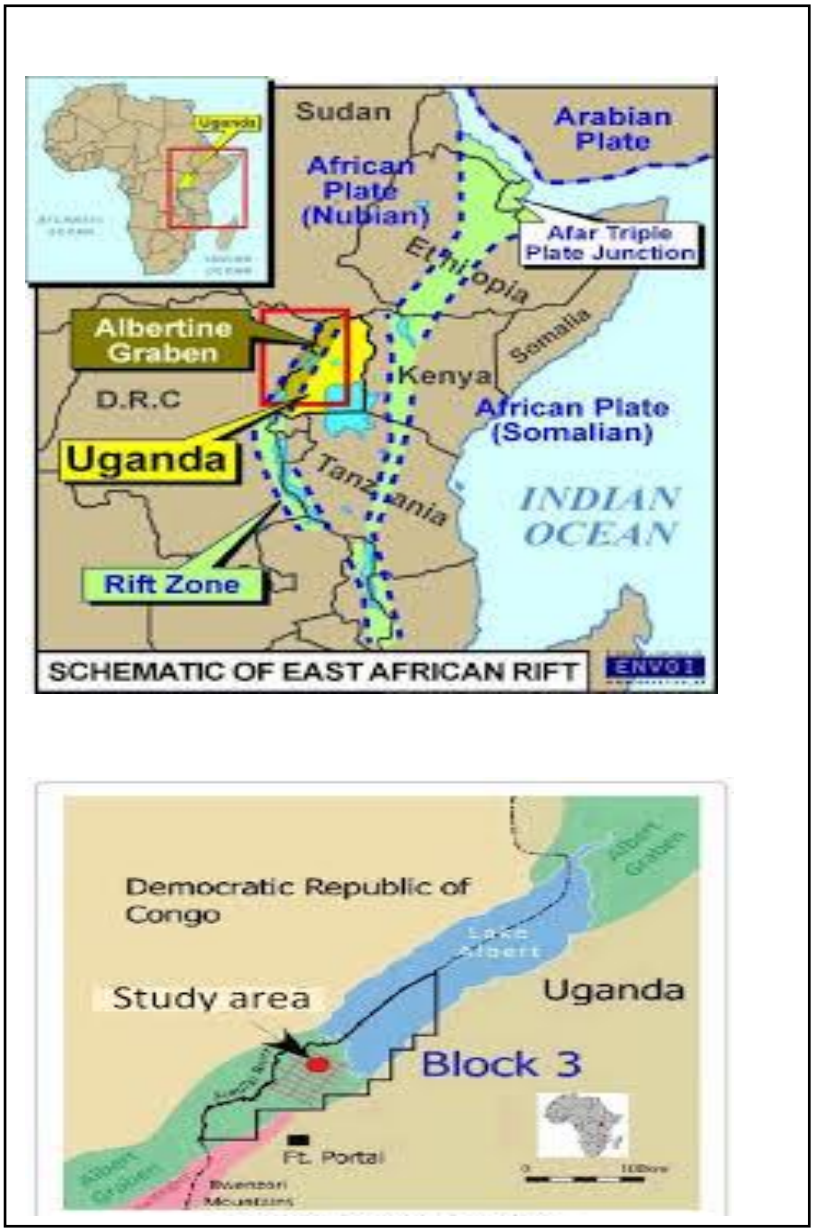

Figure.1.1 Maps showing the Location of the Albertine graben in Africa and in Uganda (top) (Source; walshmedicalmedia.com). Block 3 exploration area showing the location of the Albertine graben (bottom) (Source; ejatlas.org)

1.2 Accessibility

The research area is accessible via road from Kampala through Mubende, Kyenjojo, and Fort-Portal districts to Ntoroko. The primary route follows the Fort-Portal-Bundibugyo highway,

covering approximately 290 km from Kampala to Fort-Portal, with an additional 25.6 km stretch connecting to Karugutu Town in Ntoroko District (Fig. 1.2).

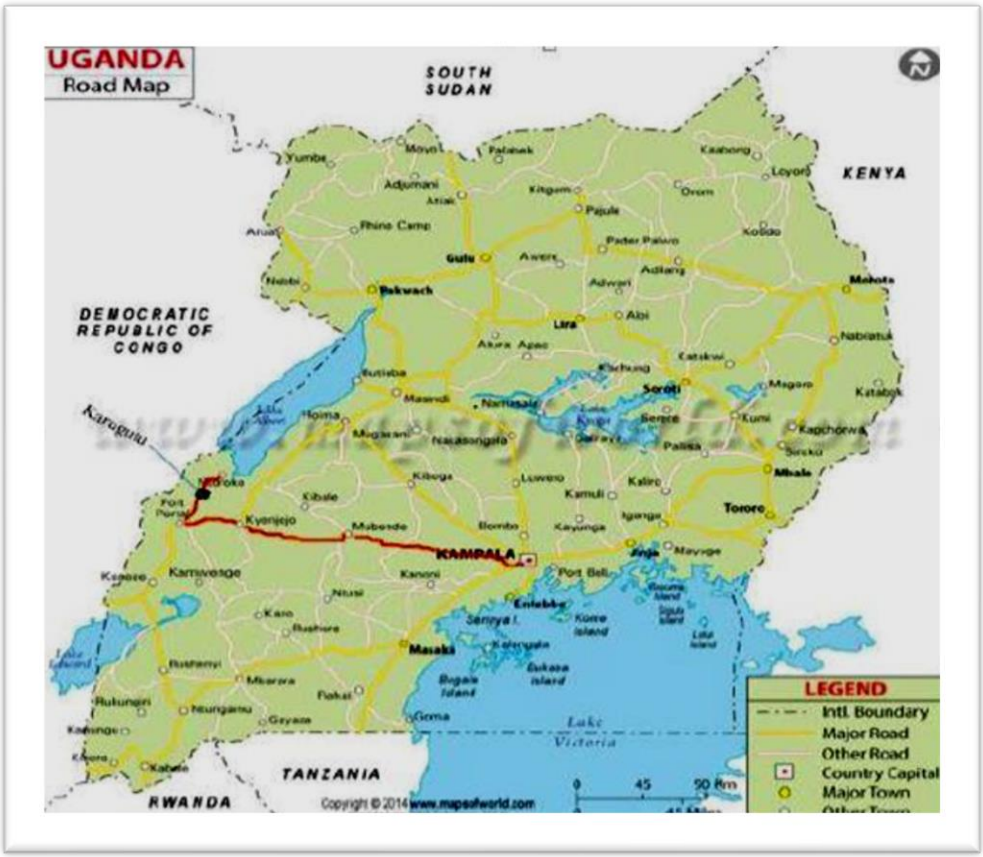

Figure 1.2. A map of Uganda showing the road used to access the Study Area.(indicated by the red line) (Source; mapsofworld.com)

1.3 Objectives of the study

- **Main Objective:**
  Field training on how to collect and interpret stratigraphic, petrographic, sedimentologic and structural data; which are very important in hydrocarbon exploration.
- **Specific Objectives:**

- To identify the lithologies in Semliki Basin.
- To identify and relate structures observed in the basement and sediments.
- To study the lithologies and environments in order to identify the different elements of the petroleum system.
- To Identify facies and depositional environments.

1.4 Geologic Setting of The Study Area

The Albertine Graben forms the northernmost segment of the Eastern African Rift System (EARS), extending over 500 km with a variable width of 45 km from the Uganda-Sudan border to Lake Edward. Initial rifting began approximately 30 Ma, with volcanic activity commencing around 20 Ma (Fig. 1.3). In the northern Virunga province, volcanism initiated later during the Middle Miocene (~12.6 Ma), while thermal up-doming and faulting in the western branch started in the Early Miocene (Bellon & Pouclet, 1980).

By ~12 Ma, basin formation began through shallow down-warping, accumulating fluvial and evaporite deposits of the Kisegi Formation (Pickford et al., 1993). The first major rifting phase (11-10 Ma) created Lake Obweruka, a 550 km-long basin. Permanent lacustrine conditions developed at 8-7 Ma when subsidence outpaced sedimentation. Significant rift shoulder uplift occurred by 4 Ma, followed by renewed rifting at 2.6 Ma that segmented the graben and separated Lake Obweruka into Lakes Edward and Albert (Pickford et al., 1993). The most recent rifting phase (14,000-12,000 years ago) altered drainage patterns northward (Aanyu, 2011). Major normal faults exhibit throws of 1-6 km, with rift polarity changes occurring along ~100 km asymmetric segments.

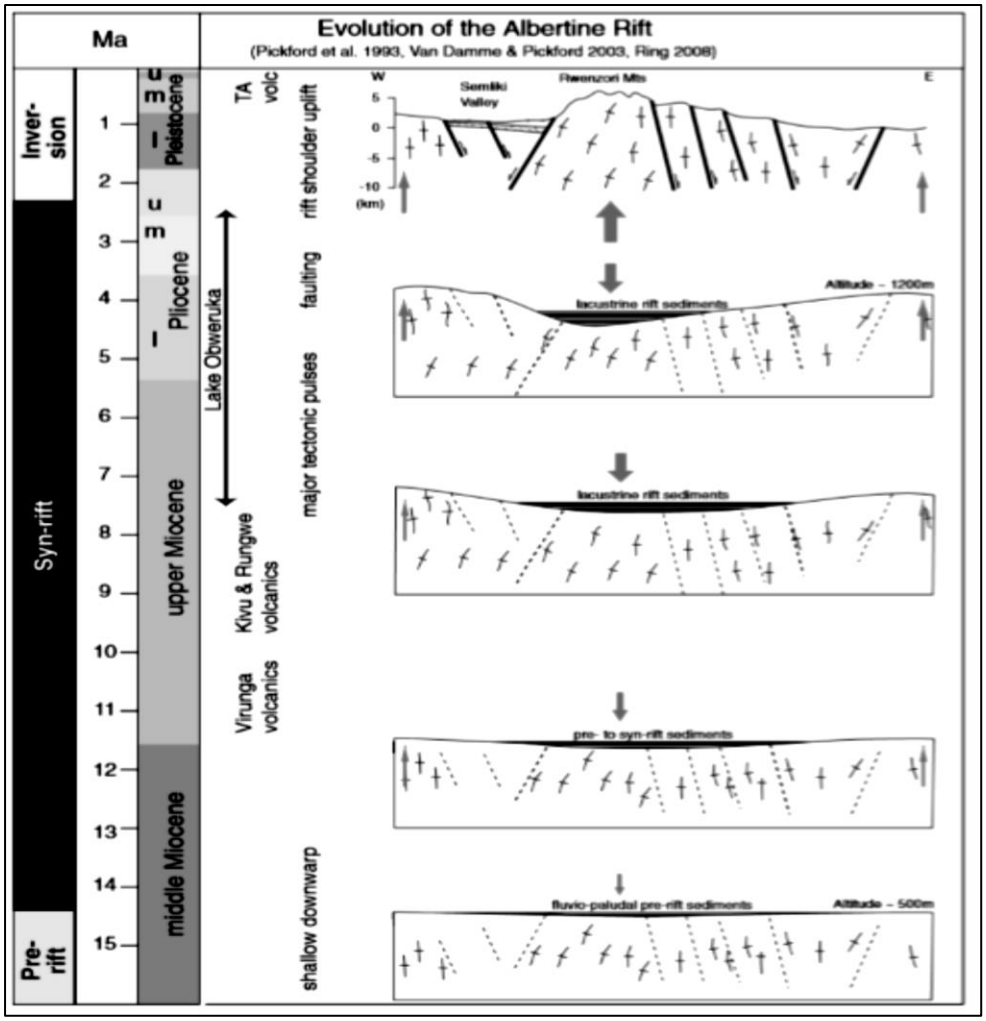

Figure 1.3: Geological evolution timeline of the Albertine Graben (modified after Pickford et al1993, Van Damme and Pickford 2003, Fling 2008).

Structural Setting

The Albertine Graben developed as a Cenozoic rift basin within the Precambrian orogenic belt of the African Craton. Initial rifting commenced during the late Oligocene/early Miocene period. The graben's formation has been influenced by multiple tectonic events across both extensional and compressional regimes.

The basin's structural architecture reveals stress regimes oriented both perpendicular and oblique to boundary faults, evident through fault system geometries. The graben's northern termination aligns with the Aswa shear zone, a prominent sinistral strike-slip structure. Similar shear zones are observed in Tanzania's Kivu and Rukwa regions along the East African Rift.

These structural features suggest the Albertine Graben evolved under a strike-slip dominated tectonic regime, consistent with other basins in the Central African Rift System (Figure 1.4).

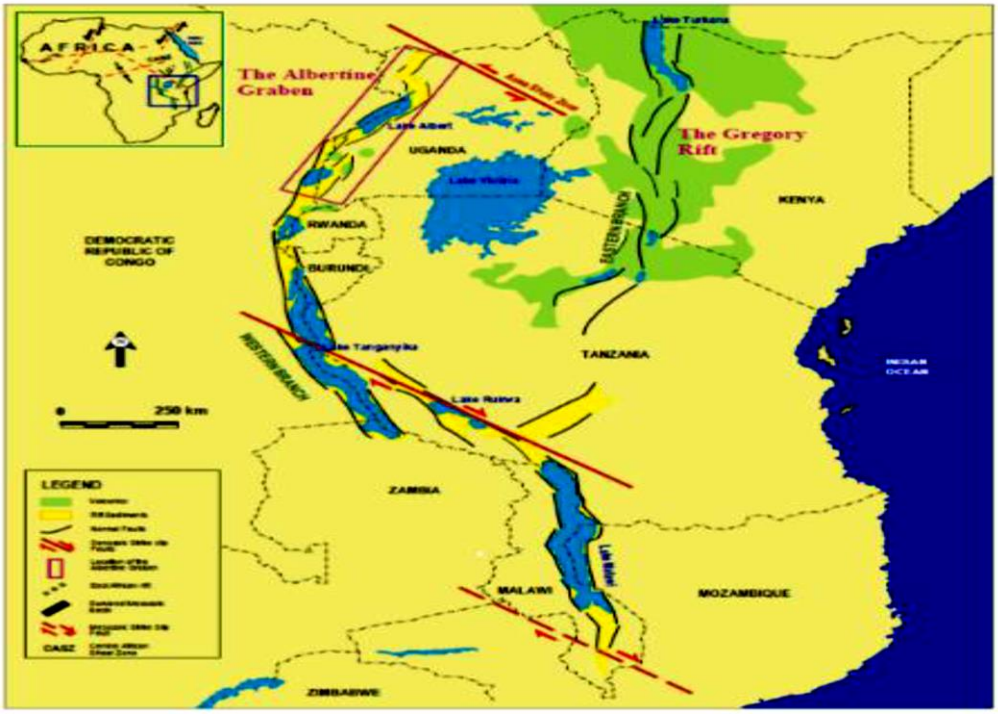

Figure1. 4: East African map showing the three strike-slip shear zones along which the Albertine graben formed (Source: Lukaye, et al 2016)

The Albertine Graben exhibits three distinct structural domains (Figure 1.5):

- The northern domain (NNE-SSW trend) containing the Rhino Camp and Pakwach basins
- The central domain (NE-SW trend) encompassing Lake Albert's Butiaba-Wanseko and Kaiso-Tonya areas plus the Semliki Basin

- The southern domain (NNE-SSW trend) comprising the Lakes Edward-George basin

Throughout most of its extent, the graben maintains a predominant NE-SW orientation, aligning with pre-existing basement structural trends.

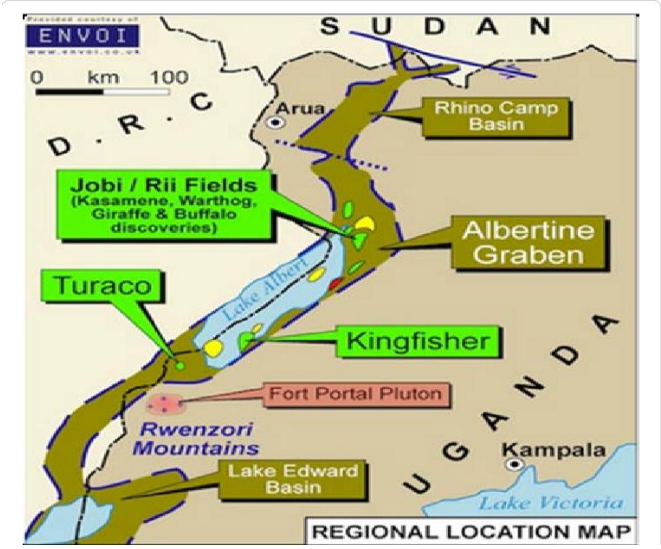

Figure1. 5: A map of Uganda showing the three structural domains of the Albertine Graben (Kiraye M. et. Al, 2016.Research gate)

Overview of Topography Albertine Graben

Grotzinger et al. (2007) define topography as the Earth's surface configuration characterized by elevation variations. Jarrett (2014) analyzed the Graben's morphology using satellite-derived digital elevation modeling (Figure 1.6), with cross-section "D" specifically illustrating the Semliki basin's topographic profile.

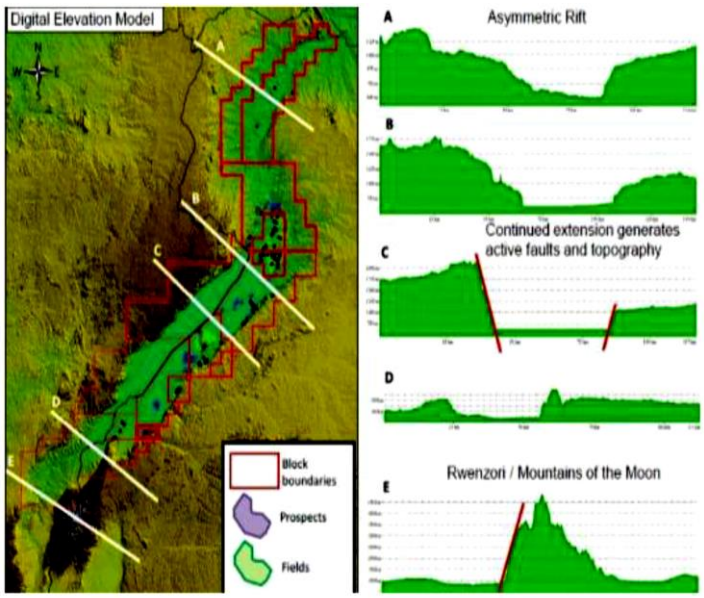

Figure1. 6: Topographic profiles along the Albertine graben (left) and the resultant cross sections (right).(Source: Jarret, 2014).

Overview of stratigraphy of Albertine Graben.

The Albertine Graben's sedimentary succession consists predominantly of fluvial-deltaic and lacustrine deposits, influenced by tectonic activity, climatic shifts, and lake-level fluctuations. Multiple researchers including Wayland (1925), Bishop (1965), and Pickford (1993) have documented the stratigraphy, with recent efforts by PEPD and oil companies working to reconcile historical discrepancies and establish a unified stratigraphic framework.

The Proterozoic basement, exposed along rift flanks, comprises high-grade metamorphic and igneous Precambrian rocks. Seismic data reveals localized Pre-Cenozoic rift sediments, particularly in Lake Albert depocenters. The syn-rift sequence was first identified in the 1938 Waki-1B well, which penetrated Mid-Upper Cenozoic conglomerates and sandstones before reaching Mesozoic pre-rift sections and basement. The well-exposed Kisegi and Kaiso Formations (Cenozoic) feature conglomerate-sandstone alternations deposited in fluvial-shallow lacustrine environments. While the Kisegi Formation often directly overlies meta-quartzite basement, in some areas it may rest on Mesozoic (Karoo) strata.

Physiography of the Semliki Basin.

The study area comprises the Semliki flats and adjacent Toro plains, located southwest of Lake Albert. The Semliki flats feature predominantly flat to gently undulating terrain with savanna vegetation, sharply demarcated from the Toro plain's rolling hills by the prominent Makondo fault along the Semliki River's eastern banks. This meandering river forms the natural Uganda-DRC border as it traverses the flats.

Covering approximately 340 km² of the Northern Rwenzori Block, the Semliki Basin connects to the Rwenzori Mountains through steep, fault-controlled escarpments. The basin's southeastern boundary rises abruptly ~1,000 m along a fault scarp to the Rwenzori's northern spur. Two major fault systems define its western margin: the NNE-SSW trending Semliki fault and NE-SW oriented Bunya fault (Figure 1.7), which separate the basin from the Congo escarpment.

The Semliki Basin exhibits uniformly low-lying terrain, with elevations ranging between approximately 630 and 750 meters above sea level (Figure 1.8). This relatively flat topography characterizes the entire study area.

The basin's peripheral valleys support agricultural activities due to their optimal soil depth-to-slope ratio. Structural analysis reveals significantly greater vertical displacement along the western bounding Semliki fault compared to its eastern counterpart. Post-depositional development has resulted in pronounced basin asymmetry, with the Congolese sector (western flank) exhibiting substantially greater depth than the Ugandan portion (eastern flank). This asymmetric morphology confirms the basin's classification as a half-graben system.

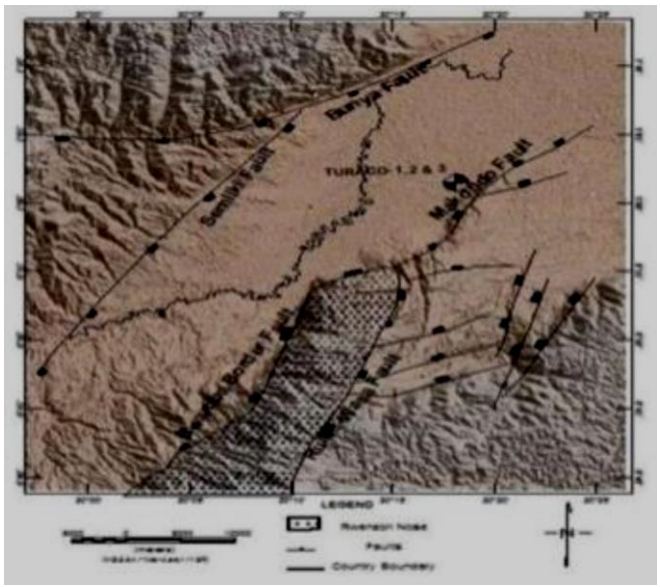

Figure1.7: Physiography map of Semliki area showing the major faults oriented mostly in NE-SW direction (Source: Semanticscholars.org and Lukaye et al 2016)

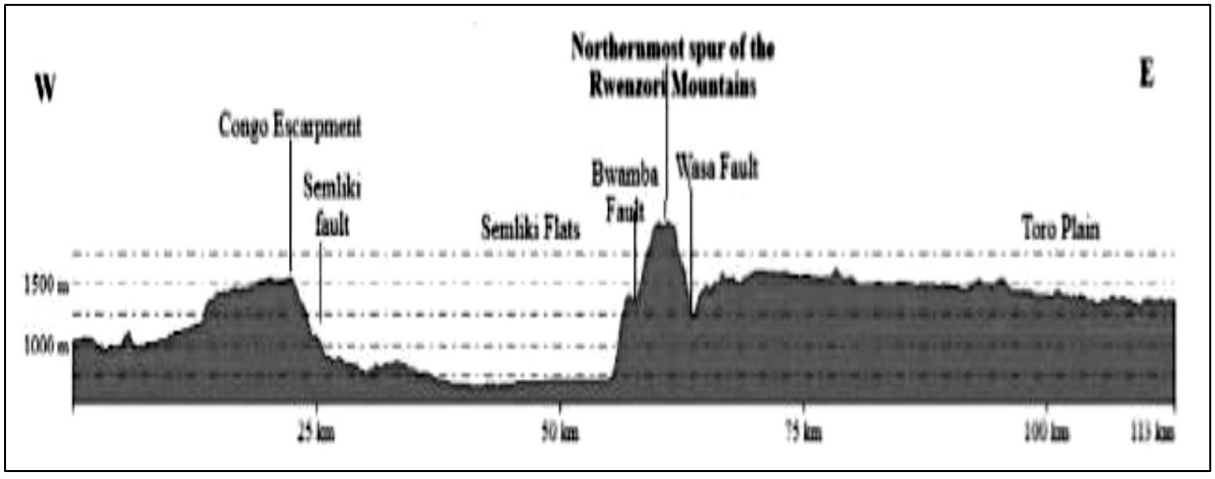

Figure1. 8: Cross section of the topography of Semliki Basin (Source: PEPD, 1995)

CHAPTER TWO: MATERIALS AND METHODS

2.0 Introduction

This chapter details the field techniques employed to achieve multiple objectives, including measuring bedding thickness, analyzing structural trends, and determining grain size distribution. It outlines various approaches for facies interpretation and data processing.

The chapter also documents the field investigation of Sempaya Hot Springs within the Albertine Graben, focusing on thermal influences on hydrocarbon generation. Additionally, it describes the geophysical equipment, methods, and protocols utilized during the study, all of which were provided by the department to each research team.

2.1 Equipment and Materials

Table 1: Equipments and materials used in the field

Material/Equipment	**Purpose**
GPS	For locating ourselves on the base map, and determining the elevation of the different stations visited
Geological Compass	To measure structure trends like dip and strikes of the various structure. For base map orientation since it gives the compass directions.
Jacob's staff	To measure vertical bedding-thickness during stratigraphic logging.
Base maps (topographic and geologic).	For locating and orienting ourselves in the field and show the type of geologic structural framework to expect in a given location.
Hand lens	To magnify the grain sizes of especially fine to very fine materials that cannot be readily distinguished by the naked eye.
Phones	To take pictures of outcrops and structures.
Tape measure	To measure bedding-thickness and extent of structures.
Shovel and hoe	For cleaning sediment surfaces so as to clearly view beds to be logged.
Geological Hammer	For breaking off samples of rocks from in situ rock outcrops especially in the basement
Wentworth grain scale	For gauging grain-sizes, shapes and the types of grain sorting while in the field
Field notebooks	For taking field notes, sketching structures and recording of structural readings taken.
Graph paper	For drawing sedimentological logs.
Well logs	For petrophysical analysis.

Backpack	To carry notebooks, pencils, pens, food, water bottle.

2.2 Methods.

2.2.1 Desk Study.

This stage involved outlining all field research tasks during project planning. At the camp, speakers presented the comprehensive strategy, proper methodologies, and implementation procedures through literature reviews. The team instructed us on field equipment usage, data collection techniques, recording methods, and data synthesis. We were divided into working groups and issued all necessary field supplies and tools. These preparations were completed the day after arriving at the research site.

2.2.2 Field Work Methods.

This component constituted the study's primary focus, occupying most of the fieldwork duration. Through comprehensive outcrop examination and station surveys, we: Documented lithologies and structural features, measured bedding thickness and structural orientations, conducted basement investigations, performed sedimentary logging and analyzed facies and depositional environments

These methods enabled paleocurrent determination and petroleum potential assessment, as detailed in subsequent sections. Field discussions and joint interpretations supplemented the data collection process.

2.2.2.1 Basement studies

The basement rocks along the Kichwamba Trading Center to Bundibugyo route consist predominantly of granitic gneiss and amphibolite, displaying visible joints, foliation, and structural discontinuities. Structural measurements were obtained using compass techniques to record strike and dip orientations of basement formations.

Our investigation documented the sedimentary units directly overlying the basement, analyzing their depositional processes and mechanisms. A detailed stratigraphic log was compiled, specifically capturing the unconformable contact between crystalline basement and unconsolidated sediments adjacent to Kibuku quarry.

Other techniques employed in these investigations include;

Mineral analysis

The technique was employed during basement investigations to mineralogically characterize rocks through visual inspection. Macroscopic minerals were identified by color and physical properties, while a hand lens aided observation of finer-grained components. This mineralogical analysis enabled accurate lithological classification and subsequent interpretation of depositional environments and formation processes.

- ✓ **Structural measurements**

This methodology was applied to both basement and sedimentary rock investigations. Structural orientations (strike, dip, plunge, and trend) were measured using geological compasses for in-situ outcrops. Bed thickness measurements were obtained using Jacob's staffs or tape measures, particularly in sedimentary sequences. All structural data collected during the study are presented in Appendices 1-3, with comprehensive interpretation provided in Chapter 5. The right-hand rule convention was consistently applied for recording strike and dip directions throughout the study. Measured structural features included: Joints (orientation and spacing), Bedding planes, Fault surfaces and Foliation planes.

- ✓ **Use of Geological Compass.**

To measure fracture strike, the compass (oriented face-up) was positioned flat on a clean fracture surface, ensuring its alignment with the horizontal plane. For dip determination, the compass was aligned vertically along the fracture surface, with its edge parallel to the plane. Measurements were then recorded directly from the compass dial.

Through systematic analysis of structural measurements and rock characteristics, we reconstructed the area's geological history and tectonic development. Notably, basement structures provided critical analogs for interpreting sedimentary deformation patterns.

2.2.2.2 Sediment study.

Vertical lithostratigraphic logging was conducted along the Kibuku roadcut section, progressing from basal to uppermost sediment layers. Detailed logs recorded: bed structures, sediment coloration, grain size parameters, sorting characteristics, lithologic classifications, granulometric distributions, and unit contact relationships. These comprehensive logs facilitated critical analysis and interpretation of the Semliki Basin's depositional history.

Logging procedure.

The systematic logging procedure involved:

- Outcrop preparation using hoes and shovels to clear vegetation and expose fresh rock surfaces.
- Vertical thickness measurement with tape measures or Jacob's staffs.
- Detailed layer documentation including grain size, sorting, and color characteristics.
- Utilization of erosional contacts as basal references for logs where basement wasn't visible.
- Facies identification and depositional environment interpretation.

The resulting logs characterized diverse sedimentary environments (lacustrine, fluvial, deltaic) and evaluated hydrocarbon potential by identifying source rocks, reservoirs, and seals.

Determination of grain size and shape.

Grain characteristics were evaluated at exposures using hand lenses to assess:
i. **Roundness**: Determined by comparing clast edges to standard categories (very angular to well-rounded), indicating transport duration through abrasion effects
ii. **Sorting**: Analyzed particle size distribution to interpret: transport energy levels, depositional rates, agent type (fluvial/aeolian/mass flow)
iii. **Cementation**: Identified interstitial mineral deposits binding grains, using the Wentworth Scale (Table 2) for precise size classification.

Table 2: Wentworth Grain size scale

Grain Diameter millimeters	microns	phi	Wentworth Size Class		
256		-8.0		Boulder	Gravel
64		-6.0		Cobble	
4.0	4000	-2.0		Pebble	
2.0	2000	-1.0		Granule	
1.41	1410	-0.5	vcU	Very coarse sand	Sand
1.0	1000	0.0	vcL		
.71	710	0.5	cU	Coarse sand	
0.5	500	1.0	cL		
0.35	350	1.5	mU	Medium sand	
0.25	250	2.0	mL		
0.177	177	2.5	fU	Fine sand	
0.125	125	3.0	fL		
0.088	88	3.5	vfU	Very fine sand	
0.0625	62.5	4.0	vfL		
0.002	2.0	9.0		Silt	Mud
				Clay	

Determination of paleocurrent flow direction.

Sedimentary structures within depositional layers preserve environmental conditions during formation, enabling paleocurrent reconstruction. Specifically, cross-bed foreset orientations (both tangential and angular types) in sandy strata were measured to determine flow directions. These foreset laminae form through downcurrent avalanche deposition, naturally aligning with paleoflow.

Field measurements involved: Identifying 3D-exposed cross-beds in outcrops, Recording foreset dip directions using geological compasses and Compiling data for rose diagram construction.

Interpretation of the depositional environment.

A depositional environment encompasses the physical, chemical, and biological processes governing sediment accumulation and subsequent lithification. The Semliki Basin primarily contains fluvial and lacustrine deposits, including sandstones, basal conglomerates, clays, and silts. These deposits' characteristics reflect controlling factors such as climate, hydrology, sediment supply, basin morphology, and tectonic setting (Selley, 1978).

Key environmental indicators include: Lacustrine evidence: Freshwater bivalve and oyster fossils in Makondo area (201157, 110303), Fluvial systems: Kisegi Formation's meandering channels, alluvial fans, and floodplain deposits and Semi-arid conditions: Gypsum precipitates in Kibuku roadcut joints and sediment layers

The Turaco-3 well's 300m section reveals low-energy fluvial channels in a stable tectonic setting. Provenance analysis through textural maturity (e.g., well-rounded quartzite cobbles) indicates strong paleocurrents, while thick clay layers and evaporites suggest intermittent lacustrine conditions.

Facies Analysis and Interpretation.

Facies analysis serves to distinguish rock units within continuous geological formations based on physical, chemical, and biological characteristics, with field investigations conducted through detailed sedimentary logging of outcrops, where facies were classified according to diagnostic features including sediment coloration, granulometry, sedimentary structures,

vertical grading patterns, and paleontological content, enabling the identification of distinct depositional environments and processes within the stratigraphic sequence.

Field discussions and presentations.

Following stratigraphic logging, each student group presented and analyzed their results to the class and instructors, engaging in discussion and addressing questions as they arose during the session.

Visit to the Sempaya hot springs.

Located within Uganda's Semliki National Park (220km²), the Sempaya hot springs occupy the Buranga geothermal field, bordered by the Semliki flats, Rwenzori Mountains, and DRC. This biodiverse park hosts 460 species, including 9 primate varieties. Local folklore names the gender-differentiated springs: Nyansimbi (male) and Bamaga (female), believed to be a vanished couple.

The springs' extreme temperatures (98-103°C) result from: Low elevation (670-760m), Proximity to the deep-seated Bwamba fault (~11km depth) and Geothermal heating of meteoric water percolating through porous sediments.

Hydrothermal processes dissolve sulfur, radium, and carbonates as water circulates through fault zones. The female spring features: 60×40m area with steam jets, H_2S/CO_2 emissions, 98.4°C water, 1m travertine cone.

The male spring comprises: 30m diameter pool, Sulfurous emissions, 86°C water (5m depth), Carbonate deposits.

Figure 2. 1: Sempaya Hot Spring (Female)

Temperature Effect on Hydrocarbon Occurrence in the rift.

As one of the world's youngest rift basins, the Albertine Graben exhibits exceptional geothermal gradients, evidenced by record temperatures of 106°C (male springs) and 103°C (female springs) that significantly exceed the oil window's lower threshold (60-120°C). These elevated temperatures create dual effects: they beneficially accelerate hydrocarbon generation by thermally transforming organic matter into kerogen and subsequent petroleum, yet simultaneously risk thermal cracking that converts oil into thermogenic gases like methane through excessive "overcooking" of source rocks.

Geothermal Potential of the Study Area.

Geothermal energy generation requires a complete system analogous to petroleum systems, comprising: a heat source (localized plume), reservoir rocks (equivalent to petroleum reservoirs), impermeable seals (preventing heat dissipation), and fluid migration pathways (functioning as plumbing systems). The presence of hot springs confirms geothermal potential by demonstrating an active heat source and functional fluid conduits, while regional sandstones and clays naturally serve as effective reservoirs and cap rocks respectively for energy production.

Makondo and Turaco field study.

Located in Semliki National Park (201070/110311), the Makondo fault's NE-SW trending flower structure was identified through geophysical surveys, including Kenting Earth Sciences' 1983 airborne study and subsequent 1998 seismic investigations. Petroleum exploration focused on the fault's hanging wall, where the Turaco wells (199697, 114170) were drilled in 2001 targeting the Kisegi Formation. While Turaco-1 reached 2400m (short of its 2500m target due to equipment failure) and Turaco-2 failed, Turaco-3 achieved 2900m depth but encountered CO_2-contaminated natural gas, leading to site abandonment. The CO_2 origin remains debated, potentially from either regional volcanism or hydrocarbon overcooking.

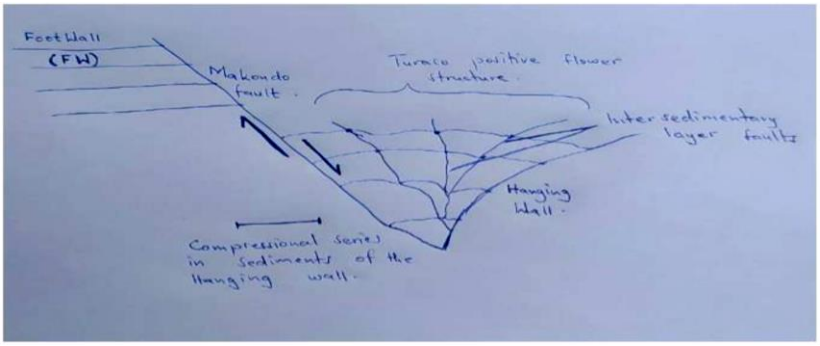

Figure 2. 2: Positive flower structure at Turaco

2.2.3 Post-field Methods.

Field data analysis.

Multiple analytical approaches were employed to enhance interpretation of geological and geophysical field data. Structural measurements (dip/strike) were processed using Stereonet software to generate stereographic projections. Stratigraphic logs were digitally reconstructed through Sedlog, while Oasis Montaj (Geosoft) facilitated gravity and magnetic anomaly mapping for subsurface evaluation.

Seismic interpretation focused on horizon tracking to identify structural discontinuities, including fault systems and roll-over anticlines. These methodologies collectively enabled comprehensive characterization of subsurface features.

Field report write-up.

This comprehensive report synthesizes all field data collected during the project, representing the culmination of rigorous research, analytical processing, literature review, and data interpretation. Organized into six systematic chapters - Introduction, Materials and Methods, Lithology and Stratigraphy, Basin and Facies Analysis, Structural Geology, Geophysics, followed by Discussions, Conclusions and Recommendations - it provides a complete documentation of the study's findings and methodologies.

CHAPTER THREE: LITHOLOGY AND STRATIGRAPHY

3.1. Basement Lithology.

3.1.1 Granitic Gneiss.

The granitic gneiss outcrop near Kichwamba Technical College (186918/79296) displays banded metamorphic rock with white, grey, pink, and black coloration, weathered to brown hues, containing quartz, feldspars, muscovite, biotite, and albite, exhibiting intense fracturing, foliation, and quartz-filled joints from hydrothermal activity, while a similar but more altered schistose variety occurs at Kibuku Quarry (192392/101800, 668m elevation) with prominent NE-SW joints and quartz veins; as a basement rock, its extensive fracturing offers potential hydrocarbon migration pathways, but compartmentalization by thick vertical clay layers—formed from joint shearing and sediment infill—limits reservoir viability, with any hydrocarbons likely being water-washed or biodegraded, yielding heavy, uneconomical oil, and quarry challenges include unstable hanging blocks from poor excavation, requiring dip-directional top-to-bottom mining, gabion stabilization, and post-extraction revegetation for safety and environmental protection.

Figure 3.1 Figure showing granitic gneiss (Location 190859E/94333N, 1037m)

3.1.3 Granites.

The granite exhibits a massive structure with pink to gray coloration, displaying weathered surfaces in brown to gray hues. This medium- to coarse-grained rock consists primarily of K-feldspars, quartz, biotite, and muscovite. Most mineral components show alteration features resulting from active faulting processes in the region margins (faster cooling causing higher friction) and core. Observed amphibolite displays dark-green, black, and brown coloration, composed predominantly of amphiboles (>90%) with subordinate plagioclase, pyroxenes, and minor biotite and quartz (<10%).

3.2 Lithology and stratigraphy of the Sediments.

3.2.1 Conglomerates.

Conglomerate is a clastic sedimentary rock containing a significant proportion of rounded to sub-angular gravel-sized clasts (>2mm diameter). In the Semliki Basin, these conglomerates occur as both polymictic and monomictic varieties with matrix-supported and clast-supported fabrics, composed of sub-angular pebbles and cobbles of varying sizes and colors. The clasts primarily consist of quartzite and granite gneiss fragments.

A representative polymictic conglomerate outcrop in the Kisegi Formation (location 192678/101935, elevation 705m) contains angular to sub-angular quartz pebbles and cobbles in a clast-supported fabric (Figure 3.2). The clast composition suggests derivation from Rwenzori Mountain basement rocks, while their sub-angular shape indicates limited transport distance from source, resulting in minimal textural modification.

The poor sorting of these conglomerates reflects deposition from high-energy sediment-laden flows that experienced sudden energy loss, characteristic of alluvial fan environments where sediments rapidly accumulate following transport from elevated source areas.

Figure. 3.2. A polymatic Conglomerate made up of angular to sub-angular pebbles found at the contact between sediments and basement (Location 192596E/102090N, 705m)

3.2.2 Sands.

The Semliki Basin's sands range from fine to coarse-grained, with colors (grey-white to iron-stained red-brown) reflecting mineralogy and oxidation. They occur in cyclic, 18-120cm thick layers, showing fluvial (fining-upward) and deltaic (coarsening-upward) deposition. Coarsening-upward sands offer optimal reservoir potential due to high porosity in upper sections, though gypsum cementation and clay interbeds cause compartmentalization, reducing permeability. Cross-bedding and planar structures dominate, with clay layers acting as seals. Lacustrine blocky sands show poorer reservoir quality compared to deltaic sequences.

Figure 3.3 *Sand layers encountered along Kibuku Road Cut. (Location 192934E/101697N, 760m)*

3.2.3 Clays.

Clays in the Semliki Basin occur as fine-grained sediments displaying grey, yellow, and reddish-brown coloration, with the latter hue indicating iron (III) oxide content. These deposits typically form thin layers (5-10 cm) interbedded between thicker sand units (Figure 3.4), though Group F documented exceptional 210 cm thick clay beds in the Kasande Formation. The ubiquitous presence of gypsum and iron oxides collectively suggests deposition under semi-arid conditions. Clay deposition occurred primarily during: Marine transgressions (low-energy conditions), flood events (overbank deposition) and periods of water column stratification

Most clay layers show discontinuous, pinch-out geometries. Sedimentary structures include laminations, faults, and desiccation cracks, along with gypsum sheets formed by precipitation from calcium sulfate-rich brines. Petroleum potential; clays serve dual roles as both source rocks (organic matter content) and effective cap rocks (impermeable nature).

Figure 3.4. Clay layers cemented by Gypsum along the Kibuku Road cut.(Location 192957E/101760,749m)

3.2.4 Silts.

The Semliki Basin's silt deposits consist of fine-grained clay minerals, feldspars, and quartz, forming thin, continuous layers in grey, white, yellow, or reddish-brown hues. Their well-sorted texture indicates low-energy depositional environments.

3.2.5 Evaporites.

Gypsum ($CaSO_4 \cdot 2H_2O$) serves as the predominant evaporite mineral within the basin's sedimentary sequence (Figure 3.5), forming under favorable paleoclimatic conditions that promoted intense evaporation. These white-to-colorless, brittle crystalline flakes function as a primary cementing agent alongside iron oxides in the Kibuku roadcut sediments. Their presence provides definitive evidence of semi-arid depositional environments characterized by periodic water scarcity and high evaporation rates.

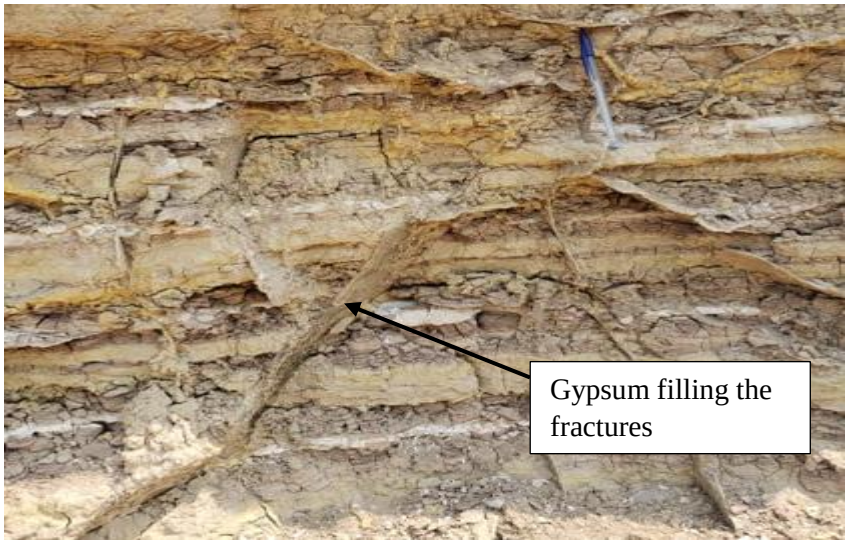

Figure 3.5. showing Gypsum filling the fractures in clay layers (Location 192961E/101768N, 745m)

3.2.6 Travertine.

Travertine represents a chemically-precipitated sedimentary rock formed through the decomposition and transport of dissolved minerals, followed by evaporative deposition. At Sempaya hot springs, this process occurs as calcium-rich groundwater, containing dissolved calcium and bicarbonate ions, precipitates calcite upon reaching the surface, forming distinctive limestone deposits through inorganic chemical processes.

3.3 Contact between basement and sediments.

The sediment-basement contact in the study area occurs at coordinates 192596/102090 (elevation 705m), marked by a distinct conglomerate layer with matrix-supported fabric composed of angular to sub-angular pebbles (indicating short transport distance) within a sandy matrix (Figure 3.6). The basement consists of granitic gneiss overlain by polymictic conglomerates and both consolidated (gypsum and iron (III) oxide-cemented) and unconsolidated sands. The sequence displays cross-stratification and features a basal, poorly-sorted, clast-supported conglomerate containing subangular cobbles, pebbles, and coarse sands.

Three fluvial depositional cycles are evident, showing progressive upward fining with smaller pebbles in upper conglomerates compared to the basal contact layer, suggesting decreased flow energy during later depositional phases. These cyclic deposits likely resulted from river rejuvenation events triggered by: Climatic changes (increased precipitation) and Tectonic uplift (enhancing source-to-basin gradient). Both mechanisms would increase flow velocity and transport capacity, enabling deposition of coarser sediments during active phases.

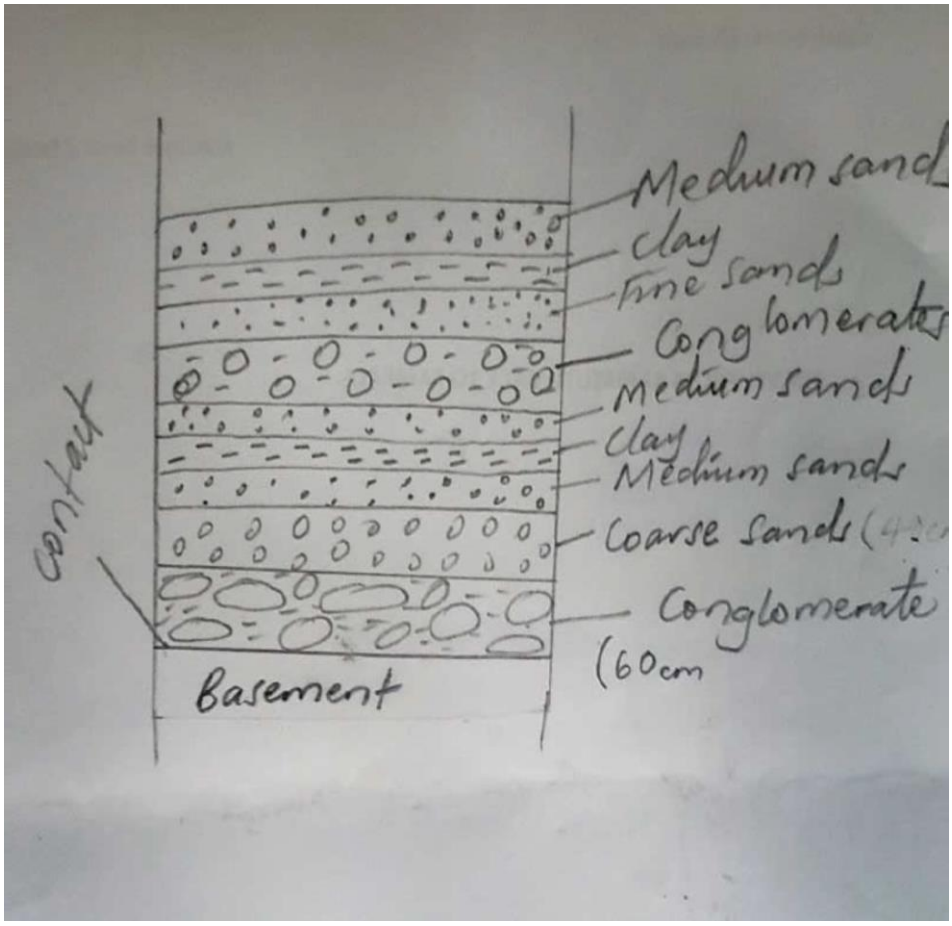

Figure 3.6 A sketch of contact between sediments and basement in Semliki basin.

CHAPTER FOUR: STRUCTURES

4.1 Primary structures

4.1.1 Bedding.

Within the study area, three principal bed types were identified: Planar bedding which are characterized by flat, parallel bedding surfaces indicating near-horizontal deposition, Massive beds which lack internal structures and Cross-bedding that features internal layers that dip at significant angles relative to the bounding surfaces of the cross-bed sets

The study area's **planar stratified beds** display thicknesses ranging from centimeters to meters, with distinct color variations (white/yellow) and parallel boundaries. These beds show a NE-SW strike, aligning with regional structural trends. Their extensive lateral continuity suggests deposition under weak currents in fine-grained environments, consistent with the Albertine Rift's tectonic setting. **Graded bedding** is prevalent in sandy units, featuring both normal (upward-fining) and reverse (upward-coarsening) sequences. These patterns indicate deposition from waning turbidity currents, reflecting fluctuating energy conditions during sediment accumulation in the basin.

Field observations reveal **tabular (angular) cross-beds** with sharp, high-angle terminations, indicating deposition by moderate- to high-energy currents transporting medium-coarse sand.

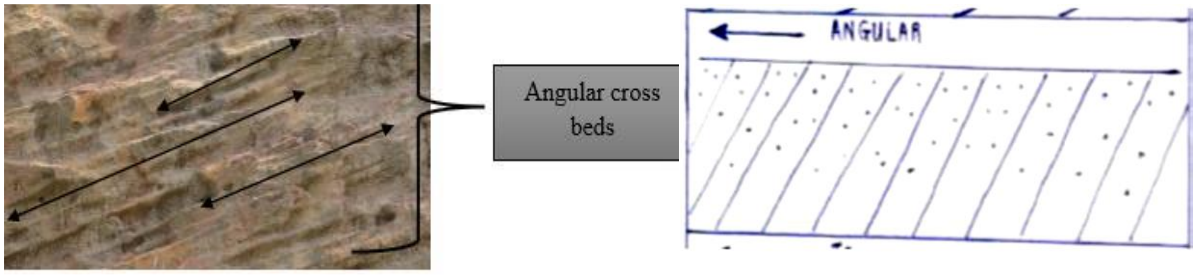

Figure 4.1 Angular cross beds(L) and Sketch of the Angular crossbeds(R)

Tangential cross-beds, characterized by asymptotic lower contacts, form from large-scale ripple migration in moderate flows. They occur in medium-coarse sands, with 5–15 cm thick foresets dipping SE.

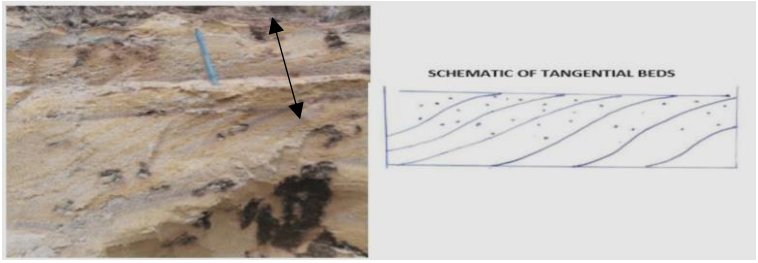

Figure 4.2 A photograph showing tangential cross beds

Stereographic analysis of beds measured in area F.

These beds show NE-SW orientation, with stereographic analysis confirming steep NE-dipping planes. The rose diagram's NE-SW trend suggests paleocurrents flowed northeastward, aligning with initial rift-related drainage patterns.
The bedding measurements used for stereographic analysis are in appendix 1.

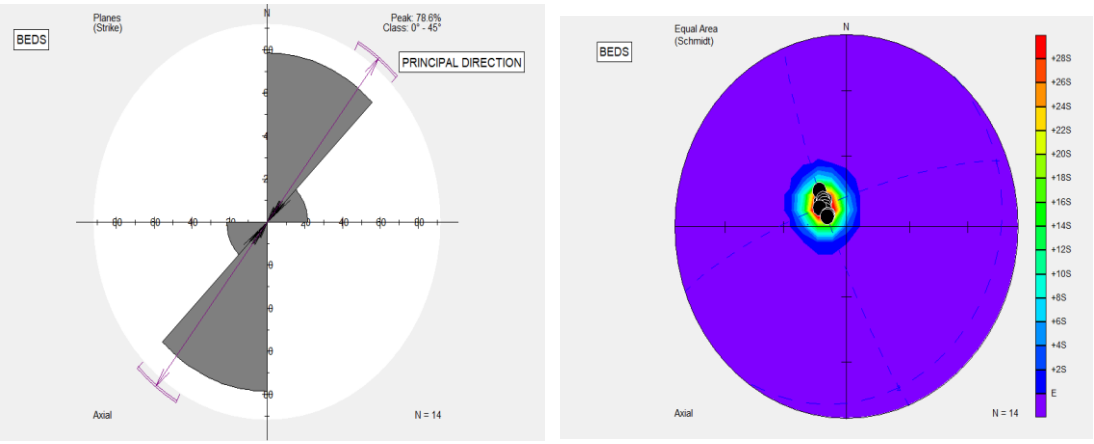

Figure 4.3. Showing the Rose Diagram(L) and Density Diagram(R) of beds measured in area F.

Trough cross-beds display curved, erosive bases and tangential foresets, formed by migrating 3D dunes under strong currents. Limited to cm-scale thickness in the study area, they lack lateral continuity. Paleocurrent interpretation is challenging due to complex geometry, though local NE-SW dips suggest rift-aligned flow.

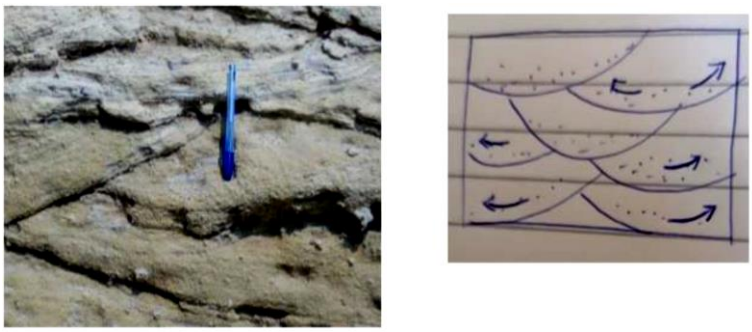

Figure 4.4 A photograph showing trough beds(L) and its sketch(R).

Herringbone cross-stratification exhibits bimodal foreset dips, reflecting bidirectional tidal currents in shallow lacustrine environments. Field observations show alternating NE and SW dips, recording flood-ebb flow reversals. The structure confirms tidal influence, with trends aligning with regional NE-SW rift orientation.

Figure 4.5. A photograph showing Herringbone Croos-stratification(L) and its sketch(L).

4.1.2. Laminations.

The study area's laminations occur as parallel or intersecting layers in clay and silt deposits, indicating low-energy deposition in deep lacustrine environments. Their delicate, undisturbed nature suggests stable conditions with periodic sediment influx. These fine-scale features align with regional lacustrine sedimentation patterns in the Albertine Rift basin.

Figure 4.6. A photograph showing laminations along the Kibuku Road cut(Location 192960E/101767N, 744m)

4.1.3. Mud cracks.

Field observations revealed polygonal mud cracks in clay-rich sediments, formed by subaerial desiccation of waterlogged deposits, with characteristic upward-curling edges serving as geopetal indicators. These features confirm periodic lake-level fluctuations in the study area, where submerged sediments underwent repeated exposure and drying, reflecting alternating wet and arid phases in the depositional environment.

Figure 4.7. A photograph showing Mud cracks of Kisengi River Channel(Location 192393E/102917N, 674m)

4.1.4. Fossils (body fossils).

The presence of carbonate fossils, including bivalves (Figure 5.19), gastropods, and oysters within the Makondo formation, provides clear evidence of freshwater depositional environments in the Semliki Basin. These bioclasts specifically indicate lacustrine or fluvial

paleoenvironments, as such organisms typically inhabit shallow freshwater systems. The fossil assemblage serves as reliable palaeoecological indicators, confirming the existence of aquatic conditions suitable for supporting these freshwater faunae during the depositional period.

Figure 4.8. A bivalve shell found at Makondo area.(Location 201158E/109998N, 702m)

4.1.5 Unconformity.

The study area contains two unconformity types: non-conformities (sedimentary rocks overlying eroded basement, marked by basal conglomerates) and disconformities (erosional gaps between parallel strata). These contacts reveal significant depositional hiatuses, recording periods of erosion or non-deposition in the basin's geologic history.

4.2 Secondary Structures.

Secondary structures develop in response to tectonic stresses induced by plate movements. In the study area, these tectonic features predominantly resulted from basement rock deformation that propagated upward into overlying sediments. Consequently, the secondary structures observed in sedimentary layers likely mirror those present in the underlying basement rocks of the basin. The sediment-hosted secondary structures identified include:

4.2.1. Faults.

Both basement and sedimentary layers in the Semliki Basin exhibit NE-SW-oriented faults, aligning with the Albertine Rift's regional trend. In the basement, major dip-slip normal faults (e.g., Makondo, Semliki, Bunya, and Kichwamba faults) form graben structures under tensional forces, influencing topography and drainage. Sedimentary units display minor NE-SW normal and reverse faults with modest displacements (~4 cm), reflecting the same tectonic regime as basement structures. The consistent orientation indicates stress propagation from basement deformation into overlying sediments, linking both layers to a shared extensional tectonic activity. Faults in both domains are discontinuous, with basement faults larger and sedimentary faults smaller but structurally congruent.

Figure 4.9. Fault zone in the Semliki basin.

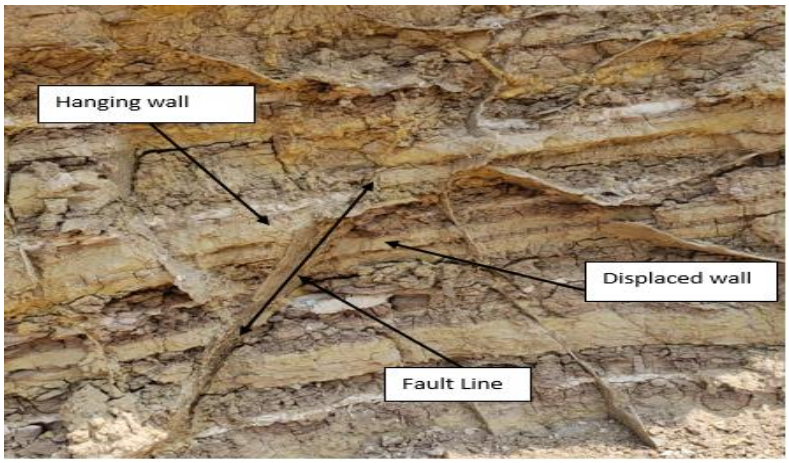

Figure 4.10. A minor fault in across the sedimentary layer along the Kibuku road cut.(Location 192961E/101767, 745)

4.2.2. Joints.

Both sedimentary and basement rocks in the Semliki Basin exhibit NE-SW-oriented joints, aligning with the Albertine Rift's regional trend. In sedimentary units, joints are gypsum- and iron-filled, confirming tectonic stress propagation from basement deformation. Basement rocks (e.g., near Kichwamba Technical College and Kibuku quarry) display dominant NE-SW and minor NW-SE joint sets, with the former matching the Kichwamba Fault trend. Average spacings are 15 cm (NE-SW) and 19 cm (NW-SE). The consistent NE-SW orientation across lithologies indicates a shared extensional stress regime, though basement joints are more systematic and widely spaced, while sedimentary joints are smaller and mineral-filled.

Figure 4.11. Joints at the Basement outcrop along the Kicwamba road cut.(Location 192452E/101453N, 689m)

Stereographic analysis of basement joints reveals two sets: a primary NE-SW trend (Set 1) and a secondary NW-SE trend (Set 2). The NE-SW joints, steeply dipping and clustered near the great circle's periphery, indicate NW-SE-directed compressional stress (σ_1), while the NW-SE set reflects NE-SW-directed forces. The contour diagram confirms this bimodal distribution, with σ_3 near the center suggesting strong compression. The rose diagram further validates two distinct deformation episodes, marked by intersecting joint orientations. These findings demonstrate that the basement rocks experienced multiple compressional stress regimes, aligning with the Albertine Rift's tectonic evolution. All the measurements used for stereographic analysis are in appendix 2.

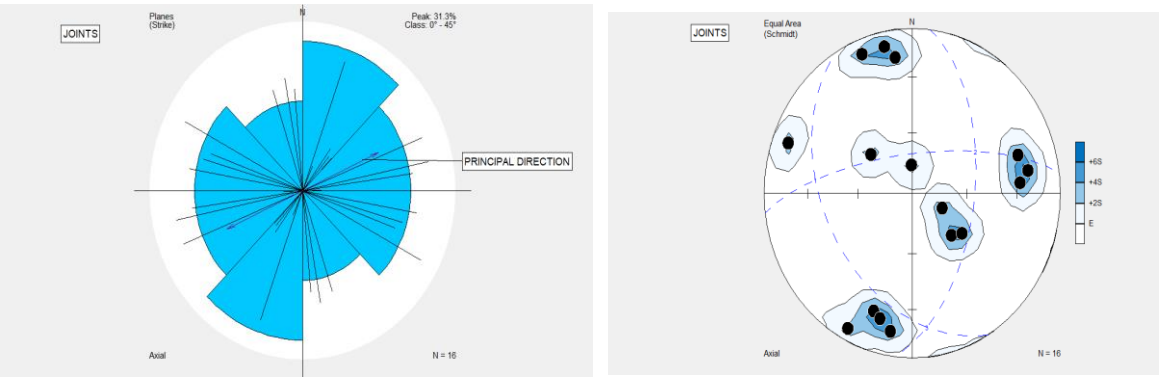

Figure 4.12. A rose diagram(L) and Density diagram(R) for joints of basement rocks.

4.2.3. Veins.

In sedimentary rocks, gypsum veins ($CaSO_4 \cdot 2H_2O$) appear as white to translucent deposits along bedding planes and joint surfaces (Figure 4.14). These veins formed under evaporative conditions, suggesting arid environments like ephemeral lakes or supratidal flats. Their cross-cutting relationships—penetrating sedimentary layers and filling interstitial spaces—confirm a post-depositional origin, where mineral-rich fluids precipitated during secondary mineralization. The presence of gypsum indicates periodic drying and sulfate-rich groundwater circulation, common in semi-arid to arid depositional settings.

In basement rocks, two vein types are observed: pink to white quartz veins (figure 4.13) and reddish-brown iron-rich veins. The quartz veins are larger (centimeters to meters in length) and form through hydrothermal fluid circulation, filling NE-SW-oriented fractures that align with regional joints. The iron-rich veins are shorter (centimeter-scale) and narrower, likely derived from iron oxide precipitation. Both vein types exploit pre-existing fractures, confirming post-formation mineralization. Their NE-SW trend matches the dominant structural orientation, linking them to the same tectonic stresses that shaped the Albertine Rift. The colors reflect mineral composition—quartz (pink-white) and iron oxides (reddish-brown).

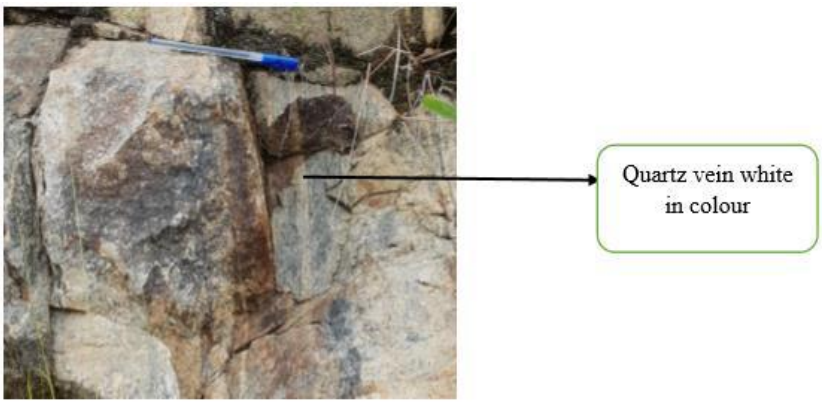

Figure 4.13. Quartz veins in the granitic gneiss At Kichwamba (Location 192492E/101899N, 678m)

Figure 4.14. Gypsum filled veins.(Location 192960E/101767N, 743m)

4.2.4. Flower Structures.

revious studies of seismic data from the Turaco area in the Albertine Graben have identified positive flower structures, where fault systems diverge upward. Detailed examination of these features shows that the region enclosed by the boundary faults exhibits anticlines, indicating their formation through transpressional tectonic activity. These anticlines present within the flower structures are significant, as they can serve as effective structural traps for hydrocarbon accumulation.

4.2.5 Banding.

This is reflected by the segregation of light-colored (felsic) and dark-colored (mafic) minerals in high-grade metamorphic rocks such as gneiss. In the research area, this banding feature is evident in granitic gneiss (found within the basement rocks) outcrops near Kichwamba Technical College, resulting from varying concentrations of different minerals within alternating layers.

4.2.6. Foliation.

Foliation in the study area's gneisses exhibits a dominant NE-SW trend, particularly near Kichwamba Technical College, reflecting alignment with regional faults and joints. This planar fabric developed perpendicular to maximum compressive stress during metamorphism, though

local shear zones show minor deviations. The consistent NE-SW orientation, with a secondary NW-SE component, indicates prolonged tectonic activity under a unified stress regime. Field measurements confirm foliation planes dip NW, mirroring the basin's structural framework.

Figure 4.15. *Foliated granitic gneiss at Kichwamba (Location 192392E/101814N, 669m)*

Stereographic analysis reinforces these observations, showing clustered poles in the SE quadrant corresponding to NW-dipping foliation. The Rose diagram's strong NE-SW peak aligns with major basement faults, while a weaker NW-SE signal suggests later deformation. Contour plots reveal a single density maximum, confirming uniform NW dips. Together, these data demonstrate foliation formed under persistent NW-directed stresses, recording the region's tectonic evolution. The minor NW-SE trend may represent reactivation during subsequent stress event. The measurements used for stereographic analysis of foliation are in appendix 3.

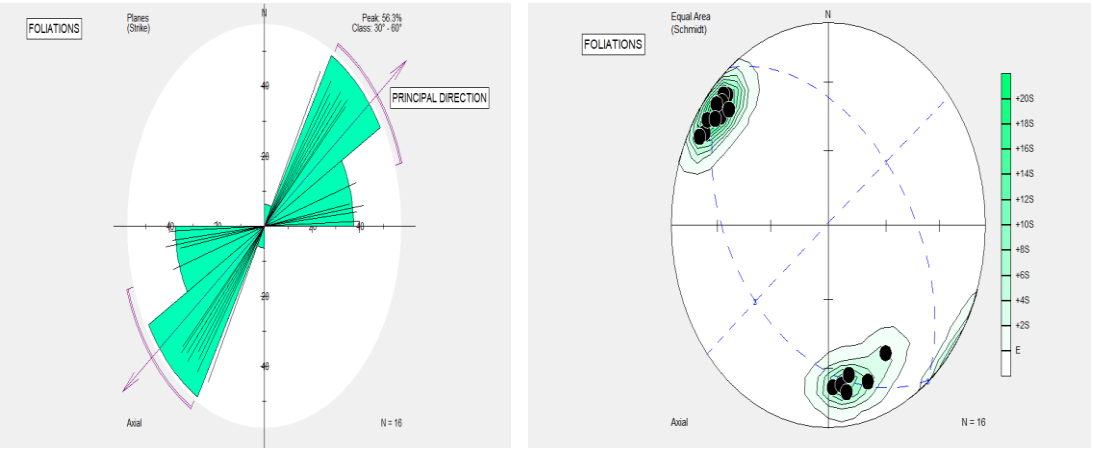

Figure 4.16. A rose diagram(L) and Density diagram(R) for foliation.

CHAPTER FIVE: BASIN AND FACIES ANALYSIS.

5.1 Integration of basin analysis concepts in interpretation of Semliki sedimentary basin.

Sedimentary basins form through tectonic subsidence, creating depressions that accumulate thick sediment packages. Analyzing sediment composition, stratigraphy, and structures reveals basin evolution, depositional processes, and provenance, enabling reconstruction of subsidence patterns and accommodation space development.

5.1.1. Formation and Evolution of Semliki basin.

The Semliki Basin represents a classic rift basin formed through crustal extension, characterized by an elongated depression bounded by normal faults that create half-graben geometry (Burke, 1985). This pull-apart basin developed in the central western arm of the Albertine Graben through trans-tensional deformation along pre-existing NE-SW trending faults during active rifting. The basin exhibits a complex three-phase syn-rift evolution (Figure 4.1): Mid-Late Miocene (Dominated by extensional faulting), Late Miocene-Early Pleistocene (Marked by transpression and rift shoulder uplift) and Early Pliocene-Recent (Continued transpression with fault reactivation)

These alternating extensional and transpressional regimes (combining compression and strike-slip) fundamentally controlled sediment provenance and basin topography through time. The basin's half-graben structure features a listric fault along one margin, typical of rift systems formed through crustal thinning. Sediment deposition generally accelerates subsidence. At the center of this graben, fine sediments and alluvial fan deposits are deposited while the shallower parts contain coarse sediments and this shallower section is where the Semliki Basin falls.

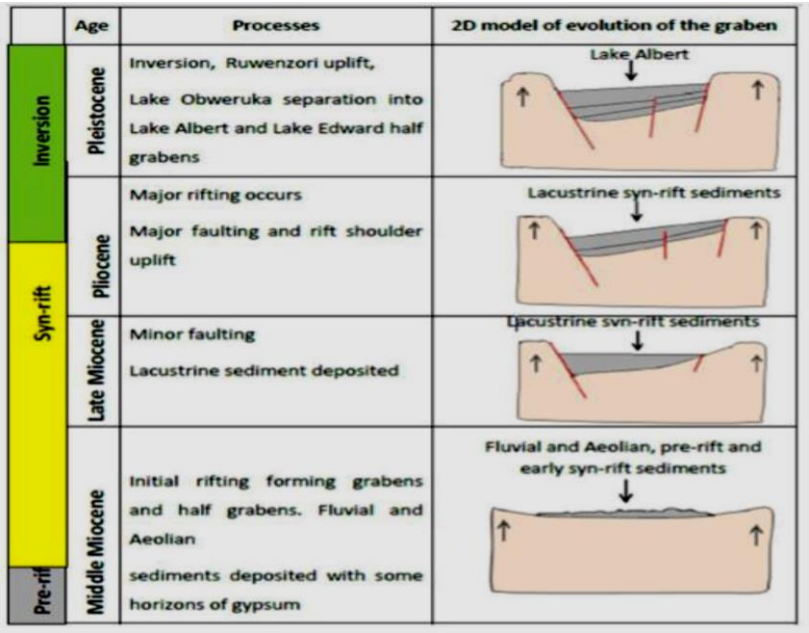

Figure 5.1. Stages of the evolution of the Semliki basin (modified after Pickford et al 1993; Van Damme and Pickford 2003; Ring 2008)

5.1.2. Basin Structure.

The Semliki Basin displays characteristic wedge-shaped geometry filled with fluvial, deltaic, and lacustrine deposits (Figure 5.2). Lithological and structural analyses reveal a depositional framework where reservoir units developed in shallow lacustrine/flexural margins and deep lacustrine environments as sub-lacustrine turbidites within claystone sequences

The stratigraphic succession begins with fluvial-deltaic sands and deep lacustrine turbidites directly overlying basement. Alluvial fan systems deposited up to 6 km of sediment that transition into deltaic sandstones (later fault-disrupted) and lacustrine formations. The basal section above the nonconformity consists predominantly of fluvial-deltaic sediments, overlain by lacustrine clays interbedded with fluvial-deltaic deposits. Facies distribution shows marked lateral discontinuity and strong contrasts, consistent with freshwater depositional systems where precipitation exceeds evaporation (Carroll & Bohacs, 2001). This facies assemblage reflects: Rapid lateral facies changes, distinct fluvial-lacustrine transitions and syn-rift tectonic controls on sedimentation.

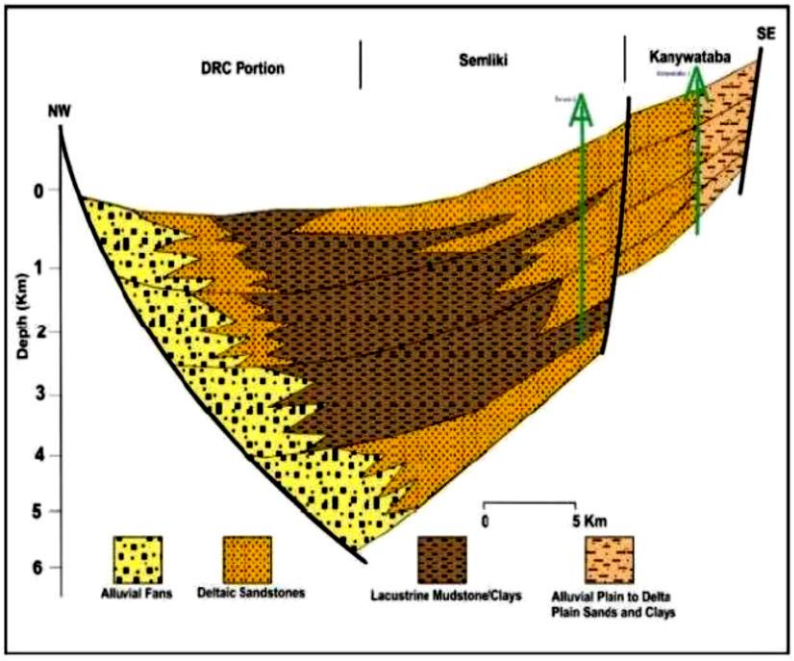

Figure 5.2The structure of the Semliki basin showing major sediment deposits and their location (Source: association (Carroll and Bohacs, 2001).

5.1.3. Stratigraphy of Semliki basin.

Based on stratigraphic relationships and bed succession analysis, Pickford et al. (1987, 1994) established a seven-fold formation scheme for the Semliki Basin sedimentary sequence (Figure 5.3), comprising in ascending order: Kisegi Formation, Kasande Formation, Kakara Formation, Oluka Formation, Nyaburogo Formation, Nyakabingo Formation and Nyabusosi Formation

This stratigraphic framework was developed through comprehensive examination of age relationships, lithological characteristics, and vertical stacking patterns observed throughout the basin.

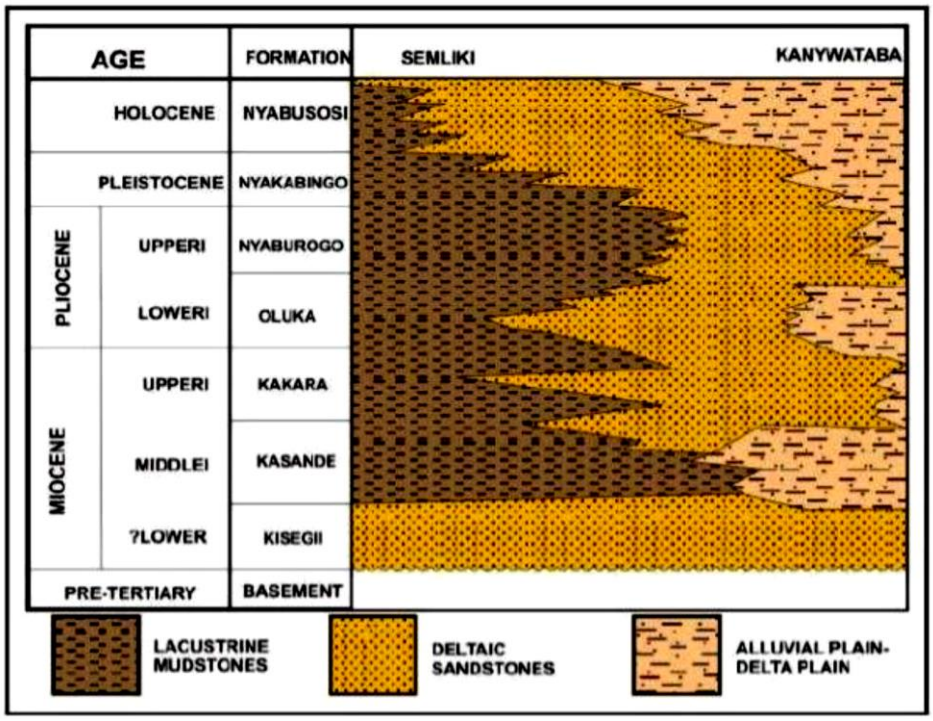

Figure 5.3. Arrangement of the Formations in the Semliki basin from the youngest (Nyabusosi) to the oldest (Kisegi)(Source: Pickford et al 1987 and 1994)

The **Kisegi Formation**, the basin's basal unit, unconformably overlies Precambrian basement with polymictic conglomerates, transitioning to yellow, well-sorted sandstones with gypsum veins and fluvial-deltaic-lacustrine deposits, evidenced by hydrocarbon seeps at Kibuku. The **Kasande Formation**, a source rock and seal, comprises dark brown mudstones, channelized sandstones, and coaly shales, transitioning from lacustrine to delta plain environments, with subsurface thicknesses up to 115m. The **Kakara Formation** consists of interbedded ferruginous sandstones, conglomerates, and claystones, deposited in coastal plain settings, reaching 542m in wells but thinning to 40m in outcrops. The **Oluka Formation** features black shales, ironstone layers, and tuff beds, with subsurface thicknesses >390m, interpreted as lacustrine to fluvial-deltaic deposits of Late Miocene age. The **Nyaburogo Formation** contains claystones, pisolitic ironstones, and fining-upward fluvial sandstones, indicating humid tropical conditions during the late Miocene-middle Pliocene. The **Nyakabingo Formation** comprises lacustrine shales, iron-stained siltstones, and coarsening-upward cycles, with ages debated between Late Pliocene (mollusks) and Late Miocene-Pleistocene (palynomorphs). The **Nyabusosi Formation** is divided into the Makondo (clays/silts), Behanga (ironstone-rich), and Kagusa (artifact-bearing) Members, reflecting coastal-lacustrine and floodplain deposition during the Pleistocene, with evidence of hominin activity. Collectively, these formations record fluvial, lacustrine, and deltaic sedimentation influenced by tectonic and climatic changes in the Semliki Basin.

5.2 Elements of facies analysis and facies analysis interpretation from observed lithologic units.

Facies represent distinct rock units characterized by unique combinations of lithological, physical, and biological attributes that differentiate them from adjacent strata. Facies analysis involves interpreting depositional environments through comprehensive examination of sedimentary features. Each depositional setting leaves distinctive imprints on sediments, creating varied facies associations.

These facies relationships critically influence hydrocarbon accumulation patterns. Specific lithological characteristics and facies distributions determine favorable exploration targets. Reservoir quality varies significantly across different facies types, with key differentiating factors including structural attributes, mineral composition, grain size distribution, sorting efficiency, and bed thickness.

The following section details the sedimentary facies observed along the Kibuku roadcut exposure in the study area:

5.2.1 Lithofacies.

Four principal lithofacies were identified during field investigations: sandstones, conglomerates, silts, and clays.

Sandstone Facies: The sandstone units display variable sorting (poor to well) and grain size (fine to coarse), with color variations including white, grey, yellow, pink, and brown. The brown coloration results from iron (III) oxide precipitation, indicating oxidative conditions, while associated gypsum suggests semi-arid paleoenvironmental conditions. These sandstones exhibit both angular and tangential bedding surfaces, predominantly dipping NW-SE, providing reliable paleocurrent indicators.

Clay Facies: Field observations revealed very fine-grained clays in brown, grey, and dark green hues. Clay beds range from continuous/persistent to discontinuous, with thickness varying from massive 2m units to thin centimeter-scale layers. The blocky, massive clay units within the Kasande Formation particularly signify low-energy lacustrine depositional settings.

Silt Facies: These very fine-grained deposits typically appear grey-white, with some yellow coloration from iron (III) oxide coatings. Characterized by good sorting and fine grain size, the silt beds generally form thin, continuous layers displaying minor cyclicity patterns.

Conglomerate Facies: Poorly sorted conglomerates dominate the sediment-basement contact zone, exhibiting matrix-supported fabrics with coarse sands, pebbles, and cobbles. Their predominant brown color derives from iron-rich mineral content. These deposits form the critical transition between basement rocks and overlying sediments.

5.2.2. Biofacies.

A biofacies represents a stratigraphic unit distinguished by distinctive fossil assemblages that differ from adjacent sections. The Semliki Basin's biofacies preserve both floral and faunal remains that reveal depositional contexts: the Makondo locality contains fish bones, bivalves, and white oyster shells indicating freshwater lacustrine environments, while the Kisegi river channel biofacies includes plant roots, fossil timber, gastropods, and snail shells, reflecting fluvial and marginal aquatic conditions. These fossil assemblages demonstrate the basin's varied paleoenvironments through diagnostic biological remains.

5.2.3. Summary of the depositional environments in the Semliki basin from facies analysis.

Fossil assemblages provide critical environmental indicators, as specific organisms inhabit particular depth ranges and ecological conditions. The basin exhibits three primary facies types: clay-dominated, fine-to-coarse sandy, and conglomeratic units. Fluvial systems are identified through fining-upward sequences (documented in Chapter 3 logs), Kisegi River point bar deposits, floodplain silts, cross-bedding structures, meander channels in Kisegi Formation coarse sands, and aquatic fossils like bivalves. Paleocurrent data derives from cross-beds and ripple marks, while sand-clay intercalations reflect fluctuating energy conditions - clays deposited during low-energy floods, coarser sands during high-energy flow periods.

Thick clay and blocky sand layers in Group F's study area indicate lacustrine conditions, with deltas likely forming transitional zones between fluvial and lacustrine environments. Coarsening-upward sequences in Kibuku roadcut exposures further support deltaic deposition. Semi-arid conditions are evidenced by red iron-oxidized sands and gypsum precipitates, the latter forming through intense evaporation. Organic-rich layers suggest periodic anoxic conditions. Collectively, these features demonstrate the Semliki Basin's fluvial-lacustrine-deltaic depositional systems.

5.2.4. Paleocurrent flow and paleocurrent analysis.

Paleocurrent indicators represent geological features, typically sedimentary structures, that enable reconstruction of ancient water flow directions - a crucial method for understanding past depositional environments (Prothero & Schwab, 1996). In this study, paleocurrent analysis

employed cross-stratification measurements, clast imbrication patterns, and parting lineation observations, collectively indicating a predominant NW-SE flow direction during sediment deposition. These directional data provide critical constraints for interpreting the basin's hydrodynamic conditions and sediment transport pathways in geologic history.

5.2.5. Hydrocarbon potential of Semliki Basin.

The Semliki Basin's elevated geothermal gradient, evidenced by active hot springs like Sempaya, presents both opportunities and challenges for hydrocarbon potential. While the high temperatures facilitate thermal maturation of organic matter in the Kasande Formation source rocks, pushing them into the oil window, there is significant risk of over-maturation if temperatures exceed optimal ranges. Excessive heat from these geothermal systems can lead to thermal cracking of hydrocarbons, converting valuable liquid petroleum into less economically favorable thermogenic gases. This over-maturation risk is particularly acute in deeper sections of the basin where temperatures may surpass the oil window's upper stability limits (typically 150-175°C). Furthermore, sustained high temperatures may accelerate diagenetic processes in reservoir rocks, promoting additional cementation that could reduce porosity and permeability in the Kisegi and Nyaburogo Formation sandstones. The thermal effects also extend to seal integrity, as clay-rich sealing units in the Kasande Formation may become more brittle under prolonged heat exposure, increasing susceptibility to fracturing and potential seal failure. This is evidenced by hydrocarbon seepages like the Kibuku oil seep, which may indicate localized thermal overpressuring and seal breaching. Additionally, the basin's extensive fault network, while providing migration pathways, may become more active under high thermal regimes, potentially disrupting trap configurations. The challenge lies in balancing the positive aspects of thermal maturation against these destructive processes - while the geothermal activity ensures source rock maturation, careful evaluation of thermal history and present-day temperature profiles is crucial to identify zones where optimal conditions persist for hydrocarbon preservation. Exploration strategies must therefore incorporate detailed thermal modeling to delineate areas where temperatures remain within the oil window without causing destructive over-maturation or adversely affecting reservoir and seal quality.

5.3 Sedimentary Logs and Interpretation.

5.3.1 Group F log.

The sedimentary log from Group F's Kibuku Road cut section reveals thick clay and blocky sand layers with minor silt deposits, suggesting a lacustrine depositional environment. The cyclical bedding reflects repetitive changes in energy levels, water depth, or tectonic activity, possibly due to seasonal fluctuations in lake levels, leading to alternating sand, clay, and silt deposition. Sand layers range from very fine to coarse, with fine grains dominating, typical of low-energy lacustrine settings. Most sands are yellow from iron (III) oxide coatings, while some are white; some layers are unconsolidated, whereas others are cemented by gypsum or iron minerals. These features indicate an oxidizing, semi-arid paleoenvironment. The clays contain dark brown organic material, making them potential source rocks, and their mud cracks suggest subaerial exposure, implying lake desiccation or level drops. Overlying the Kisegi

Formation (reservoir rocks) and underlying the Kakara Formation, these clays may also act as hydrocarbon seals for the underlying sands, aligning with the Kasande Formation's documented characteristics.

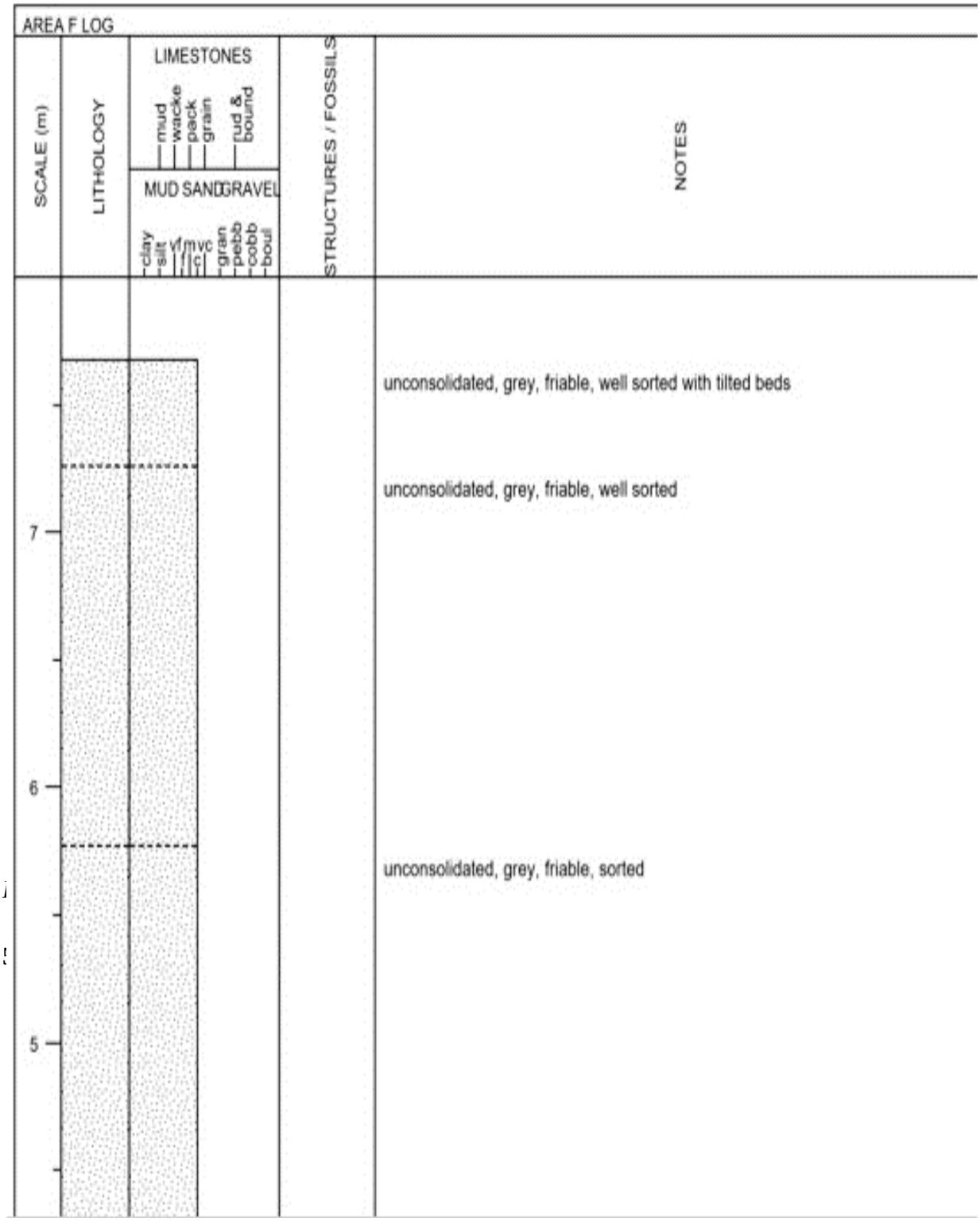

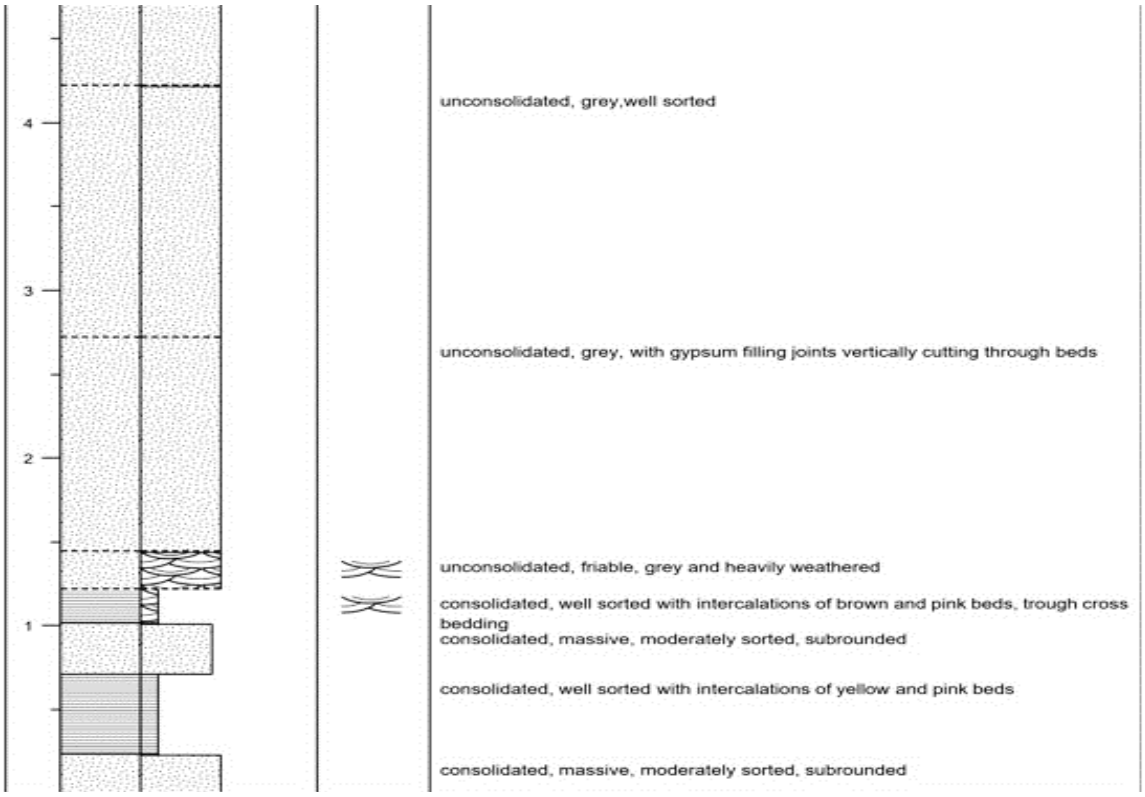

Figure 5.4. Log for Group F

5.3.2. Combined log

Figure 5.5 presents a composite sedimentary log of the Kibuku area, combining data from base, the section for Group A, to top which is the section of Group G. The base section displays fining-upward cycles, with cross-bedded sands (angular, planar, and trough stratification) interlayered with thin clay laminations, indicating a fluvial paleoenvironment. The cyclicity reflects fluctuating sediment supply and river rejuvenation, while smaller pebbles in upper conglomerates suggest declining flow energy. Southeast-dipping cross-beds imply a paleocurrent direction, and the sedimentology—point bar deposits (coarser channel sands) alongside floodplain fines—supports a meandering river system. Iron and gypsum cementation points to semi-arid conditions. The section in between the base and top transitions from a fining-upward (fluvial) to a coarsening-upward sequence, the latter typical of deltaic settings due to lake/ocean regression-transgression cycles. This shift suggests a fluvial-lacustrine transition zone, with yellow, iron- and gypsum-cemented sands and matrix-supported conglomerates. The upper section (discussed separately) is dominated by lacustrine clays and sands. The interbedded clays and finer sands likely represent floodplain or oxbow lake deposits, while coarser sands denote channel fills. Together, the log reveals dynamic depositional shifts—from high-energy fluvial systems to lower-energy lacustrine/deltaic environments, under semi-arid conditions, evidenced by recurring iron oxides and gypsum cementation.

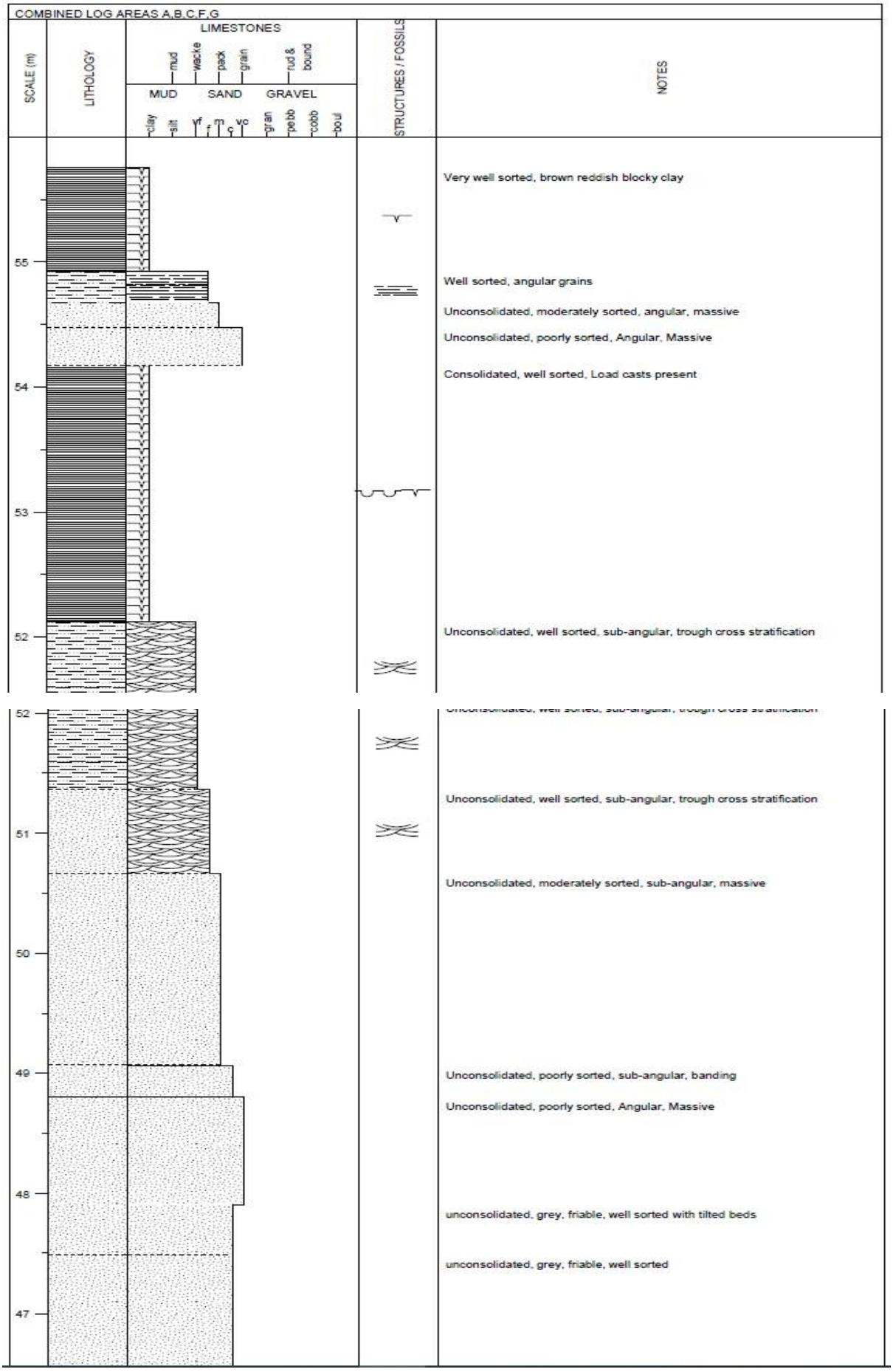
COMBINED LOG AREAS A,B,C,F,G
SCALE (m)
LITHOLOGY
LIMESTONES
mud
wacke
pack
grain
rud &
bound
MUD
SAND
GRAVEL
clay
silt
vf
f
m
c
vc
gran
pebb
cobb
boul
STRUCTURES / FOSSILS
NOTES
Very well sorted, brown reddish blocky clay
Well sorted, angular grains
Unconsolidated, moderately sorted, angular, massive
Unconsolidated, poorly sorted, Angular, Massive
Consolidated, well sorted, Load casts present
Unconsolidated, well sorted, sub-angular, trough cross stratification
Unconsolidated, well sorted, sub-angular, trough cross stratification
Unconsolidated, moderately sorted, sub-angular, massive
Unconsolidated, poorly sorted, sub-angular, banding
Unconsolidated, poorly sorted, Angular, Massive
unconsolidated, grey, friable, well sorted with tilted beds
unconsolidated, grey, friable, well sorted
55
54
53
52
52
51
50
49
48
47

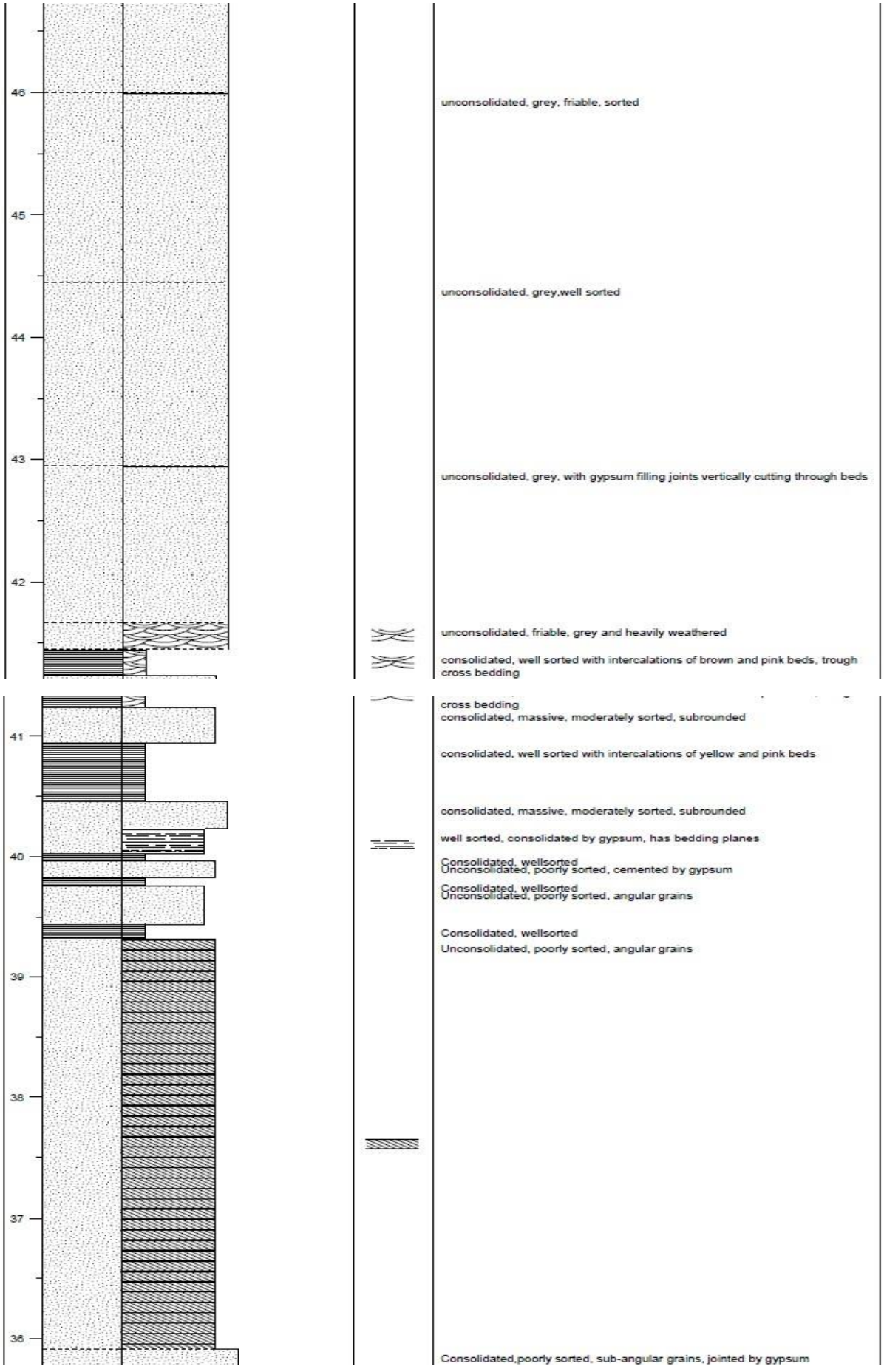
46
45
44
43
42
41
40
39
38
37
36
unconsolidated, grey, friable, sorted
unconsolidated, grey,well sorted
unconsolidated, grey, with gypsum filling joints vertically cutting through beds
unconsolidated, friable, grey and heavily weathered
consolidated, well sorted with intercalations of brown and pink beds, trough cross bedding
cross bedding
consolidated, massive, moderately sorted, subrounded
consolidated, well sorted with intercalations of yellow and pink beds
consolidated, massive, moderately sorted, subrounded
well sorted, consolidated by gypsum, has bedding planes
Consolidated, wellsorted
Unconsolidated, poorly sorted, cemented by gypsum
Consolidated, wellsorted
Unconsolidated, poorly sorted, angular grains
Consolidated, wellsorted
Unconsolidated, poorly sorted, angular grains
Consolidated,poorly sorted, sub-angular grains, jointed by gypsum

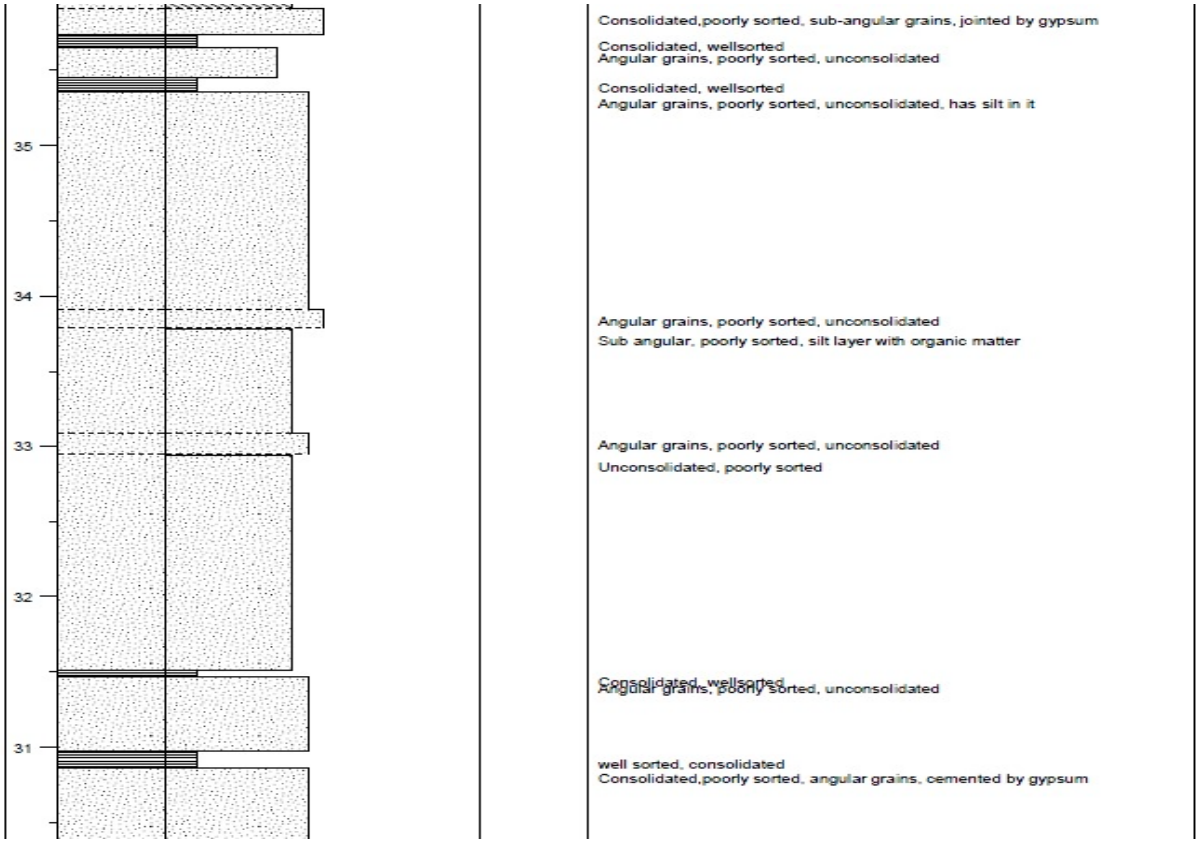
35
34
33
32
31
Consolidated,poorly sorted, sub-angular grains, jointed by gypsum
Consolidated, wellsorted
Angular grains, poorly sorted, unconsolidated
Consolidated, wellsorted
Angular grains, poorly sorted, unconsolidated, has silt in it
Angular grains, poorly sorted, unconsolidated
Sub angular, poorly sorted, silt layer with organic matter
Angular grains, poorly sorted, unconsolidated
Unconsolidated, poorly sorted
Consolidated, wellsorted
Angular grains, poorly sorted, unconsolidated
well sorted, consolidated
Consolidated,poorly sorted, angular grains, cemented by gypsum

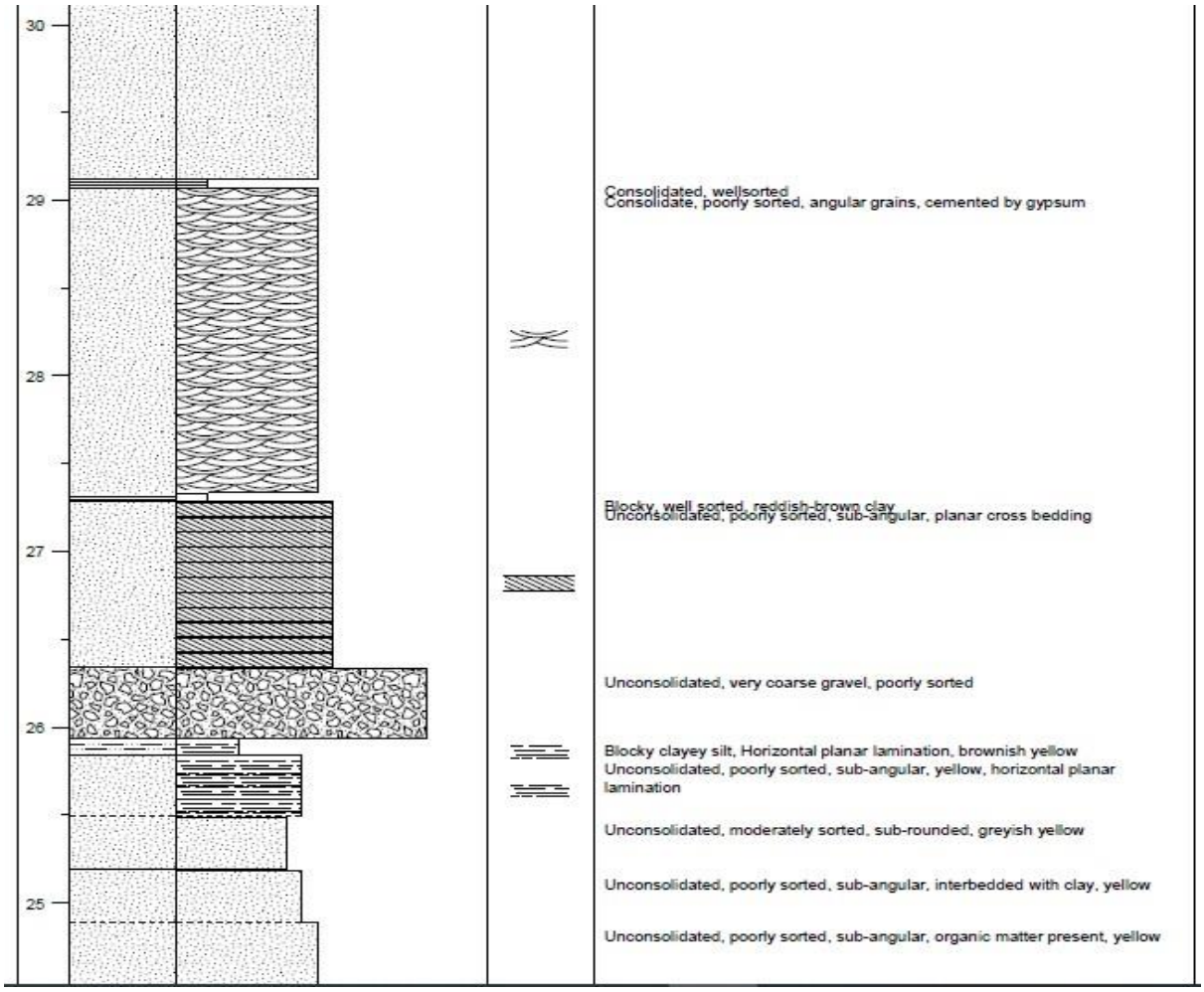
30
29
28
27
26
25
Consolidated, wellsorted
Consolidate, poorly sorted, angular grains, cemented by gypsum
Blocky, well sorted, reddish-brown clay
Unconsolidated, poorly sorted, sub-angular, planar cross bedding
Unconsolidated, very coarse gravel, poorly sorted
Blocky clayey silt, Horizontal planar lamination, brownish yellow
Unconsolidated, poorly sorted, sub-angular, yellow, horizontal planar lamination
Unconsolidated, moderately sorted, sub-rounded, greyish yellow
Unconsolidated, poorly sorted, sub-angular, interbedded with clay, yellow
Unconsolidated, poorly sorted, sub-angular, organic matter present, yellow

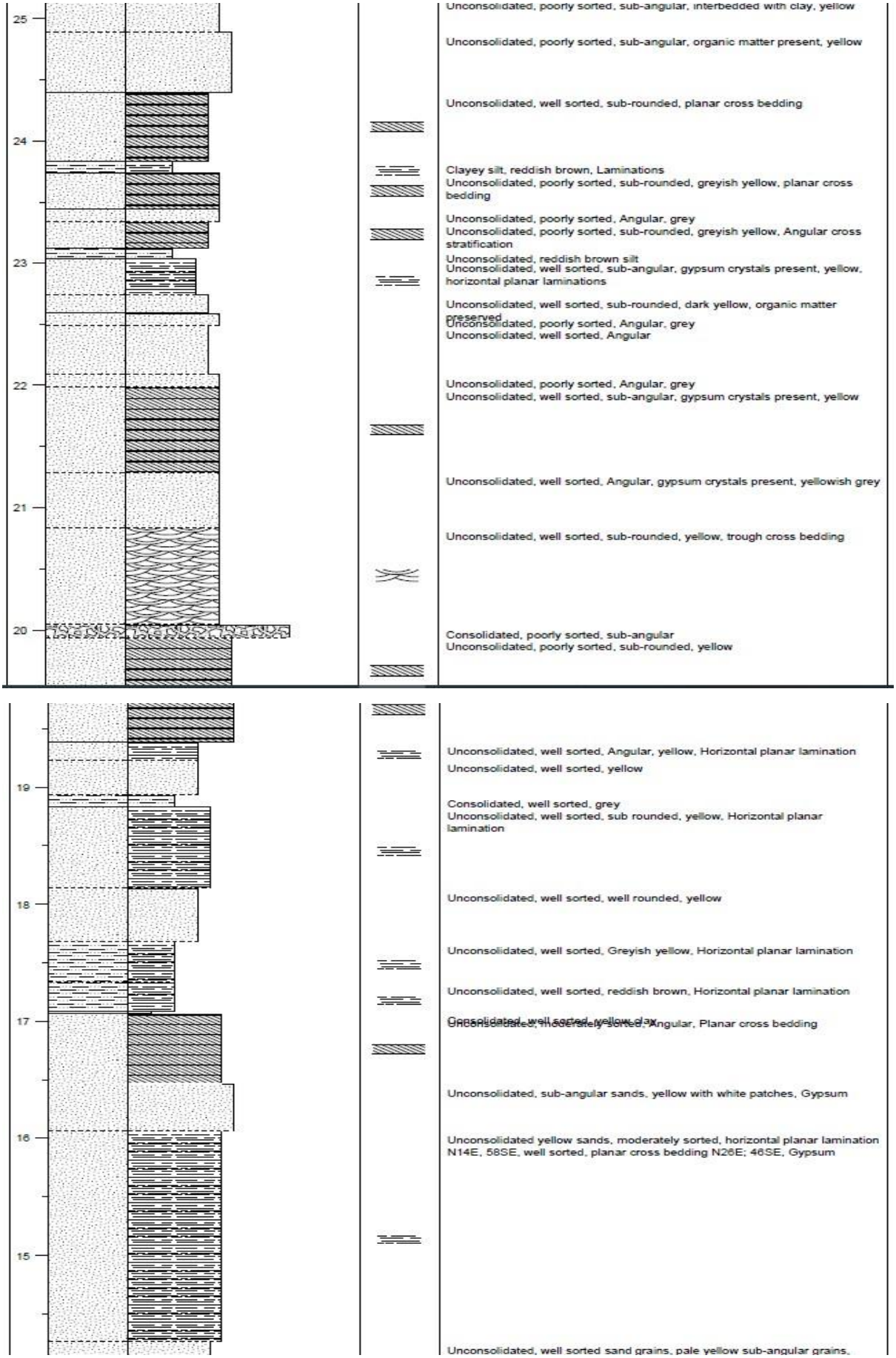
25
24
23
22
21
20
19
18
17
16
15
Unconsolidated, poorly sorted, sub-angular, interbedded with clay, yellow
Unconsolidated, poorly sorted, sub-angular, organic matter present, yellow
Unconsolidated, well sorted, sub-rounded, planar cross bedding
Clayey silt, reddish brown, Laminations
Unconsolidated, poorly sorted, sub-rounded, greyish yellow, planar cross bedding
Unconsolidated, poorly sorted, Angular, grey
Unconsolidated, poorly sorted, sub-rounded, greyish yellow, Angular cross stratification
Unconsolidated, reddish brown silt
Unconsolidated, well sorted, sub-angular, gypsum crystals present, yellow, horizontal planar laminations
Unconsolidated, well sorted, sub-rounded, dark yellow, organic matter preserved
Unconsolidated, poorly sorted, Angular, grey
Unconsolidated, well sorted, Angular
Unconsolidated, poorly sorted, Angular, grey
Unconsolidated, well sorted, sub-angular, gypsum crystals present, yellow
Unconsolidated, well sorted, Angular, gypsum crystals present, yellowish grey
Unconsolidated, well sorted, sub-rounded, yellow, trough cross bedding
Consolidated, poorly sorted, sub-angular
Unconsolidated, poorly sorted, sub-rounded, yellow
Unconsolidated, well sorted, Angular, yellow, Horizontal planar lamination
Unconsolidated, well sorted, yellow
Consolidated, well sorted, grey
Unconsolidated, well sorted, sub rounded, yellow, Horizontal planar lamination
Unconsolidated, well sorted, well rounded, yellow
Unconsolidated, well sorted, Greyish yellow, Horizontal planar lamination
Unconsolidated, well sorted, reddish brown, Horizontal planar lamination
Consolidated, well sorted, yellow clay
Unconsolidated, moderately sorted, Angular, Planar cross bedding
Unconsolidated, sub-angular sands, yellow with white patches, Gypsum
Unconsolidated yellow sands, moderately sorted, horizontal planar lamination N14E, 58SE, well sorted, planar cross bedding N26E; 46SE, Gypsum
Unconsolidated, well sorted sand grains, pale yellow sub-angular grains,

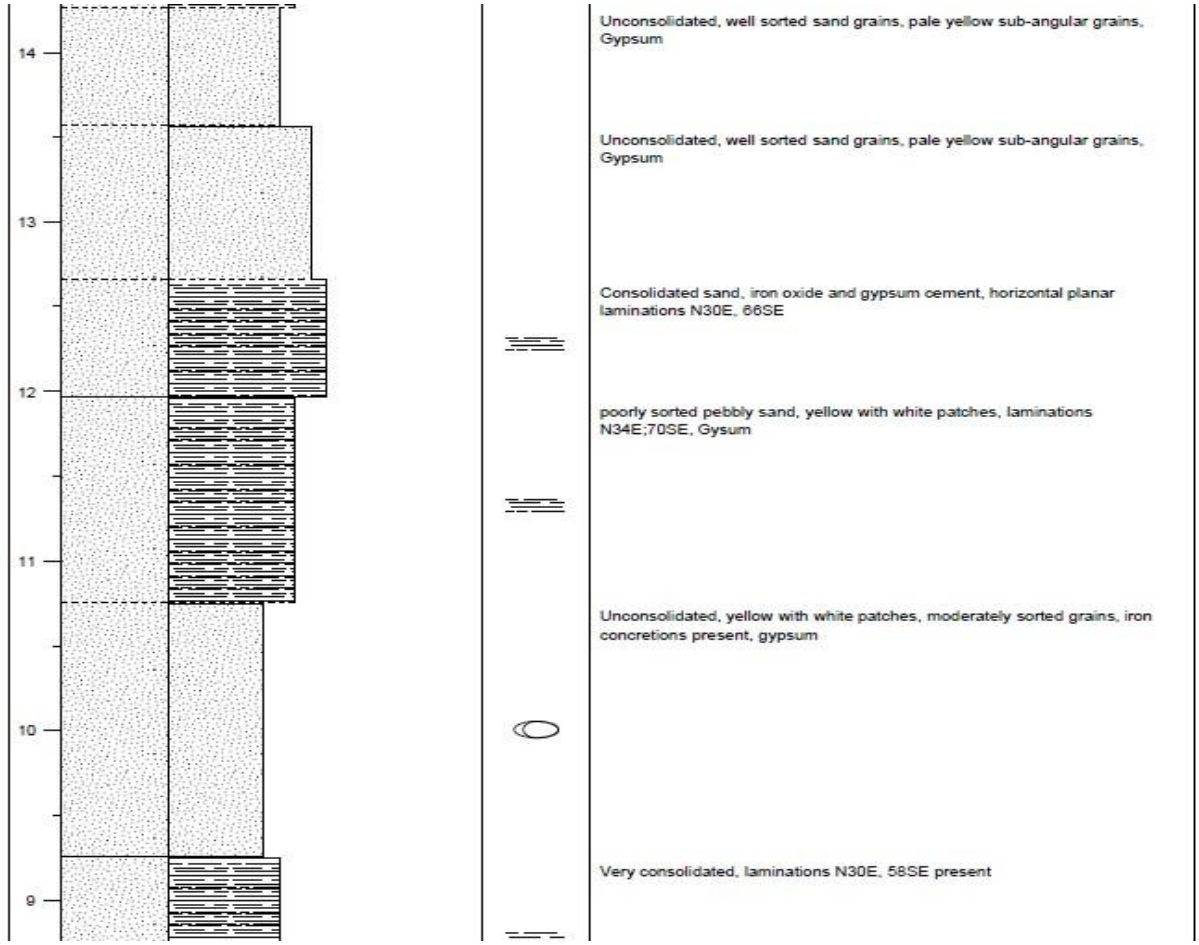
14
13
12
11
10
9
Unconsolidated, well sorted sand grains, pale yellow sub-angular grains, Gypsum
Unconsolidated, well sorted sand grains, pale yellow sub-angular grains, Gypsum
Consolidated sand, iron oxide and gypsum cement, horizontal planar laminations N30E, 66SE
poorly sorted pebbly sand, yellow with white patches, laminations N34E;70SE, Gysum
Unconsolidated, yellow with white patches, moderately sorted grains, iron concretions present, gypsum
Very consolidated, laminations N30E, 58SE present

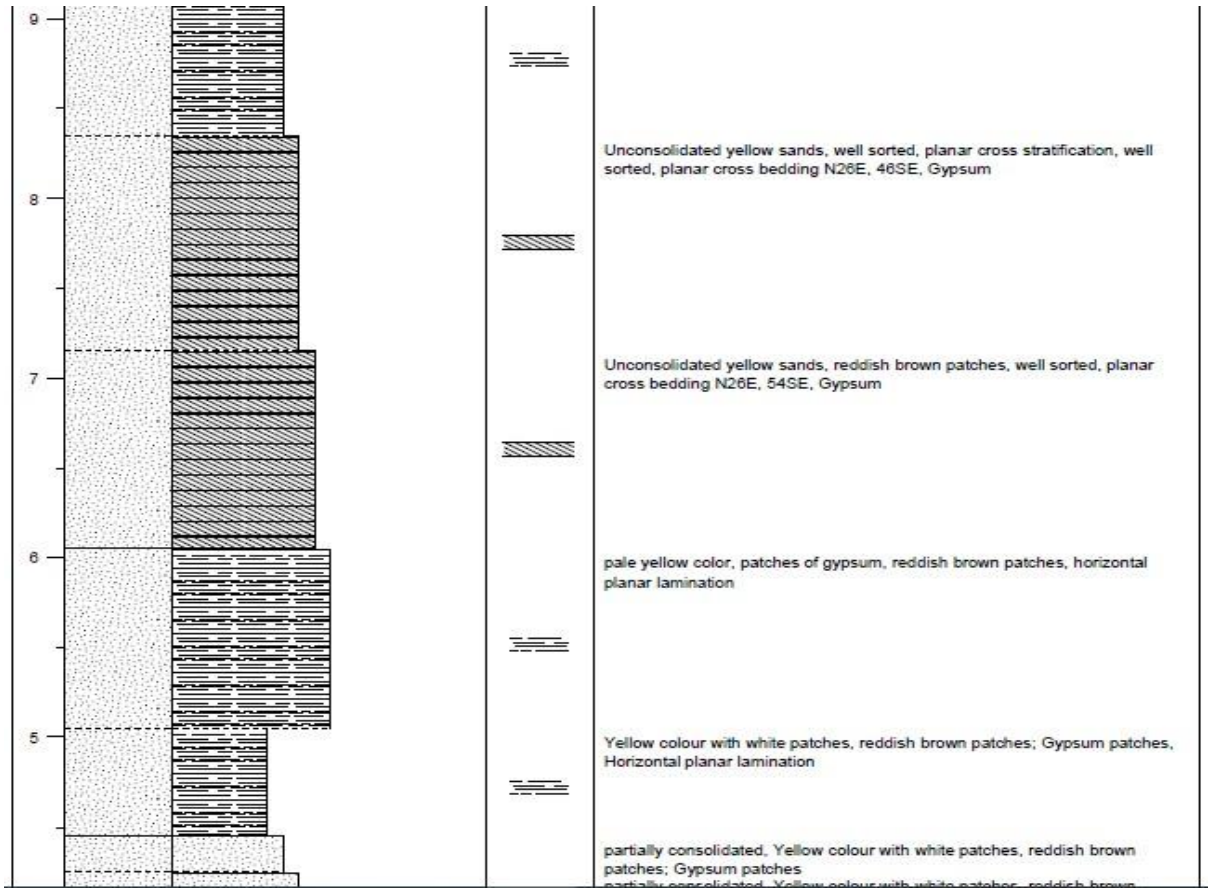
9
8
7
6
5
Unconsolidated yellow sands, well sorted, planar cross stratification, well sorted, planar cross bedding N26E, 46SE, Gypsum
Unconsolidated yellow sands, reddish brown patches, well sorted, planar cross bedding N26E, 54SE, Gypsum
pale yellow color, patches of gypsum, reddish brown patches, horizontal planar lamination
Yellow colour with white patches, reddish brown patches; Gypsum patches, Horizontal planar lamination
partially consolidated, Yellow colour with white patches, reddish brown patches; Gypsum patches

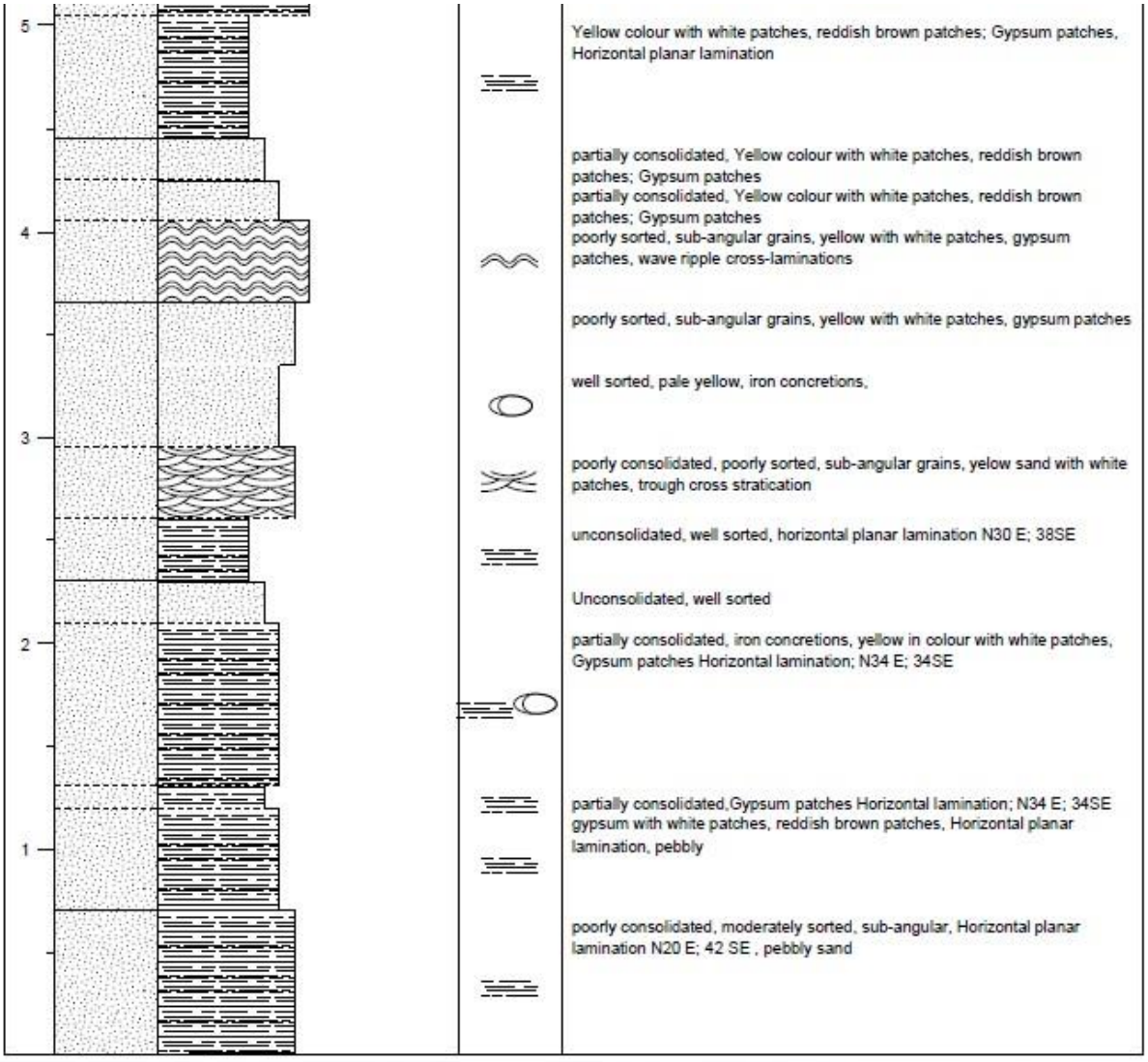

Figure 5.5. Combined log for Group A, B, C, F and G

CHAPTER SIX: GEOPHYSICS OF SEMLIKI SEDIMENTARY BASIN.

6.0 Introduction.

This chapter examines the geophysical characteristics of the Semliki Basin, particularly through the analysis of potential field data, including gravity and magnetic surveys. These datasets have been studied to enhance understanding of the petroleum system within the Albertine Graben.

Geophysics is the scientific discipline that applies physical principles to study the Earth's structure. It focuses on investigating the subsurface by leveraging variations in lithology and the physical properties of rocks. Different geophysical exploration methods target specific rock properties—for instance, the gravity method detects density contrasts, while the magnetic method measures magnetic susceptibility.

Geophysical techniques can be broadly classified into two categories: active and passive methods. Active methods, such as electrical and seismic surveys, involve introducing energy into the ground to assess rock properties. In contrast, passive methods, like gravity and magnetic surveys, analyze natural spatial variations in existing fields without external energy input. These passive approaches are also referred to as potential field methods.

Acquisition of potential field data in the Albertine graben and Uganda at large.

Over the years, Uganda has been comprehensively mapped through airborne geophysical surveys. In 1980, Geo-survey conducted aeromagnetic and gamma-ray spectrometry surveys over the onshore southern region (south of 10°00' N) with a 1 km line spacing. Later, in 1983, Kenting Earth Sciences carried out aeromagnetic surveys under the "Great Lakes" program, covering Lake Victoria at 40 km line spacing and the western part of Uganda, including the Albertine Graben, at 5 km line spacing. Earlier, in 1959, Hunting Aviation performed surveys in the northern and northeastern regions, collecting magnetic, electromagnetic, and radiometric data. The African Magnetic Mapping Project later compiled and reprocessed these magnetic datasets.

The African Magnetic Mapping Project identified five sedimentary basins in Uganda: the Albertine Graben, Hoima Basin, Lake Kyoga Basin, Lake Wamala Basin, and Kadam-Moroto Basin. In 1992, Kenting conducted another aeromagnetic survey focused on petroleum exploration in the Kidepo Valley, Moroto, and Mount Elgon areas. However, due to safety concerns, the aircraft flew at a 2 km altitude over the Karamoja region, which affected data resolution. According to MEMD, Kenting acquired 15,454 line-kilometers of raw aeromagnetic data over the Albertine Graben, which Edcon later processed. This data interpretation revealed three major sub-basins with basement depths exceeding 3 km (shown in Appendix I), leading to the division of the graben into three exploration zones.

In 1991, the Petroleum Unit within the Geological Survey and Mines Department (GSMD) of MEMD was upgraded to the Petroleum Exploration and Production Department (PEPD), tasked with assessing and promoting Uganda’s petroleum potential. From 1991 onward, PEPD

began collecting ground geophysical data in the Albertine Graben. Gravity surveys provided insights into subsurface structures, refined basement depth estimates, and allowed the graben to be further subdivided into five exploration areas instead of three. The data used in this study was obtained through these efforts. Currently, PEPD has shifted focus to the Moroto-Kadam Basin, gathering additional geological and geophysical data following significant discoveries in the Albertine Graben.

6.1 Potential Field Survey Method.

6.1.1 Gravity Survey Method.

The Earth's gravity field is not uniform; it varies based on the distribution of subsurface mass. These lateral variations can be measured and interpreted to infer the underlying geological composition. A gravity survey is an indirect (surface-based) technique used to assess subsurface density variations, higher gravity readings typically indicate denser underlying rocks.

Ground-based gravimeters precisely measure local gravity fluctuations at different locations. To determine gravitational anomalies, the regional background field is subtracted from the observed data, revealing density contrasts in subsurface materials. Positive anomalies often correspond to shallow, high-density structures, while negative anomalies suggest shallow, low-density formations.

For example, low-density deposits like halite, weathered kimberlite, and diatomaceous earth produce gravity lows, whereas high-density minerals such as chromite, hematite, and barite generate gravity highs. Additionally, the gravity method can estimate the total anomalous mass (ore tonnage) responsible for an anomaly. Gravity data is useful for identifying lithological variations, structural features, and even mineral deposits (Wright, 1981). However, gravity surveys are less effective for detecting small anomalous bodies, such as underground cavities, unless they are very shallow.

In petroleum exploration, gravity surveys help geologists refine their targets by providing insights into sediment thickness and basement depth, guiding further exploration efforts.

Results from gravity data interpretation for Semiliki basin.

The gravity low values, ranging from below -221.3 to -203.0 mGals (represented by blue to green zones), are predominantly located in the central to northern sections of the map, particularly in grids A2, B2, B1, C1, C2, and portions of A3, B3, C3, as well as the central part of grid B4 on the Bouguer anomaly map. In contrast, gravity highs, associated with high-density rocks, range from -203.0 to above -111.3 mGals (yellow to pink zones) and are concentrated in the southern region, covering grids A4, B4, C4, and the southern parts of A3, B3, and C3.

A distinct yellow line in cells A3, B3, and C3 likely marks the contact zone between sedimentary deposits and basement rocks, as areas south of this line exhibit gravity highs while those to the north display gravity lows.

The gravity high regions suggest minimal sediment thickness (very thin layers), indicating that the high-density basement formations, rich in dense minerals, are shallow and contribute significantly to the elevated gravity readings. Conversely, the gravity lows result from density deficiencies caused by thick sedimentary accumulations within the basins. The intensity of these low gravity values correlates with the thickness of the sedimentary cover overlying the Pre-Cambrian rift floor.

Based on this interpretation, it can be concluded that the Semliki depocenter is situated in the northwestern part of the study area (around grid B2), where the Bouguer anomaly values are relatively low (blue zones on the map).

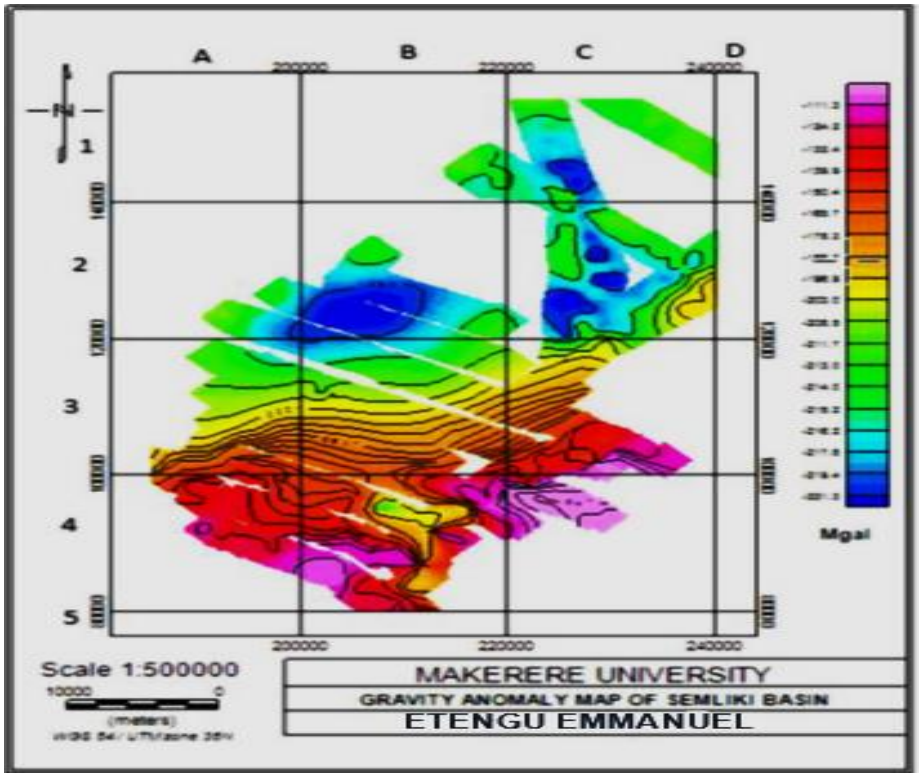

Figure 6.1. A bouguer anomaly map of Semliki basin.

Positions of geological bodies. Gravity maps help identify the lateral distribution of geological formations by detecting density contrasts between subsurface bodies and their surrounding rocks. The observed gravity lows in grid cells C2, C1, and B4 likely result from density variations caused by features such as igneous intrusions or salt domes, which typically exhibit different density properties compared to the host rock.

6.1.2 Magnetic Survey Method.

The magnetic method detects variations in Earth's magnetic field caused by differences in the magnetic properties of rocks. A magnetometer measures these regional magnetic field differences, which indirectly helps estimate the thickness of sedimentary layers that may contain hydrocarbons. Areas with thick accumulations of non-magnetic sedimentary rocks typically show lower magnetic susceptibility values.

Magnetic surveys can reveal buried basins (like grabens) beneath sedimentary cover or identify basement highs under overlying strata. However, magnetic contour maps provide only limited structural or stratigraphic detail. The method can be conducted aerially (via aircraft or satellite), enabling efficient large-scale mapping. Similar to gravity surveys, magnetic surveys are often used in early exploration phases.

Rock magnetization is a vector quantity with both direction and magnitude, combining induced magnetization (dependent on rock susceptibility) and remanent magnetization (dependent on the rock's geological history). Because magnetic fields originate from dipole sources, anomaly amplitudes remain unaffected by scale changes. This occurs because magnetic effects stem from interface surfaces rather than bulk volumes, and because magnetic fields attenuate rapidly with distance. Consequently, magnetic maps predominantly highlight shallow sources rather than deep ones. In areas lacking shallow volcanic rocks (which are typically highly magnetic), magnetic maps primarily reflect crystalline basement characteristics. Basic igneous/metamorphic rocks, iron ores, and banded iron formations produce strong magnetic anomalies, while acid gneisses and metamorphic rocks yield moderate readings, and sedimentary rocks show the weakest responses.

Results from Magnetic data interpretation for Semiliki basin.

The zones exhibiting magnetic highs correspond to the sediment-dominated depositional basin in the northern and northwestern portions of the study area (Figure 6.2). This suggests that the sediments incorporate magnetic minerals eroded from rocks that once overlay the rift valley flanks and the Rwenzori mountain block. The total magnetic intensity map reveals variations between high and low magnetic signatures, ranging from 33,337.7 nT to 34,033.6 nT respectively.

The relatively subdued magnetic values in the southeastern sector are attributed to basement rocks that were previously buried at substantial depths beyond the Curie temperature, causing their magnetic minerals to lose magnetization. The localized magnetic highs observed in southern areas may represent igneous intrusions containing magnetic minerals such as magnetite and hematite.

A key magnetic interpretation tool is the analytic signal filter, which helps pinpoint the sources of magnetic anomalies. This filter's maxima consistently align with source boundaries regardless of magnetization direction (Cheyney et al., 2011), effectively converting data

collected under Earth's inclined magnetic field to what would be observed under vertical field conditions.

Complementary processing techniques included applying the Tilt Derivative (TDR) and computing both horizontal and vertical derivatives of the Total Magnetic Intensity (TMI) maps. These methods enhanced structural mapping in the Semliki basin (Figure 6.3) by sharpening magnetic anomaly edges and improving contrast between geological units and structural features like faults and lineaments (Macleod, Jones, & Dai, 1993).

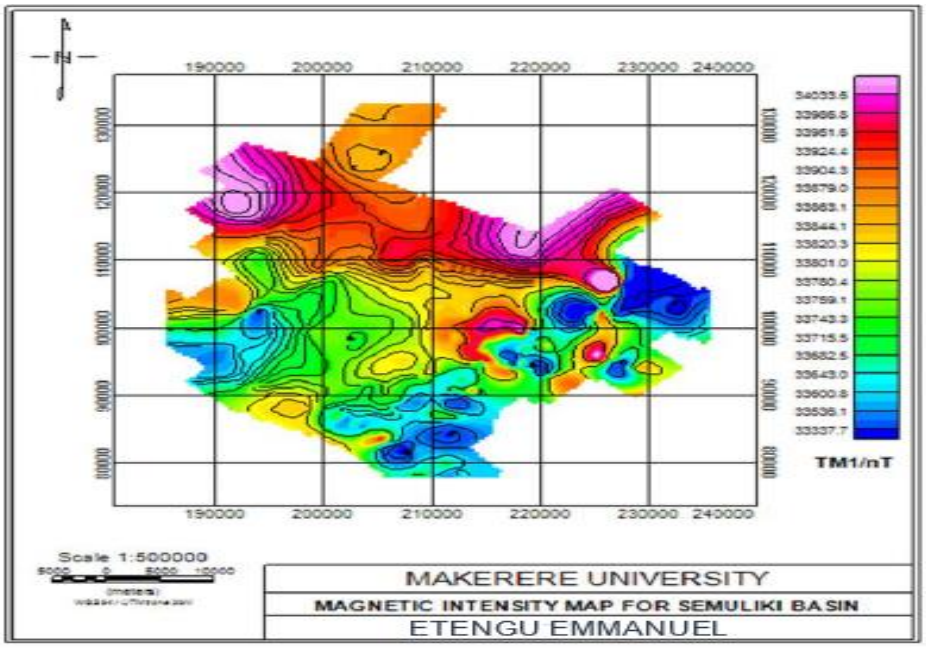

Figure 6.2 A total magnetic intensity anomaly map of the Semliki basin

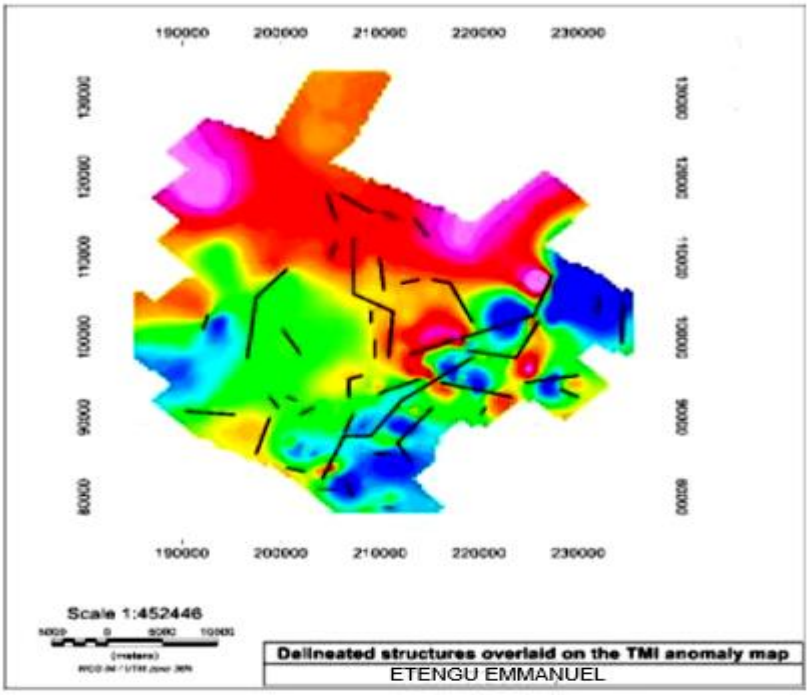

Figure 6.3. Structures delineated from magnetic intensity data.

6.2 Seismic Surveys.

Seismic methods provide superior subsurface imaging compared to other geophysical techniques. The technique involves generating seismic waves at or near the surface using vibroseis trucks, airguns, or explosives, then recording the reflected/refracted waves that return after interacting with underground layer boundaries. When a seismic pulse propagates through sedimentary layers, different rock formations transmit these sound waves at varying velocities. Surface sensors (geophones for land surveys, hydrophones for marine surveys) capture the returning wave data, which is subsequently analyzed for hydrocarbon indicators.

These methods excel at detecting and mapping subsurface interfaces, typically with simple geometries, making them particularly valuable for studying layered sedimentary sequences - hence their widespread use in oil and gas exploration. Seismic interpretation, whether for energy exploration or geotechnical investigations, involves extracting geological meaning from seismic data. Each reflection visible on a seismic profile possesses distinct timing and waveform characteristics that reveal subsurface features. Key advantages include: Superior resolution of subsurface structures, Effective imaging of sedimentary layering, Quantitative analysis of wave properties for rock characterization and Adaptability to both land and marine environments.The technique's effectiveness stems from its ability to provide: Depth information through travel time measurements, Rock property insights via amplitude analysis, Structural details from reflection patterns, and Stratigraphic information through sequence interpretation.

6.2.1 Results of Seismic Study and Interpretation of Structures for Semliki Basin.

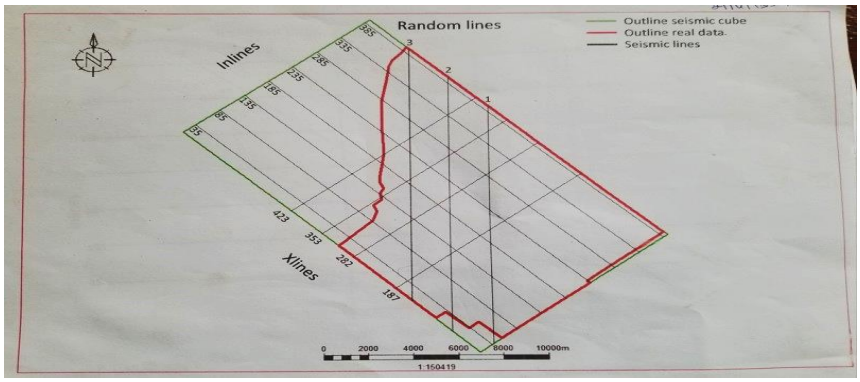

Figure 6.4. The random lines from which the seismics were shot.

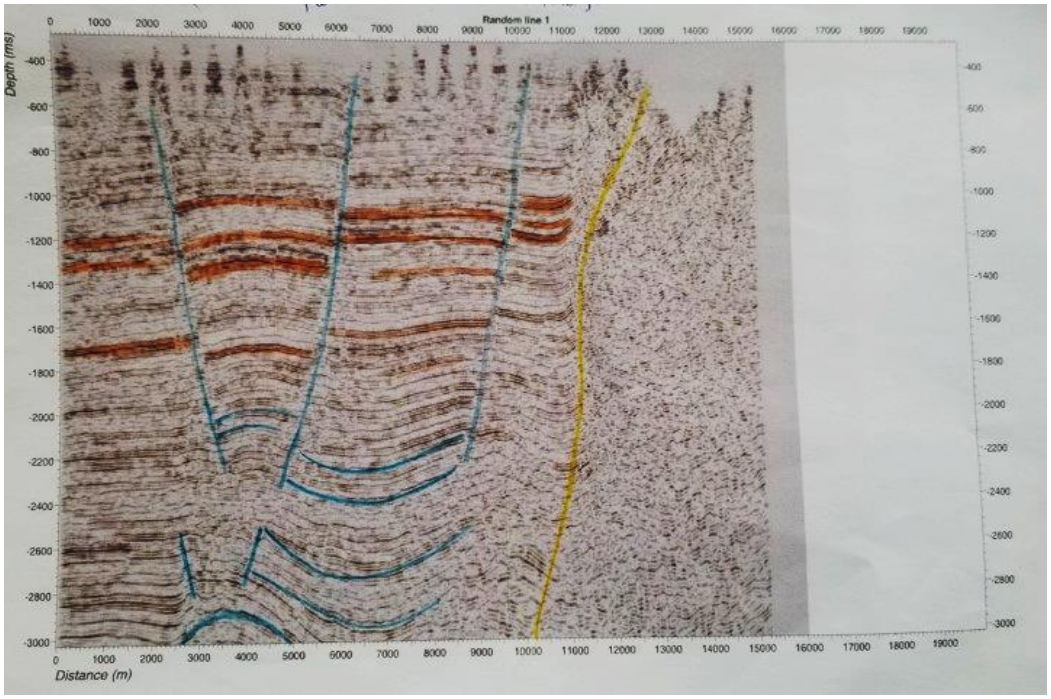

Figure 6.5. Structures interpreted from Random line 1.

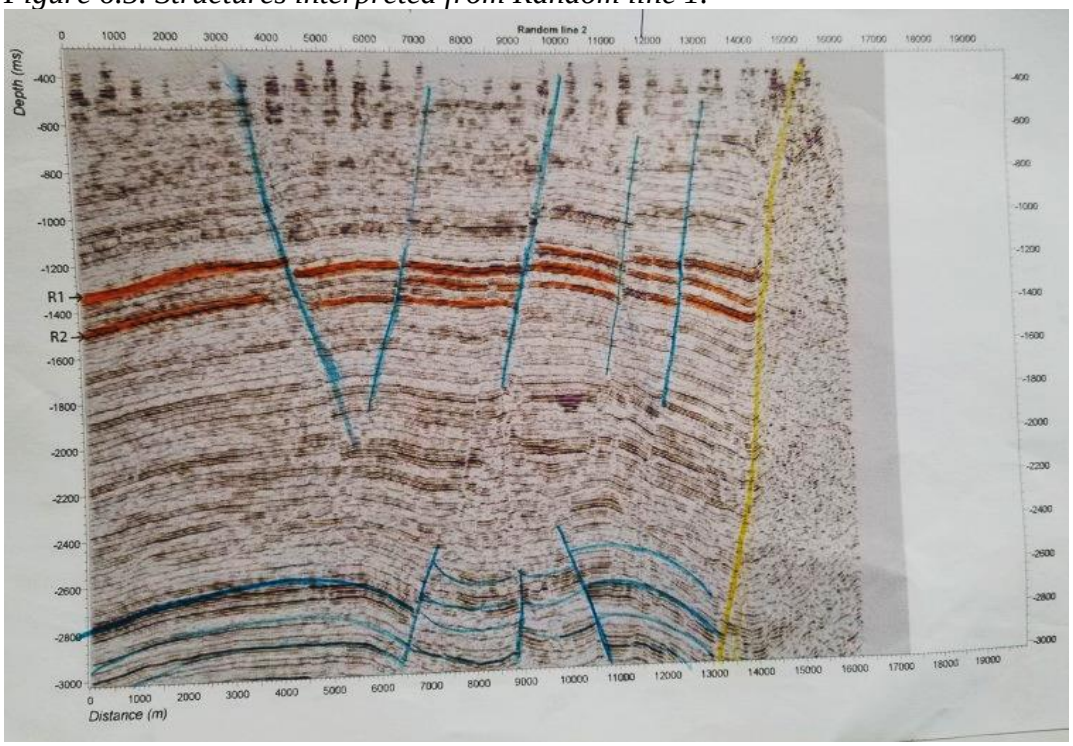

Figure 6.6. Structures interpreted from Random line 2.

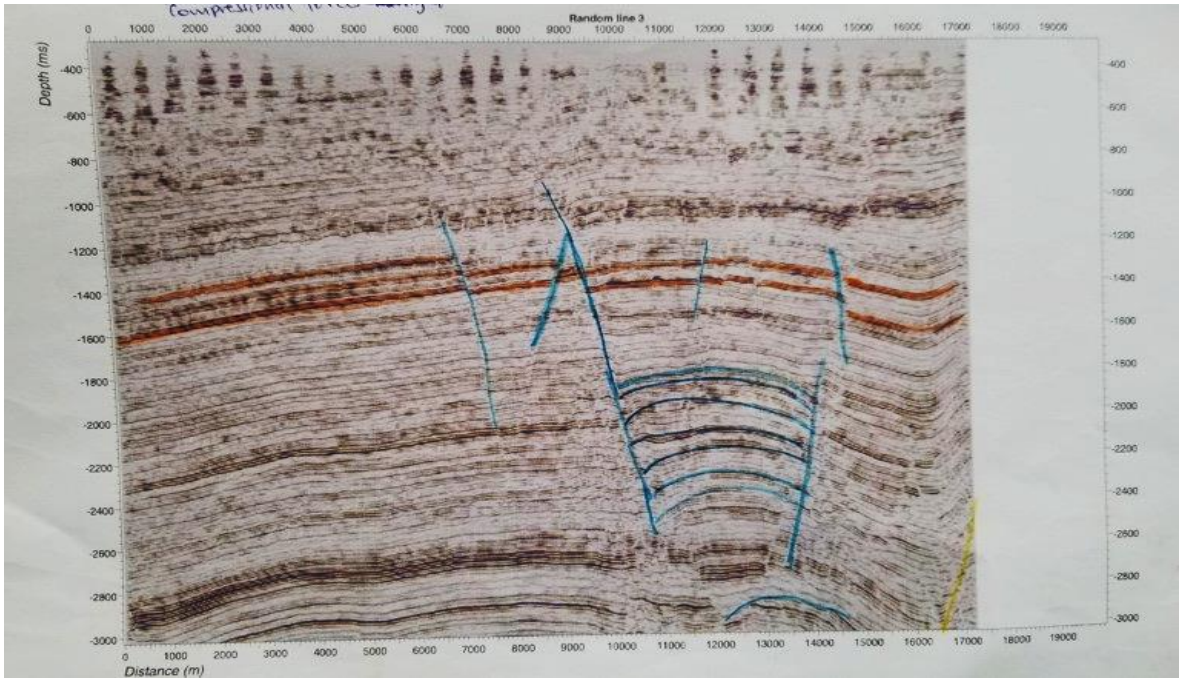

Figure 6.7. Structures interpreted from Seismic Random line 3

The seismic sections presented in Figures 6.5-6.7 reveal high-quality data from the Semliki Basin, clearly imaging subsurface horizons and structural features. Interpretation shows significant fault activity evidenced by horizon displacements along the light blue fault traces. The fault system displays an upward-diverging pattern characteristic of positive flower structures, with internal anticlinal features suggesting transpressional tectonic origins. While predominantly composed of dip-slip normal faults, some dip-slip reverse faults are present. These concave-upward planar reverse faults create reservoir compartmentalization - a phenomenon well-documented across the Albertine Graben. The transverse anticlines represent accommodation zones between major border faults, which serve as persistent fluid conduits through networks of fault breccias and fractures. Such zones, marked by intersecting normal faults with opposing dips, often form effective hydrocarbon traps, particularly where rollover anticlines develop in the downthrown blocks of growth faults. The basement-Sediment contact is represented by the yellow line seen in the seismic section.

6.2.2 Results of seismic study and interpretation of facies/lithology for Gulf of Mexico

For the Gulf of Mexico study, the field supervisor utilized exceptional resolution seismic data (150-200 Hz, 3m vertical resolution) from an intra-slope salt withdrawal mini-basin. This dataset, comprising eight 2D lines (including dip line D1 connecting strike lines S1-S7) from an ExxonMobil training exercise, exemplifies characteristic seismic facies of deepwater

depositional systems. The educational objectives focused on structural/stratigraphic interpretation and uncertainty assessment through: (1) identifying reflection terminations on D1; (2) correlating strike line S6 with dip line D1; and (3) propagating interpreted surfaces/facies from D1 across S6. This interpretation workflow was systematically applied to all strike lines (S1-S7), ensuring consistent feature mapping throughout the seismic grid. The exercise particularly emphasized understanding depositional elements and their seismic expression in salt-influenced deepwater environments.

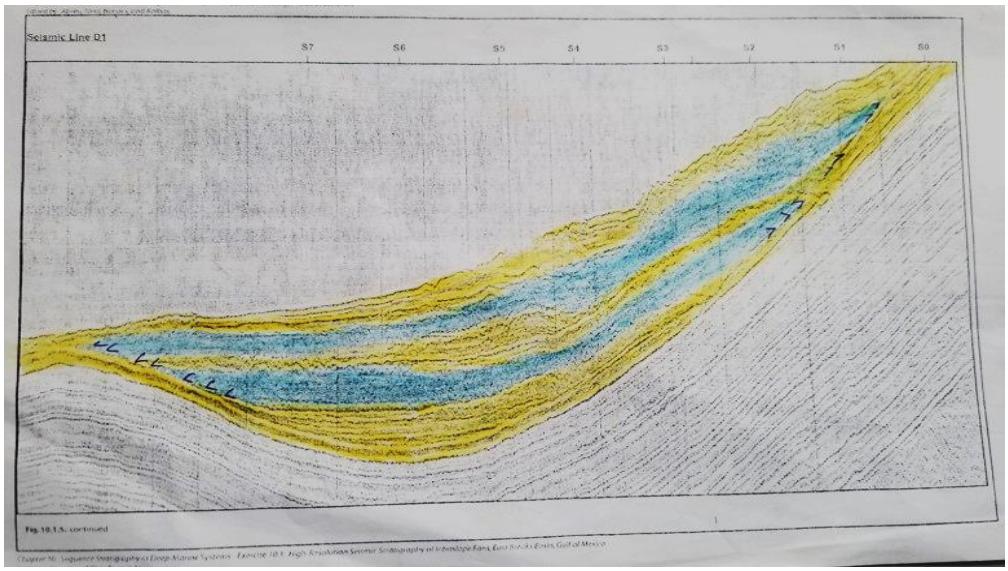

Figure 6.8. Seismic line D1

The figure 6.8 above shows cyclic sedimentation with two major facies shown by yellow and blue colours. It also shows a pinch-out and layers on-lapping onto a surface.

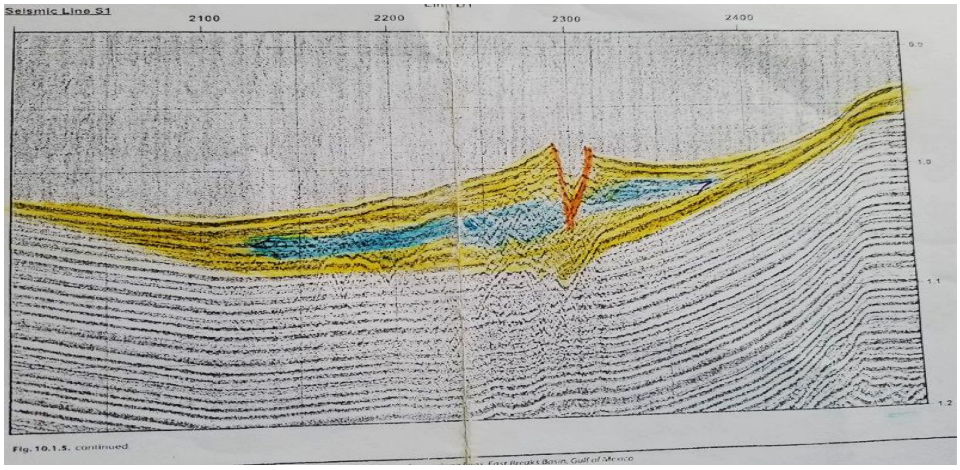

Figure 6.9. Seismic line S1

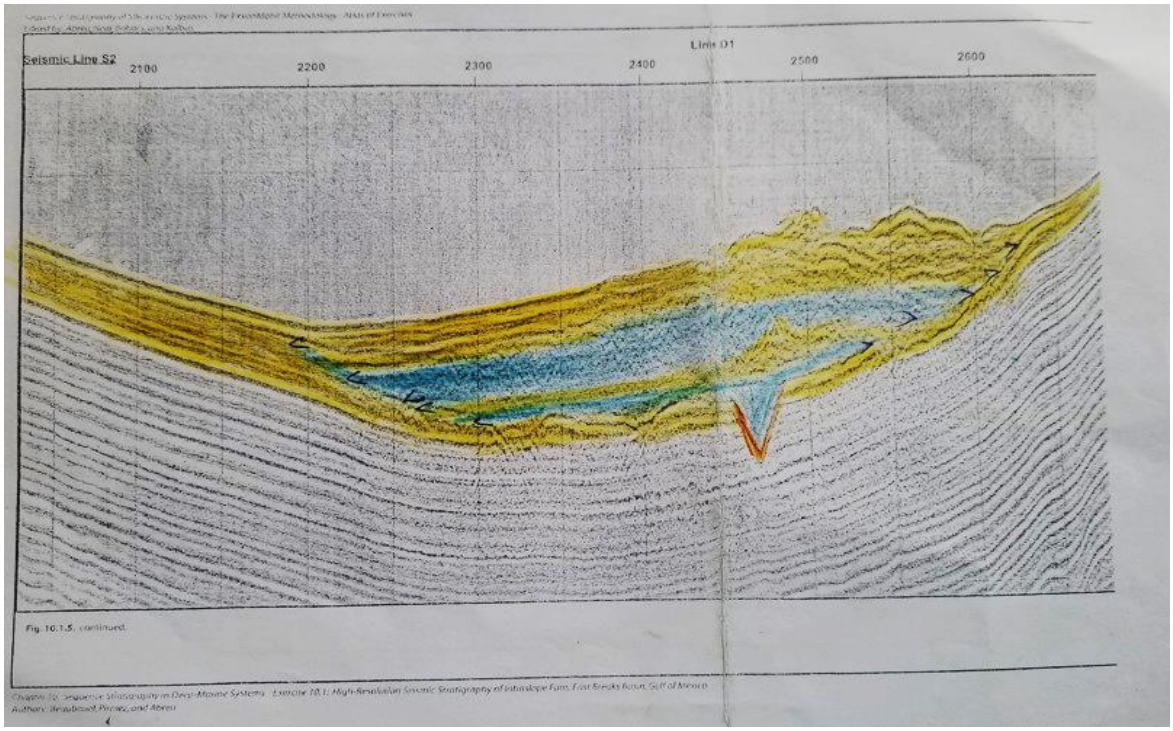

Figure 6.10. Seismic line S2.

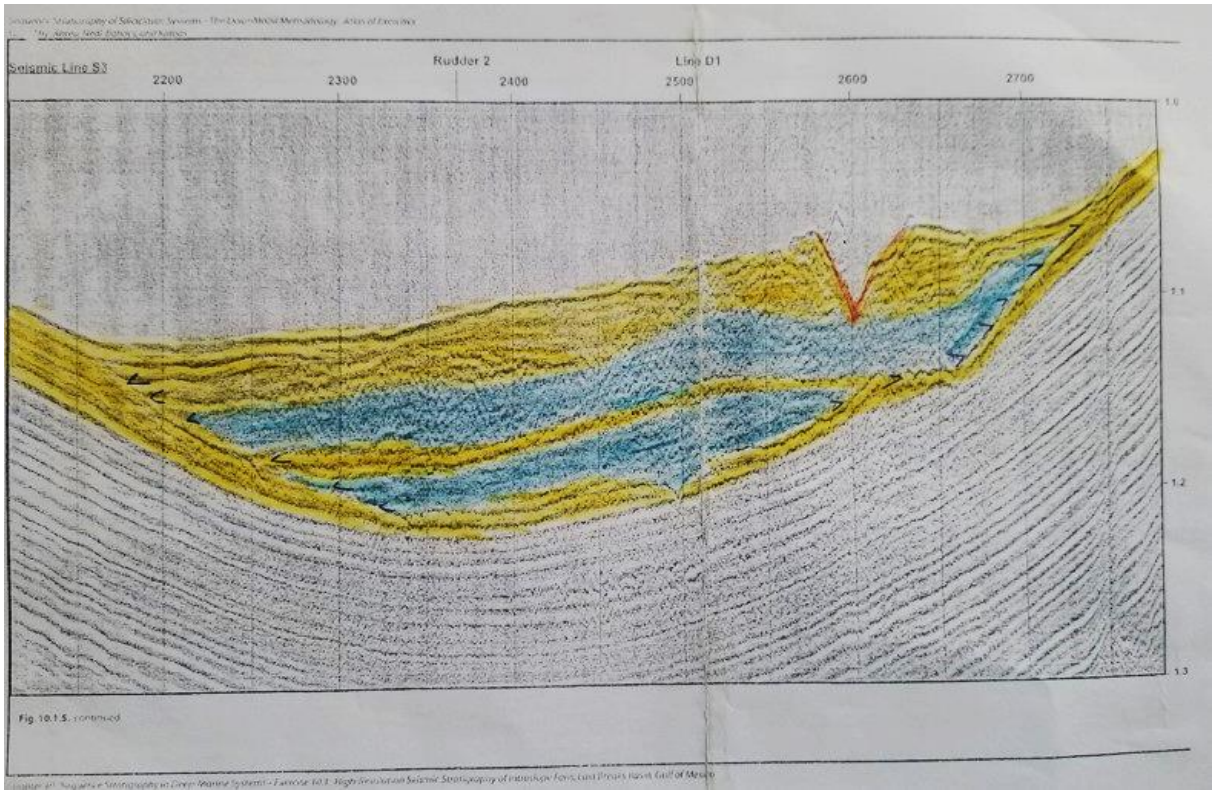

Figure 6.11. Seismic Line S3.

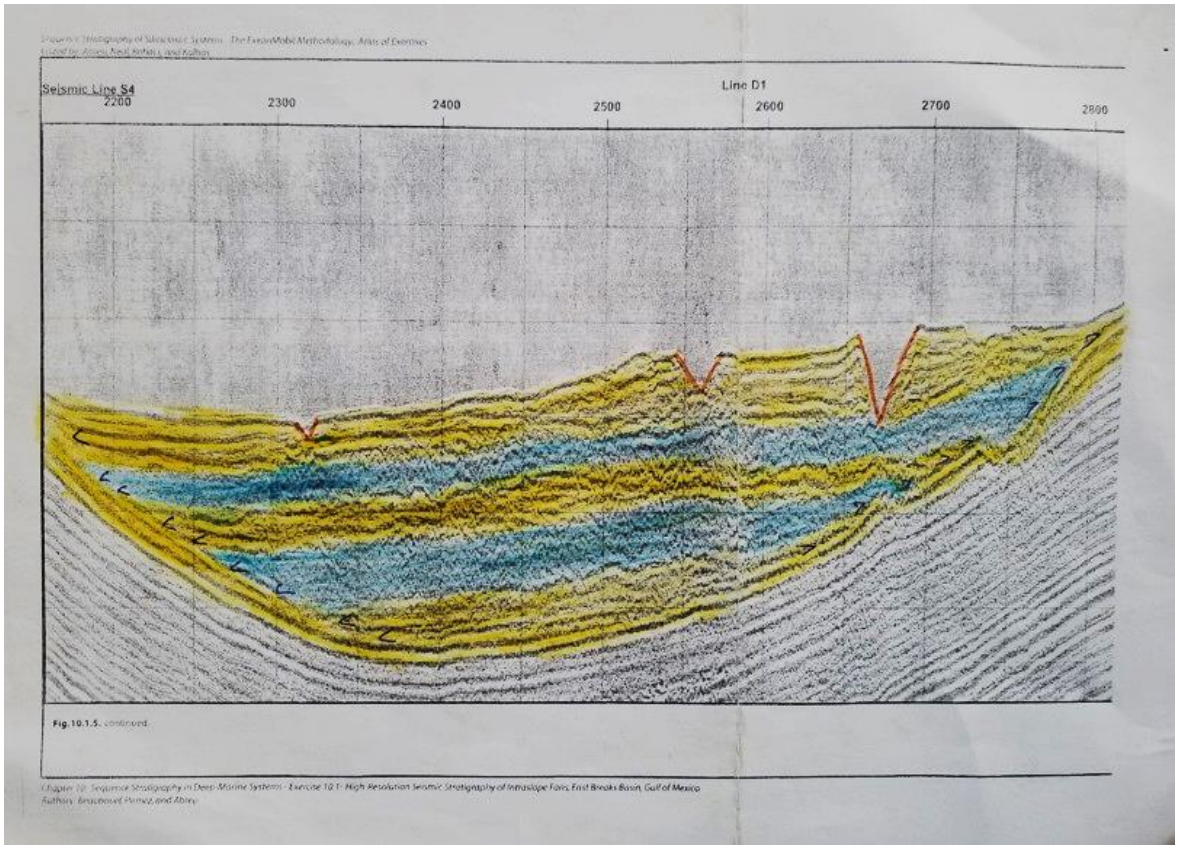

Figure 6.12. Seismic line S4.

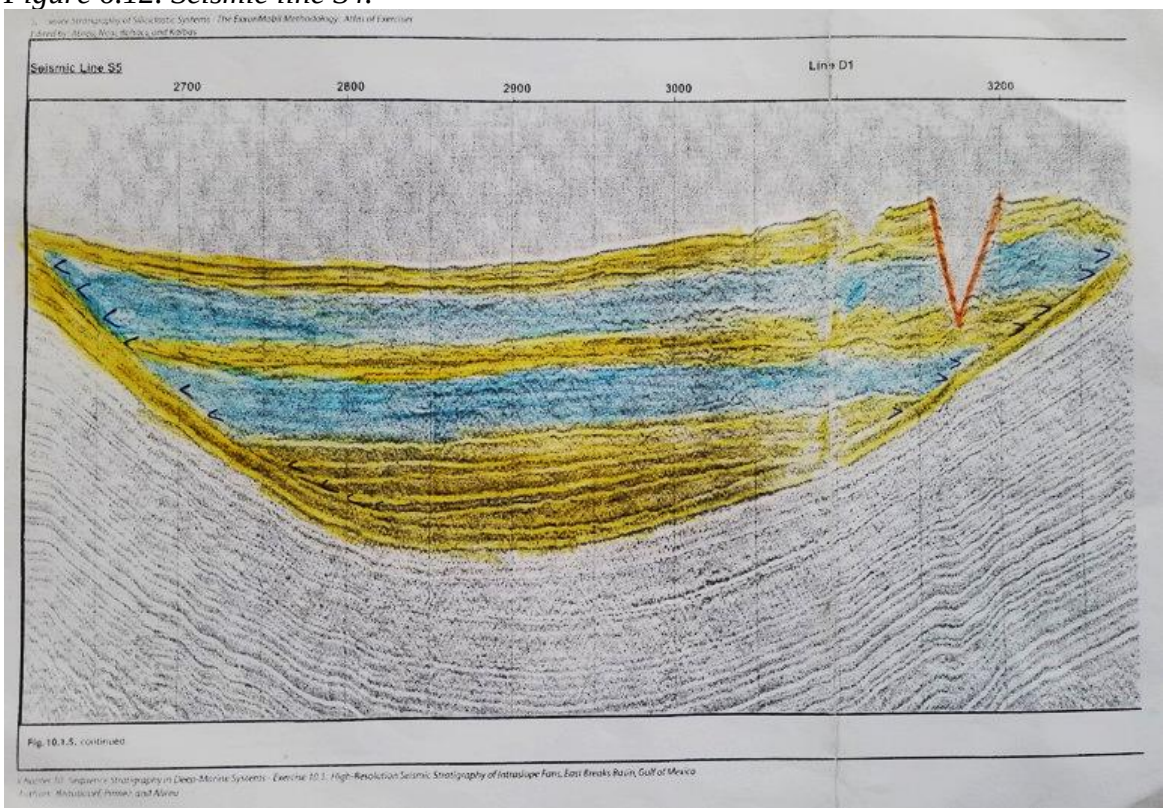

Figure 6.13. seismic line S5.

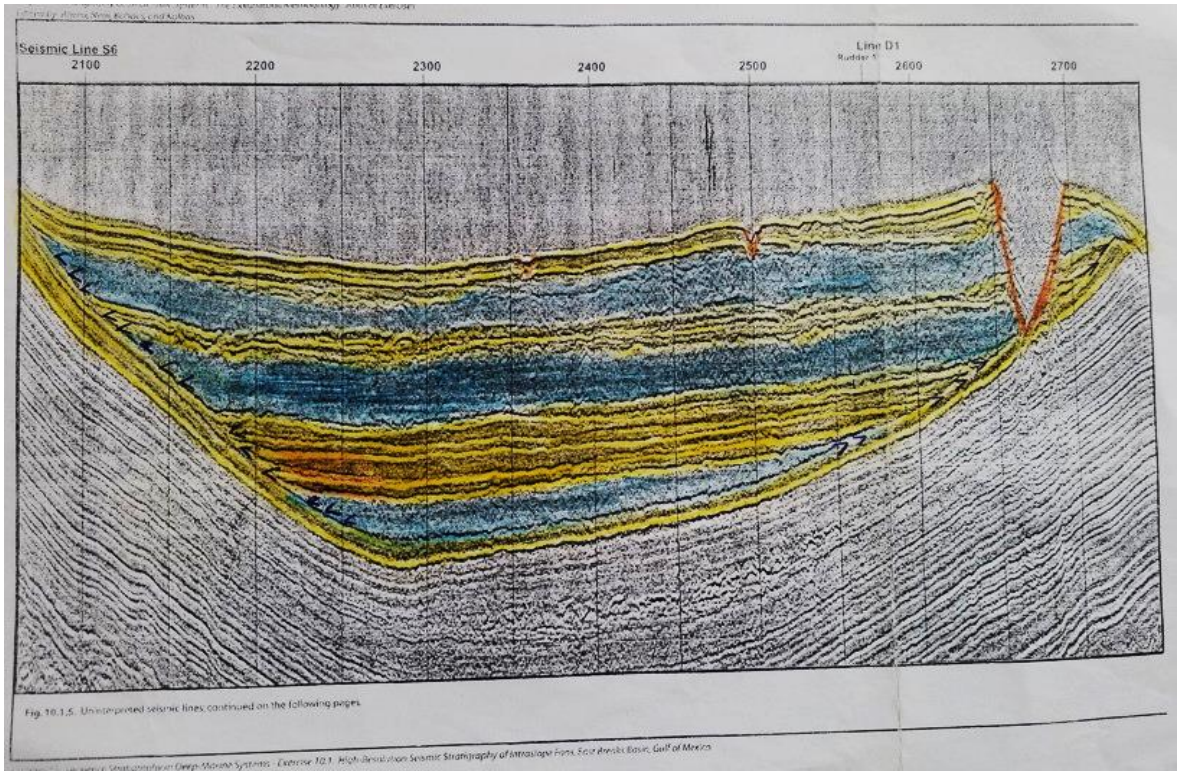

Figure 6.14. seismic line S6.

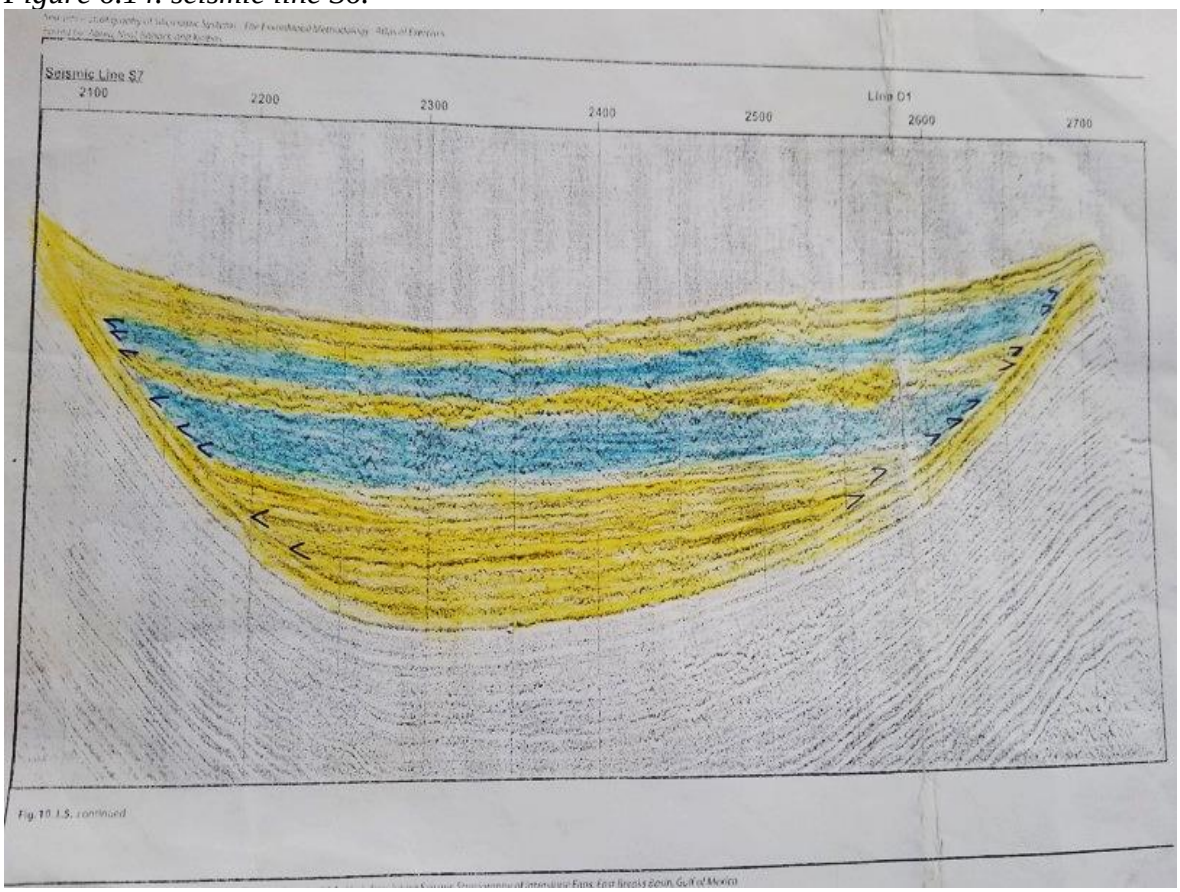

Figure 6.15. seismic line S7.

Figures 6.8 through 6.15 reveal two distinct facies with cyclic sedimentation patterns in seismic lines S1-S7, represented by grey and green shading. The green-colored facies display continuous parallel reflections, suggesting deposition in stable, laterally extensive environments such as low-energy deepwater settings. In contrast, the blue-shaded facies exhibit discontinuous reflections, indicative of environments with lateral facies variations like high-energy fluvial and alluvial systems.

The seismic lines S1-S7 show sequence boundaries comprising both gradational conformable surfaces between facies and a potential unconformity marked by onlapping seismic facies. These onlapping relationships appear as low-angle reflections terminating against steeper seismic surfaces.

Geometric analysis reveals that seismic line S1 contains just two facies types that pinch out to the right, likely representing fluvial channel deposits at a river mouth entering the basin. Progressing through lines S2-S7, the basin demonstrates increasing width, depth, sediment cyclicity, and thickness, with maximum basin depth evident in line S7. This configuration suggests a cone-shaped depositional geometry with clear onlap terminations.

Based on the seismic geometries and attributes, the sediments were deposited in a fluvial/alluvial fan environment. Subsequent river channel incision during regressive phases eroded these deposits, creating stratigraphic truncations and abandoned channel features. The seismic evidence thus records both the initial depositional system and later erosional modification of the basin sediments.

6.3 Petrophysics For Formation Evaluation.

6.3.1 Results from wireline logging.

The wireline log interpretation focuses on an interesting 500-foot interval (1500ft-2000ft) from the Turaco 2 well. The complete log is available for reference in Appendix 5.

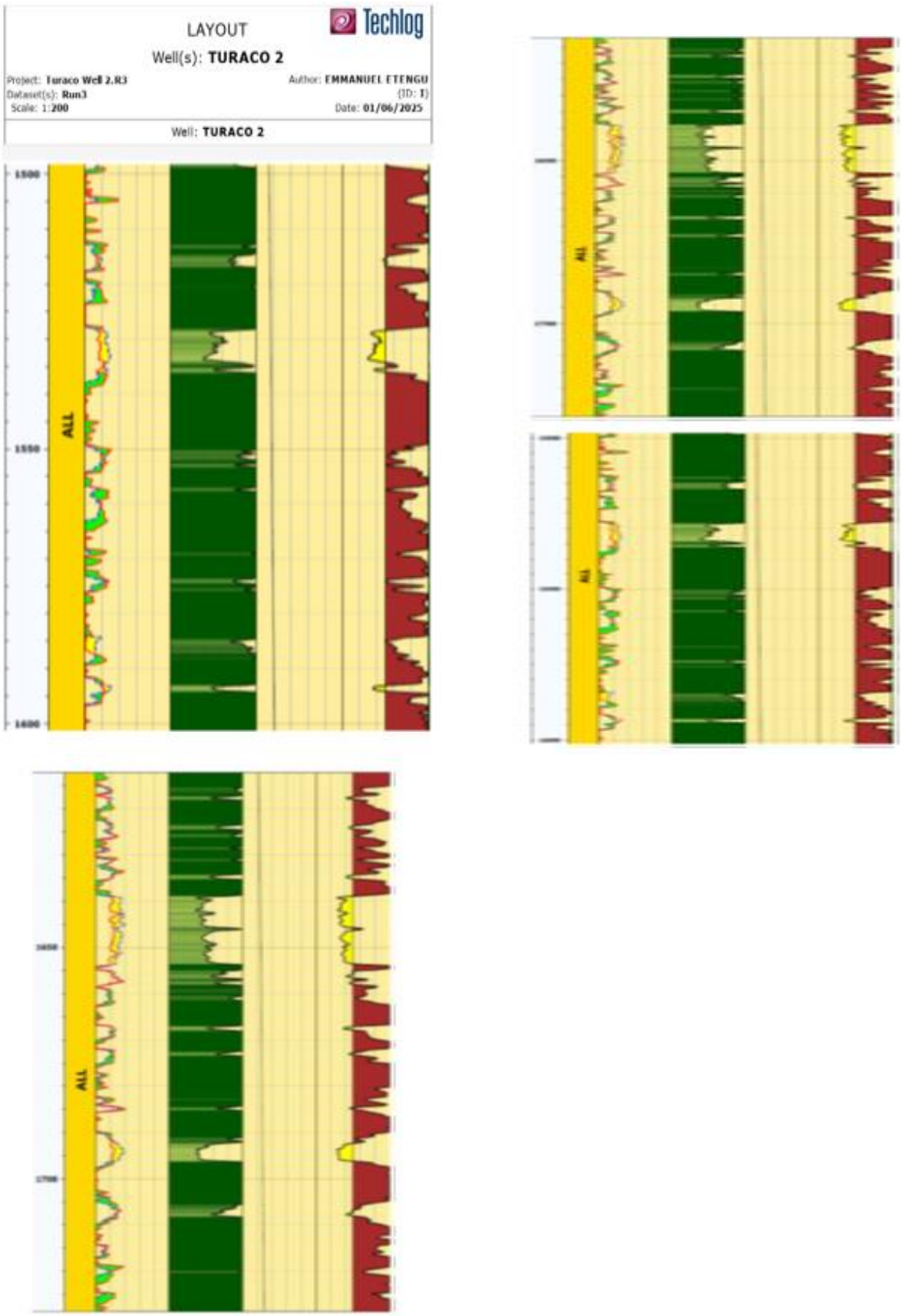

Figure 6.16. Wireline log for Run 3 Turaco 2 from depth 1500ft t0 2000ft.

Neutron and Density porosity logs.

Track 1 presents the density porosity log (red) and neutron porosity log (blue), which measure electron density and hydrogen concentration respectively. Gas-bearing zones are identified by significant separation between the logs - the neutron log shows low readings due to gas's reduced hydrogen content, while the density log registers higher values. Conversely, closely overlapping or parallel neutron and density porosity curves indicate the presence of either water or oil in the formation. This diagnostic separation pattern allows for clear fluid identification in the logged interval.

$$\Phi = \frac{\rho(matrix) - \rho(\text{densit log})}{\rho(matrix) - \rho(fluid)}$$

Where, Φ =porosity,
ρ $(matrix)$=the density of the matrix (g/cc),
ρ $(density\ log)$ = the corresponding density read from the density log (g/cc) and $(fluid)$ is the density of the fluids (g/cc).

Average Porosities obtained for Turaco-2 well include 31%, 21%, 36%, 26%, 22%. These are very good porosities implying that the reservoirs with in this area are good.

V-Shale log.

Track 2 displays the shale volume (Vshale) log, which quantifies shale content within the formation. Lower Vshale values indicate reduced shale presence and consequently higher porosity, typically correlating with hydrocarbon-bearing zones (oil/water). The gamma ray log serves as the primary tool for calculating shale volume using the following method:

$$Vshale = \frac{GRlog - GRmin}{GRmax - GRmin}$$

Where;

$GRlog =$ reading of the gamma ray log

$GRmin =$ clean sand

$GRmax =$ is shale

Gamma ray Log.

Track 3 demonstrates how gamma ray logs distinguish between shale and sand formations. Elevated gamma ray readings characterize shales due to their concentration of radioactive elements (particularly potassium), while lower readings indicate sandstones which lack these radioactive components. The log also reveals reservoir zones through negative deflections (mudcake effects) caused by interactions between reservoir fluids and drilling mud.

Analysis of the Turaco well log shows predominantly shale-rich intervals, evidenced by consistently high gamma ray responses. This lithology likely corresponds to the Kasande, Oluka, and Nyakabingo formations - known shale/clay-bearing units within the Semliki Basin's stratigraphic sequence. The persistent high readings suggest these formations contribute significantly to the well's shale content profile.

Makondo and the decommissioned Turaco Well sites.

While we didn't conduct field visits to these locations, existing literature and prior geological surveys confirm that Makondo is situated at coordinates 201157/110303 with an elevation of 678m. Historical geophysical data reveals Kenting Earth Sciences performed aeromagnetic surveys in the area during 1993, followed by Heritage Oil and Gas's 1998 seismic survey along the Makondo fault. This fault represents an intra-sedimentary structure forming the eastern boundary of the Turaco positive flower structure (Figure 6.17). The basin preserves paleontological evidence including fish fossils, bivalves, white oysters, and hematite deposits - remnants suggesting the existence of paleolake Obweruka before its eventual desiccation.

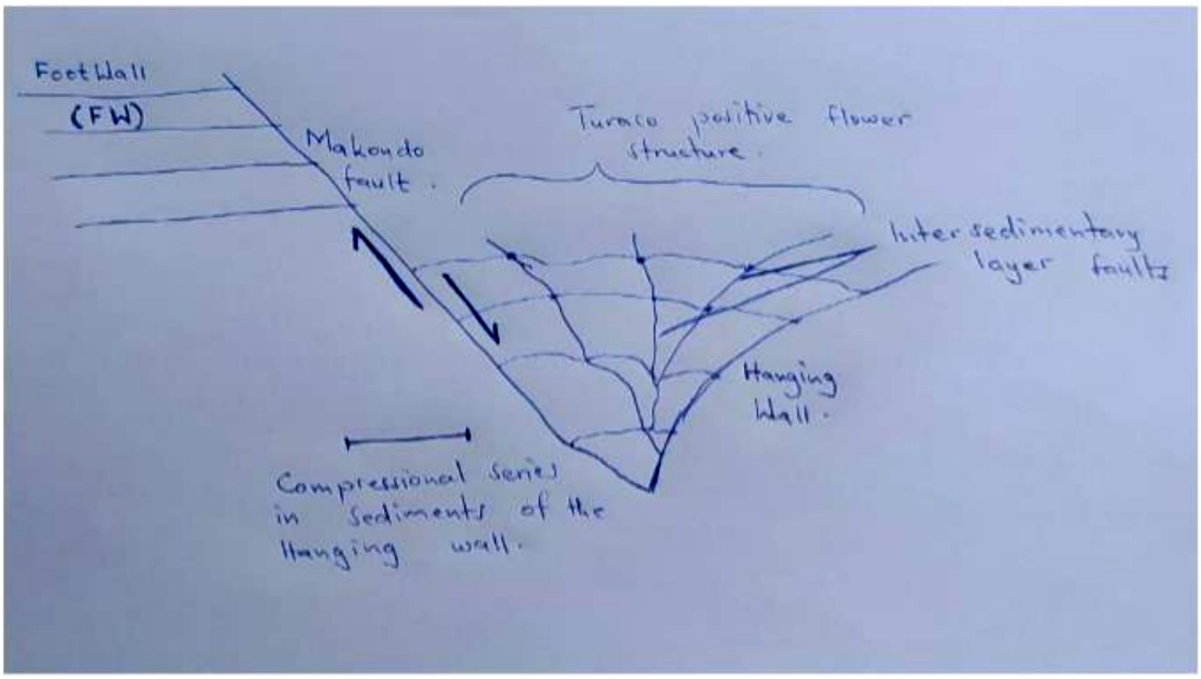

Figure 6.17. Positive flower structure at Turaco.

While direct field surveys were not conducted, documented records and previous geological investigations establish Makondo's position at coordinates 201157/110303 with an elevation of 678 meters. The area's geophysical background shows Kenting Earth Sciences executed aeromagnetic surveys in 1993, succeeded by Heritage Oil and Gas's seismic data collection along the Makondo fault in 1998. This intra-sedimentary fault constitutes the eastern margin of the Turaco positive flower structure (Figure 6.18). The basin contains fossilized remains including fish, bivalves, white oysters, and hematite minerals, likely preserved from the ancient Lake Obweruka prior to its disappearance.

Figure 6.18. Decommissioned Turaco well site.

6.4 Results of study of Geophysical methods for geothermal exploration.

A geothermal field is an area of the earth characterized by a relatively high heat flow and the elements are similar to those of a petroleum system include;

Heat source: localized thermal plume or a rock having radiactive minerals.

Reservoir: good conducting rock such as granite or sandstone

Seal: thermal blanket/ insulator and should be regional such as shale

Plumbing system: cold water moves through the hot reservoir, turns hot, percolates to surface, becomes cold, sinks back top reservoir due to high density and the cycle continues.

Uganda hosts three geothermal fields: Katwe-Kikorongo, Buranga, and Kibiro. Field studies in the Semliki basin included visits to the Sempaya hot springs, locally known as the female and male hot springs, located within the Buranga geothermal field in Semliki National Park, Bundibugyo district. This area exhibits intense geothermal surface activity where hot water emerges from rainwater that infiltrates porous sedimentary rocks. As the water percolates downward, it dissolves various minerals, including radium and sulfur, and is heated by the Earth's mantle, which is relatively shallow in this region. The heated water then rises through fractures or faults to the surface, forming hot or warm springs.

Impact of Sempaya Hot springs on Petroleum potential of Albertine Graben.

The Albertine Graben (15 million years old) remains geologically young yet contains hydrocarbons due to its elevated heat flow, demonstrated by the Sempaya Hot springs resulting from crustal thinning. Hydrocarbon generation requires source rocks to reach a specific Time-Temperature Index (TTI) threshold for thermal maturation. The Sempaya springs exhibit temperatures reaching 106°C (male) and 103°C (female), contributing to the enhanced geothermal gradients that have rapidly matured source rocks in this young rift basin. While the conventional oil window spans 60-120°C, the springs' higher temperatures risk "overcooking" oil.

CHAPTER SEVEN: DISCUSSION

7.1 Facies and Depositional Environments of the Study Area.

The Semliki Basin exhibits a diverse range of sedimentary facies that reflect varying depositional environments, including fluvial, lacustrine, deltaic, and alluvial fan systems. These facies were identified based on lithological characteristics, sedimentary structures, and fossil assemblages:

Fluvial Facies: Characterized by fining-upward sequences, cross-bedding, and channelized sandstones, indicative of meandering and braided river systems. Paleocurrent analysis (from cross-bed orientations) suggests NW-SE and NE-SW flow directions, influenced by tectonic shifts in the Albertine Graben.

Lacustrine Facies: Thick, blocky claystones and siltstones with laminations and freshwater fossils (bivalves, fish bones) suggest prolonged lake deposition. The Kasande Formation, rich in organic clays, serves as a potential source rock.

Deltaic Facies: Coarsening-upward sand sequences with interbedded clays indicate delta-front progradation, likely where rivers entered Lake Obweruka.

Alluvial Fan Facies: Poorly sorted conglomerates at the basement-sediment contact (Kisegi Formation) suggest rapid deposition in high-energy, tectonically active margins.

The Facies Associations include: **Cyclic sand-clay alternations;** implying fluctuating water levels (e.g., lake transgressions/regressions). **Gypsum and iron oxides** in sediments point to semi-arid conditions with periodic evaporation. The presence of both fluvial and lacustrine facies confirms a dynamic basin influenced by tectonics and climate.

7.2. Geological History of the Study Area

The basin's evolution is tied to the Albertine Graben's rifting phases:

Early-Mid Miocene (~12 Ma): Initial rifting formed Lake Obweruka, depositing fluvial and evaporitic sediments (Kisegi Formation).

Late Miocene (8–7 Ma): Increased subsidence led to deep lacustrine conditions (Kasande Formation).

Pliocene-Pleistocene: Uplift of the Rwenzori Mountains segmented the graben, shifting drainage patterns and depositing coarser sediments (Nyaburogo, Nyakabingo Formations).

Recent: Active faulting (e.g., Makondo Fault) and geothermal activity (Sempaya Hot Springs) indicate ongoing tectonic influence.

Key Evidence are**;** Unconformities between basement and sediments record erosion during rift initiation, Flower structures and anticlines (e.g., Turaco) reflect transpressional deformation. Fossil assemblages and sediment cyclicity correlate with lake-level changes.

7.3. Petroleum Potential of the Semliki Basin

The basin hosts all critical elements of a petroleum system, though challenges exist:

Source Rocks: Kasande Formation clays contain organic matter, but high geothermal gradients may have "overcooked" some hydrocarbons into gas.

Reservoirs: Kisegi Formation sands have good porosity (up to 36%) but are compartmentalized by gypsum and clay layers.

Traps: Anticlines in flower structures (e.g., Turaco) and fault-dependent closures provide structural traps.

Seals: Kasande Formation clays and lacustrine shales act as effective seals, though seepages (e.g., Kibuku) indicate local seal failure.

Migration Pathways: Fractures in basement and faults facilitate hydrocarbon movement.

Hight temperatures and gypsum cementation and compartmentalization affects the petroleum potential of the area. High temperatures (>100°C at Sempaya) may have degraded oil to thermogenic gas (methane, CO_2) and reservoir quality is reduced by gypsum cementation and compartmentalization.

The Sempaya Hot Springs (103–106°C) demonstrate elevated geothermal gradients, affecting hydrocarbons by: Accelerating Maturation, where source rocks reached the oil window faster but risked thermal cracking beyond 120°C, converting oil to gaProlonged exposure to >150°C can destroy hydrocarbons, leaving dry gas (methane) and non-hydrocarbon gases (CO_2, H_2S).this is evidenced when Turaco wells encountered CO_2-rich gas, possibly from volcanic input or cracked hydrocarbons.

7.4. Structural Controls on Hydrocarbon Accumulation

Observed structures (faults, folds, joints) significantly influence hydrocarbon systems:

Faults: NE-SW normal faults (e.g., Makondo) create traps but may also leak if not sealed by clay gouge.

Anticlines: Rollover folds in flower structures (e.g., Turaco) form structural traps.

Fractures: Basement joints enhance migration but may lead to biodegradation if connected to surface.

Compartmentalization: Gypsum-filled fractures and clay layers hinder fluid flow, reducing recovery efficiency.

CHAPTER EIGHT: CONCLUSION AND RECOMENDATIONS

8.1. Conclusion.

The field study in the Semliki Basin successfully addressed its objectives by analyzing lithologies, structures, and depositional environments to assess the petroleum potential of the area. The identified lithologies, including sands, clays, conglomerates, and evaporites, revealed cyclic fluvial-deltaic and lacustrine depositional environments, influenced by semi-arid conditions. Structural analysis highlighted NE-SW trending faults and joints, which play a crucial role in hydrocarbon migration and trap formation. The basin exhibits all essential elements of a petroleum system, with the Kasande Formation as a potential source rock and the Kisegi Formation as a reservoir. However, challenges such as reservoir compartmentalization by gypsum and high geothermal gradients affecting thermal maturity were noted. The findings underscore the basin's hydrocarbon potential while emphasizing the need for further exploration to optimize recovery strategies. The study also highlighted the region's geothermal energy prospects, supported by the active Sempaya Hot Springs. Overall, the fieldwork provided valuable insights into the basin's geology, supporting future petroleum and geothermal exploration efforts.

8.2. Recommendations.

The field study in the Semliki Basin provided valuable hands-on training in stratigraphic logging, structural analysis, and geophysical data interpretation, aligning with its objectives of enhancing students' fieldwork competencies. However, limited field exposure and insufficient guidance on software like Geosoft, Sedlog, and Stereonet hindered students' ability to fully interpret data. To address this, the department should organize more field projects, ensuring students gain practical experience and confidence in applying geological techniques.

Increasing the duration of fieldwork would allow students more time to engage with activities like lithostratigraphic logging and facies analysis, reinforcing their understanding of depositional environments and structural trends observed in the basin. Additionally, assigning dedicated lecturers or supervisors to each student group would provide tailored mentorship, improving learning outcomes.

Pre-fieldwork preparation is crucial. Students should be given a list of relevant literature and software tools beforehand to familiarize themselves with key concepts, such as paleocurrent

analysis or seismic interpretation, before arriving on-site. This would streamline fieldwork efficiency and deepen comprehension.

Lastly, students should participate in actual geophysical data acquisition, rather than relying solely on pre-collected datasets. Practical involvement in gravity, magnetic, and seismic surveys would enhance their technical skills and provide a holistic understanding of exploration methods. These recommendations aim to bridge gaps in field training, ensuring students are better equipped for future geological endeavors.

REFERENCES

- Aanyu, K. (2011). “Implications of Regional Fault Distribution and Kinematics for the Uplift of Rift Flanks around the Rwenzori Mountains, Southwestern Uganda”. PhD thesis, Johannes Gutenberg University. P.15-18.
- Allen, J.R.L., (1964), Parallel lamination developed from upper-stage plane beds: a model based on the larger coherent structures of the turbulent boundary layer: Sedimentary Geology, v. 39, p227-242
- Barritt, S.D. (1993). The African Magnetic Mapping Project. ITC Journal, 1993-2, p122-131.
- Bellon, H., and Pouclet, A., (1980). Datations K-Ar de quelques laves du Rift-ouest de l,Afrique Centrale; implications sur l’evolution magmatique et structural. Geol. Rundsch.
- Bishop, W. (1969). Pleistocene Stratigraphy of Uganda. Geological Survey of Uganda, Memoir X. 122.
- Boggs, Jr., (2006). Principles of Sedimentology and Stratigraphy. 4th ed. Pearson Education Inc.
- Davis, G.H., S.J. Reynolds, and C. Kluth (2012) Structural Geology of Rocks and Regions (3rd ed.): John Wiley and Sons, Inc., New york, New York. 864 pp
- Geosoft Inc., (2015). Oasis Montaj Data Processing and Analysis System for Earth Science Applications, Version 8.4 User Guide, p 5-91.
- Grotzinger, J., Jordan, T.H., & Siever, R., (2007). Understanding the Earth. 5th ed. W.H Freeman and Company New York.
- Jackson, Julia A., ed. (1997). "wedge-out". Glossary of geology (Fourth ed.). Alexandria, Viriginia: American Geological Institute. Pp50
- Jarrett, D. (2014). Oil Discoveries in the East African Rift. Gaffney, Cline & Associates
- Kasande R and Rubondo, E.N.T(1996). The geology of the Semliki Basin, unpublished report, Petroleum Exploration and Production Department.
- Kashambuzi, R.J., (2006). The Potential and Developments in Uganda’s Upstream Petroleum Sector. AAPG Convention, Dallas Texas, 2004.
- Kiconco, L. (2005). The Semliki Basin, Uganda: its sedimentation history and stratigraphy in relation to petroleum accumulation, Unpublished MSc. Thesis: University of Cape Town, South Africa, pp 1-138.
- Lukaye, J., Worsley, D., Kiconco, L., Nabbanja, P., Abeinomugisha, D., Amusugut, C., … & Sempala, V., (2016). Developing a Coherent Stratigraphic Scheme of the Albertine Graben-East, Africa. Journal of Earth Science and Engineering, vol. 6, No. 5, 2016. David Publishing Company.
- Macleod, I, A., Vieira, s., Chaves, A. c. (1993). Analytic Signal and Reduction-to-the-Pole in the interpretation of the total Magnetic Field Data at Low Magnetic Latitude, 3rd Conference of The Brazillian Geophysical Society. Pp.831-835.
- Marshak, Stephen, (2009). *Essentials of Geology,* W. W. Norton 3rd Ed, pp 40-50
- McLane, Michael, (1995). Sedimentology, Oxford University Press. pp 95-97.
- Neuendorf, K.K.E., J.P. Mehl, Jr., and J.A. Jackson, eds., 2005. Glossary of Geology (5th ed.). Alexandria, Virginia; American Geological Institute. p 61. ISBN 0-922152764.

- Okpoli. C., Akingboye, A. 2016a. Reconstruction and appraisal pf Akunu-Akoko area iron ore deposts using geologic and magnetic approaches. RMZ -Materials and Geoenvironment (Materiali in geokojie), 63(1). 19-38
- Paschier, C.W., Trouw, R.A.J, 1996, Micro tectonics. Springer (Berlin)
- Pickford, M., et al (1993). Geology and paleobiology of the Albertine Rift Valley, Uganda-Zaire. Geology, Internat. Centre Training Exchange Geosci., 1, pp.1-90
- Pickford, M., Senut, B., and Hadoto, D., (1994). Geology and Palaeobiology of the Albertine Rift Valley, Uganda-Zaire. Palaeobiology-Paléobiologie (Vol. 2). Occas. Publishing CIFEG 1994
- S. Roller, J. H. (2010). Middle Miocene to Pleistocene sedimentary record of rift evolution in the southern Albert Rift (Uganda).
- Schlueter, T., (1997). Geology of East Africa. Beitrage zur Regionalen Geologic de Erde, Gebruder Bontrager-Berlin Stuttgart, Bd. 27, 484p.
- Selley, Richard C.; Sonnenberg, Stephen A. (2015). "Chapter 8 - Sedimentary Basins and Petroleum Systems". Elements of petroleum geology (3rd ed.). Amsterdam: Academic Press. pp. 377–426.
- Simon. B., Guillocheau. F., Robin. C., Dauteuil. O., Nalpas. T., Pickford. M., Senut. B., Lays. P, Bourges. P, Bez. M (2017). Deformation and sedimentary evolution of the Lake Albert Rift (Uganda, East African Rift System). Marine and Petroleum Geology. 86, 17-37.
- The geological mapping of the Semliki Basin, Western Uganda (published).
- Tukei. I,(2019). Geologic And Stratigraphic Logging Project Report Of Semiliki Basin-Albertine Graben-Ntoroko District Western Uganda. Undergraduate report, Makerere University, DGPS.
- Wayland, E.J., (1925). Petroleum in Uganda. Memoir 1 Geological Survey of Uganda, p61.
- Wilkerson, M.S. (2019).“Primary Structures.” Geoscience 350A: Structural Geology/Tectonics, DePauw University. Pp20.

APPENDICES.

Appendix 1. Bed Measurements.

Strike	Dip
$N40^0E$	18^0SE
$N36^0E$	15^0SE
$N30^0E$	10^0SE
$N35^0E$	15^0SE
$N48^0E$	15^0SE
N40E	26SE
N50E	20SE
N46E	16SE
N44E	15SE
N42E	14SE
N38E	13SE
N34E	12SE
N32E	15SE
N28E	10SE
N25E	10SE

Appendix 2. Joint Measurements in the basement rock

Set 1		Set 2	
Strike	**Dip**	**Strike**	**Dip**
S40W	34NW	S85E	62SW
N20E	78SE	N62W	82NE
N82E	72SE	N70W	65NE
N88E	14SE	S80E	68SW
N40E	30SE	N74W	68NE
N68E	80SE	N80W	74NE
S24W	18NW	S72E	64SW
S44W	30NW		
S36W	34NW		

N78E	80SE		

Appendix 3. Measurements of foliation in the basement rocks

Strike	**Dip**
S86^{0}W	70^{0}NW
S88^{0}W	69^{0}NW
S84^{0}W	68^{0}NW
S72^{0}W	70^{0}NW
S82^{0}W	72^{0}NW
N45E	80SE
N44E	82SE
N42E	80SE
N38E	76SE
N30E	80SE
N34E	82SE
N40^{0}E	82^{0}SE
N28^{0}E	82^{0}SE
N42^{0}E	74^{0}SE
N36^{0}E	78^{0}SE
S80^{0}W	64^{0}NW
S60^{0}W	62^{0}NW

Appendix 4. Well logs for Turaco well-2

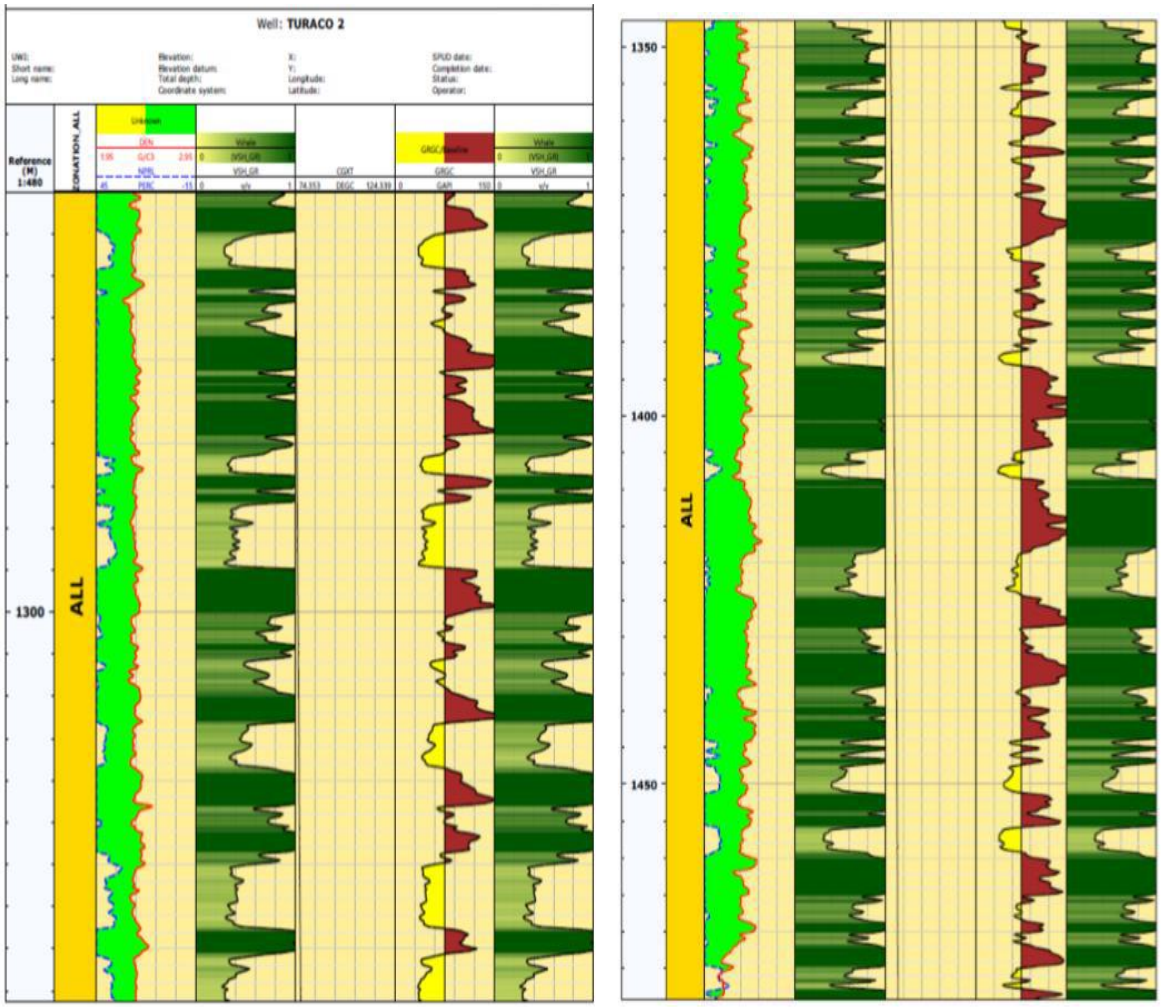

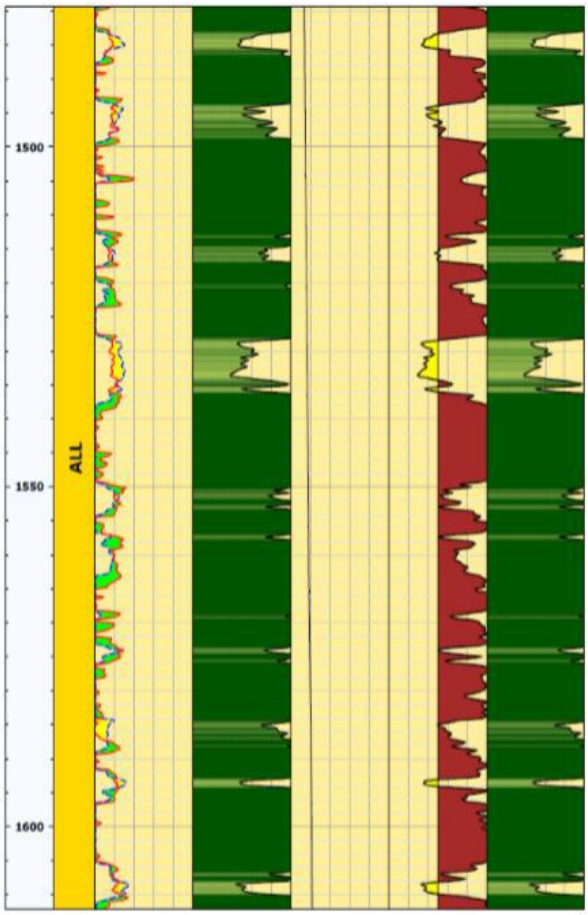
1500
1550
1600
ALL

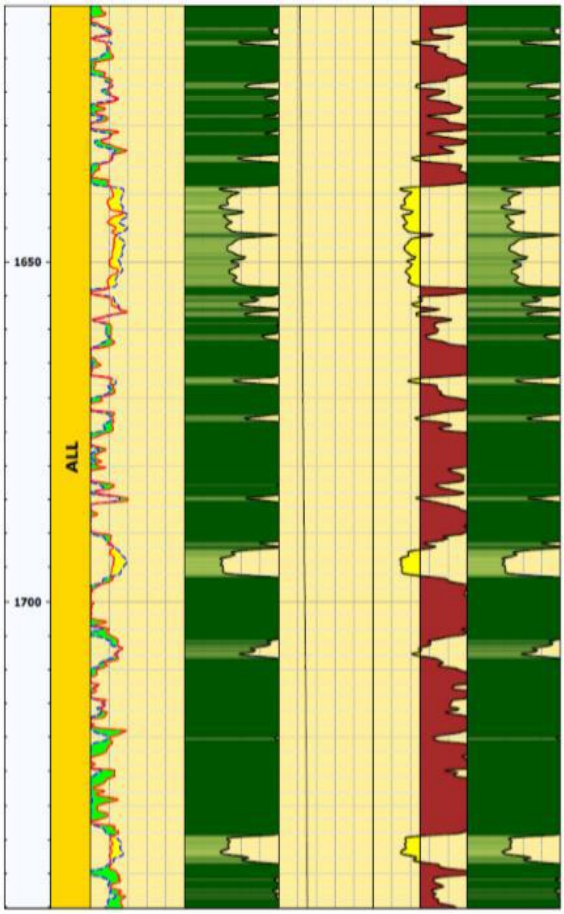
1650
1700
ALL

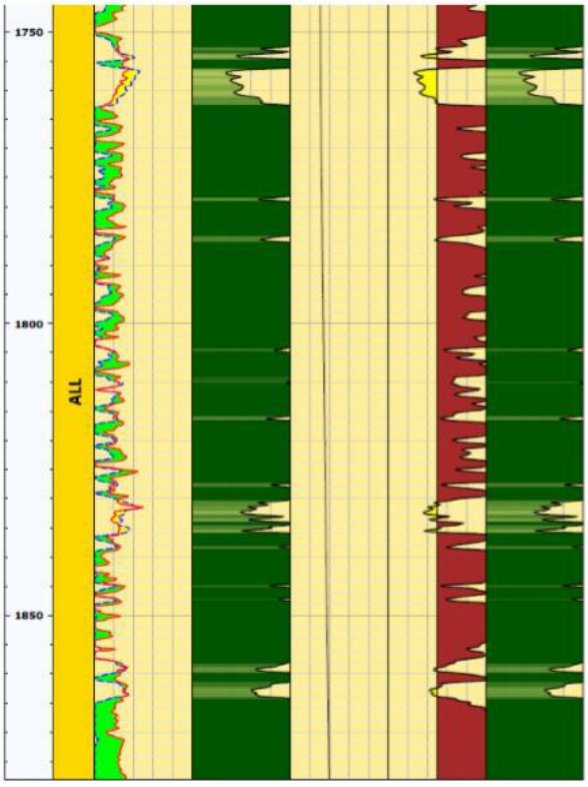
1750
1800
1850
ALL

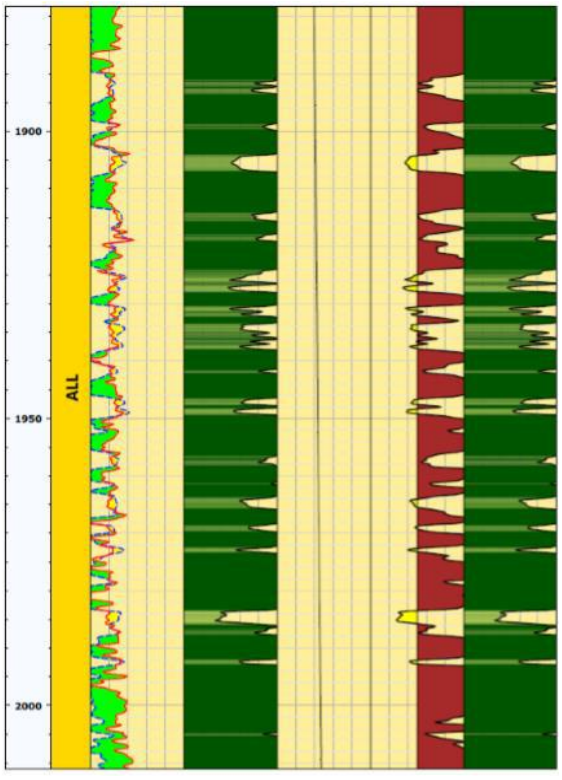
1900
1950
2000
ALL

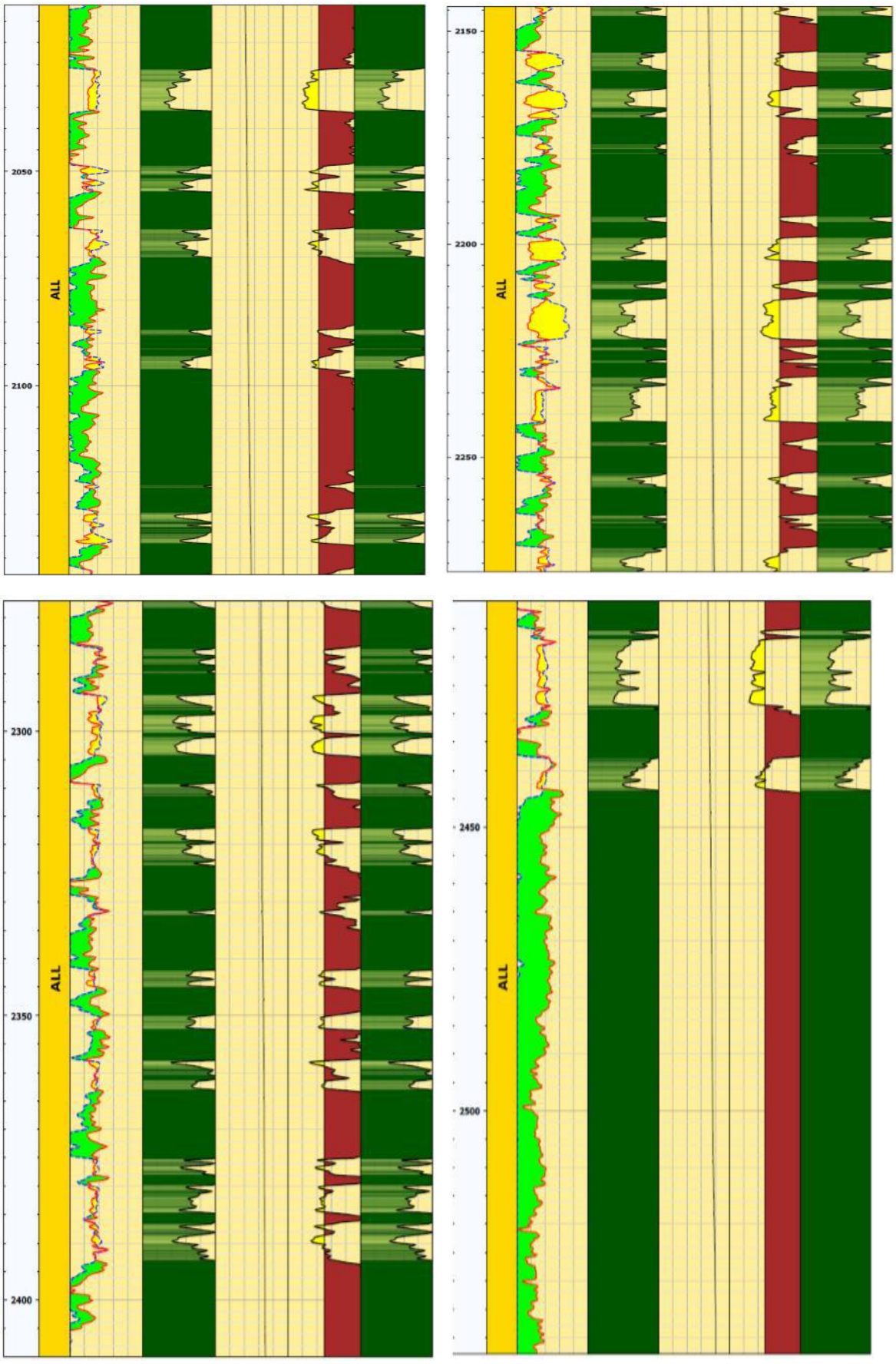
2050
2100
ALL
2150
2200
2250
ALL
2300
2350
2400
ALL
2450
2500
ALL

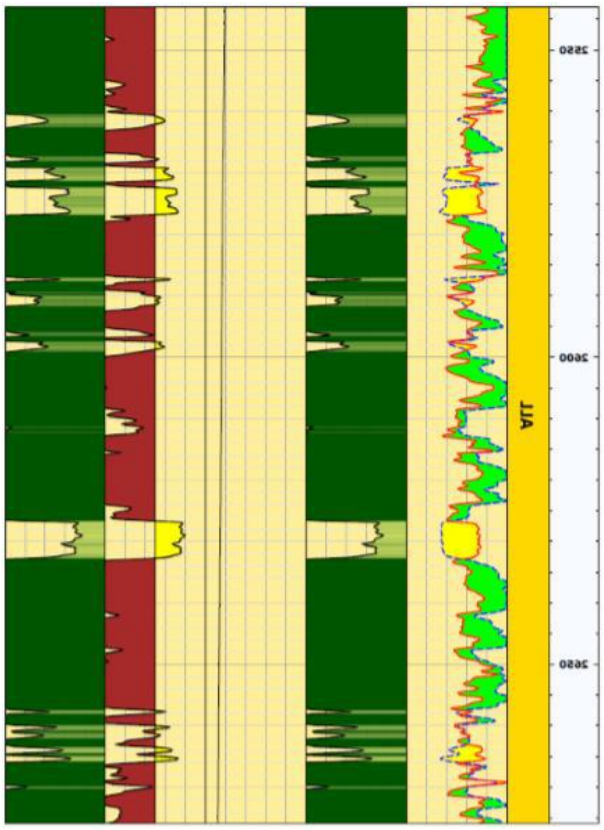
3520
3600
3680
JJA

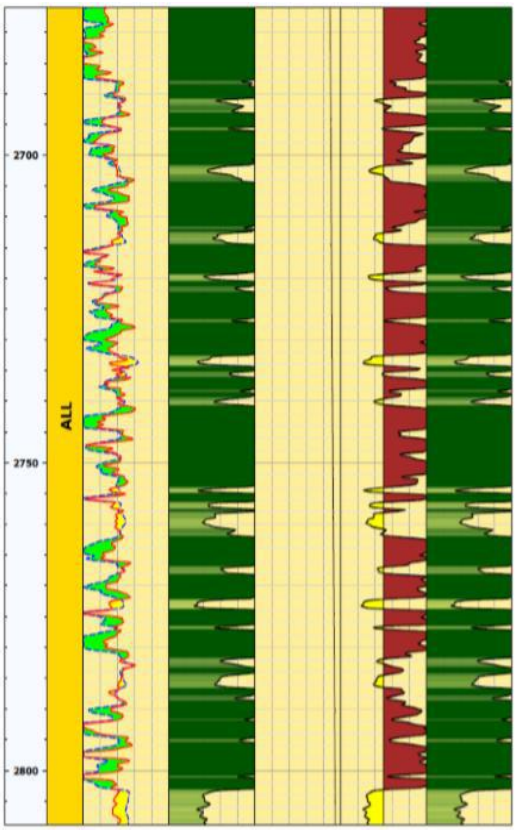
2700
2750
2800
ALL

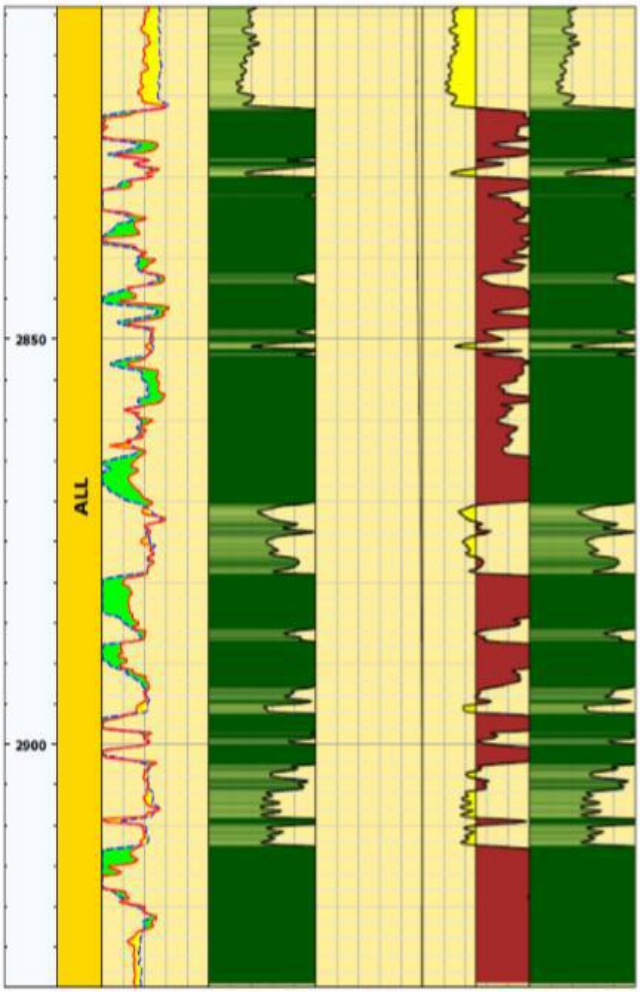
2850
2900
ALL